Ministry of Higher Education
and Scientific Research
University of Kerbala
College of Education for Pure Sciences

Pure Sciences International Journal of Kerbala

PSIJK

Year:2025
Volume : 2
ISSUE : 5

ISSN: 6188-2789 Print
3005 -2394 Online

Pure Sciences International Journal of Kerbala

(PSIJK) is published in four issues annually

A quarterly peer-reviewed scientific journal issued by the College of Education for Pure Sciences at the University of Kerbala, specializing in pure sciences, accredited for the purposes of scientific promotion Pursuant to Ministerial Resolution No. **B.T 7575** Dated **14 /9 /2023**

Licensed by

Ministry of Higher Education
and Scientific Research and Scientific Research

Issued by

University of Kerbala
College of Education for Pure Sciences

Second Year ,Volume 2 , Issue 5
31 March 2025

Ministry of Higher Education and Scientific Research

College of Education for Pure Sciences

University of Kerbala

Print ISSN: 6188-2789
Online ISSN: 3005 -2394

Consignment Number in the Housebook and Iraqi Documents: 2515, 2021

Postal Code: 56001
Mailbox: 232

Mobile: +964 7769920165
https://journals.uokerbala.edu.iq

Iraq - Holy Karbala

Workflow by OJS/PKP

About the Journal

The "Pure Sciences International Journal of Kerbala", published quarterly and distributed internationally by the College of Education for Pure Sciences provides a forum for publication of significant science advancements and developments in chemistry, biology, computer, physics, mathematics and interdisciplinary areas of science. All prospective authors are invited to submit their original contributions on new theoretical and applied aspects of growing research. All manuscripts submitted, including symposium papers, will be peer reviewed by qualified scholars assigned by the editorial board.

You are cordially encouraged to use this journal as a means of dissemination of information on the various facets of science and technical problems; and to impart specialized knowledge, quality and excellence to strengthen the perception of technological resources and needs of the world. The PSIJK is looking forward to receiving your assistance to working together to develop a worthwhile, high quality journal.

Aims and Scope

The objective of the Pure Sciences International Journal of Kerbala is to provide a forum for communication of information among the world›s scientific and technological community and Iraqi scientists. This journal intends to be of interest and utility to researchers and practitioners in the academic, industrial and governmental sectors. All original research contributions of significant value in all areas of science discipline are welcome.

This journal will publish authoritative papers on theoretical and experimental research and advanced applications embodying the results of extensive field, plant, laboratory or theoretical investigation or new interpretations of existing problems. It may also feature - when appropriate - research notes, technical notes, state-of-the-art survey type papers, short communications, letters to the editor, meeting schedules and conference announcements. The language of publication is English. Each paper should contain an abstract both in English and Arabic. However, for the authors who are not familiar with Arabic language, the publisher will prepare the translations. The abstracts should not exceed 250 words.

All manuscripts will be initially checked for plagiarism and then peer-reviewed by qualified reviewers. The material should be presented clearly and concisely:

-Full papers Authors are urged to be succinct; long papers with many tables and figures may require reductions prior to being processed or accepted for publication. Although there is not an absolute length restriction for original papers, authors are encouraged to limit the text to =5,000 words (including references) and references up to 40.

-Review papers are only considered from highly qualified well-known authors generally assigned by the editorial board or editor-in-chief. Author of review papers should have high qualifications with distinct developed research area, an outstanding scholar with an extensive publications.

-Short communications and letters to the editor should contain a text of about 3000 words and whatever figures and tables that may be required to support the text. They include discussion of full papers and short items and should contribute to the original article by providing confirmation or additional interpretation. Discussion of papers will be referred to author(s) for reply and will concurrently be published with reply of author(s).

Instructions for Authors

Submission of a manuscript represents that it has neither been published nor submitted for publication elsewhere and is result of research carried out by author(s). Presentation in a conference and appearance in a symposium proceeding is not considered prior publication.

Authors are required to include a list describing all the symbols and abbreviations in the paper. Use of the international system of measurement units is mandatory.

-On-line submission of manuscripts results in faster publication process and is recommended. Instructions are given in the PSIJK web sites https://journals.uokerbala.edu.iq/

-Hardcopy submissions must include MS Word and jpg files.

-Manuscripts should be typewritten on one side of A4 paper, double-spaced, with adequate margins.

-References should be numbered in brackets and appear in sequence through the text. List of references should be given at the end of the paper.

-Figure captions are to be indicated under the illustrations. They should sufficiently explain the figures.

-Illustrations should appear in their appropriate places in the text.

-Tables and diagrams should be submitted in a form suitable for reproduction.

-Photographs should be of high quality saved as jpg files.

-Tables, Illustrations, Figures and Diagrams will be normally printed in single column width (8cm). Exceptionally large ones may be printed across two columns (17cm).

This journal makes articles available online as soon as possible after acceptance. This concerns the accepted article (both in HTML and PDF format), which has not yet been copyedited, typeset or proofread. A Digital Object Identifier (DOI) is allocated, thereby making it fully citable and searchable by title, author name(s) and the full text. The article›s PDF also carries a disclaimer stating that it is an unedited article. Subsequent production stages will simply replace this version.

The Pure Sciences International Journal of Kerbala is an open access journal: all articles will be immediately and permanently free for everyone to read and download. To provide open access, this journal has an open access fee of USD 100 excluding taxes (also known as an article publishing charge APC) which needs to be paid by the authors or on their behalf e.g. by their research funder or institution. If accepted for publication in the Journal following peer review, authors will be notified of this decision and at the same time requested to pay the article processing charge. A CC user license manages the reuse of the article.

-Author(s)' bio-data including affiliation(s) and mail and e-mail address(es).

-Manuscript including abstracts, key words, illustrations, tables, figures with figure captions and list of references.

-MS Word file of the paper.

The following list will be useful during the final checking of an article prior to sending it to the journal for review. Please consult this Guide for Authors for further details of any item.

Publication Ethics

1. Author responsibility

The authors are exclusively responsible for the contents of their submissions, the validity of the experimental results and must make sure that they have permission from all involved parties to make the data public.

It is the responsibility of each author to ensure that papers submitted to PSIJK are written with ethical standards in mind, concerning plagiarism.

Please note that all submissions are thoroughly checked for plagiarism. If an attempt at plagiarism is found in a published paper, the authors will be asked to issue a written apology to the authors of the original material. Any paper which shows obvious signs of plagiarism will be automatically rejected and its authors will be banned for duration of three years from publishing in PSIJK. The authors will receive proper notification if such a situation arises.

Information on what constitutes plagiarism is provided below.

2.Plagiarism: Definition and Context

Plagiarism, where someone assumes another›s ideas, words, or other creative expression as one›s own, is a clear violation of scientific ethics. Plagiarism may also involve a violation of copyright law, punishable by legal action.

Plagiarism may constitute the following:

Word for word, or almost word for word copying, or purposely paraphrasing portions of another author›s work without clearly indicating the source or marking the copied fragment (for example, using quotation marks);

Copying equations, figures or tables from someone else›s paper without properly citing the source and/or without permission from the original author or the copyright holder.

Self-plagiarism, as a related issue, is the word for word or almost word for word reproduction of portions of one›s own copyrighted work without proper citation of the original material. Self-plagiarism does not apply to publications based on the author›s own previously copyrighted work (for example from conference proceedings) where proper reference was given for the original text.

International Journal of Engineering editorial board will place any plagiarism-related investigation at high priority and will take appropriate action as needed.

Editorial board

Pure Sciences International Journal of kerbala

Year: 2025 Volume : 2 Issue : 5 ISSN: 6188-2789 Print 3005 -2394 Online

Pure Sciences International Journal of Kerbala

Journal Homepage:https://journals.uokerbala.edu.iq/index.php/psijk

Computational Study for the Electronic and Molecular Properties of Zn_3Se_3 Clusters

Aula Mahdi Al Hindawi *1, Jihan Hameed Abdulameer 2, and Sharmee Sahib3

1*, 2,3 *Department* Chemistry Department, College of Education for Pure Science, University of Kerbala, Kerbala, Iraq

P A P E R I N F O

Paper history:
Received: 28 August 2024
Accepted: 1 October 2024
Published: 31 March 2025

Keywords:
Vibrational frequency, DFT, HOMO&LUMO, Zn3Se3 .

A B S T R A C T

Low affinity energy thresholds were precisely tailored into the Zn_3Se_3 cluster's molecular geometry configurations. The structural and electronic characteristics of the Zn_3Se_3 composite were examined using the 6-113G (d, p) basis set for density functional theory calculations (DFT/B3LYP). Comprehensive vibrational mode frequencies were methodically examined using potential energy distribution as a basis for analysis. The energy band gap (E_g) for the Zn_3Se_3 structured was computed and plotted HOMO and LUMO, or high occupied and low unoccupied molecular orbitals, are frontier values. The result is the value of E_g (0.0383) eV. The molecular electrostatic potential as well as surface and contour diagram of Zn_3S_3 were determined, along with electronic properties of the stated structures. These include IP, EA, Ef, E_g, Cp, χ, η, S, and ω.

1. INTRODUCTION

Zinc selenide (ZnSe) is a light-yellow binary compound (II–VI) semiconductor that has a wide band gap (2.7 eV). The low resistivity, and great photosensitivity are just a few of the extremely desirable properties of this semiconducting material. There are two crystalline forms of zinc selenium: wurtzite (a hexagonal form) and zinc blende (a cubic form), with the cubic phase being thought to be stable. The electron affinity of ZnSe is 4.09 eV. ZnSe is often manufactured as an-type semiconductor, like the majority of II-VI group 7 semiconductors, although producing a p-type is challenging [1].

Owing to its large and direct band gap, it can be used as both emitters and detectors in optoelectronic devices. It is beneficial for optical parts of windows with high strength lasers. Because of its broad transmission wavelength range of 600 nm to 2000 nm, it is also employed as an infrared optical material. It is frequently utilized as a transmission window in ATR prisms, night vision applications, and infrared spectroscopy. Electronic structure can be found in chemical and physical systems through the use of Density Functional Theory (DFT), a quantum mechanical modeling tool [2]. Additionally, ZnSe can be employed in high resolution thermal imaging systems to rectify color distortion that is frequently present in other lenses that are part of the system. To validate the results of experiments, DFT has shown to be an invaluable research tool [3].

Chemical interactions can be studied at better scales recognitions to combinatorial phenomena, in especially the low cost (DFT) technique, which theoretically gives material design predictions through geometrical structures [4].

Furthermore, when theoretical research is “confirmed" for a particular experiment, the more quantitative predictions of events the more broadly accepted the entire theory which is made and validated by experiment [5]. However, a number of theoretical investigations have been cited and considered in real-world applications as gas sensors [6].

Recently, the ZnSe molecules' electrical and structural properties as nanotubes with varying amounts of ZnSe atoms have been studied using DFT theory [7, 8].

This paper demonstrates that the ground state (GS) and other characteristics of a many-electron system may be determined using DFT.

*Corresponding Author Institutional Email:
aula.m@uokerbala.edu.iq (Aula Mahdi Al Hindawi)

2. COMPUTATIONAL DETAILS

Density functional theory (DFT) has been applied to many-electron systems to study their electronic structure and behavior, and it has influenced the quantum mechanical approach. The electron density distribution is understood in physics and chemical sciences through the application of functional analysis. DFT is by far the most popular and adaptable computational method chemistry and physics. It has also demonstrated effectiveness ins simulating the ground state properties of materials. Utilizing DFT theory and a basis set comprising 6-311G**, this study employs a modified Lee-Yang-Parr (Becke, three-parameters, Lee-Parr) strategy. The heavy-atom polarization set d-function is represented by the first asterisk above basis G. But the second symbol, which sometimes needs to be expressed as 6-311G (d, p), shows the polarization of the hydrogen atoms' p-functions [9, 10]. These formulas and theories were all part of Gaussian 09 and Gaussian View 6.0 [11]. Precise molecular geometries optimization was necessary to provide reliable results and reduce the thresholds for convergence. The frequency of typical vibrations were also determined the self-consistent field (SCF) that can solve equation, which validated the decreased energy at geometric optimization. Three Zn and three Se atoms make up the chemical structure of the Zn_3Se_3 cluster, as illustrated in Figure (1).

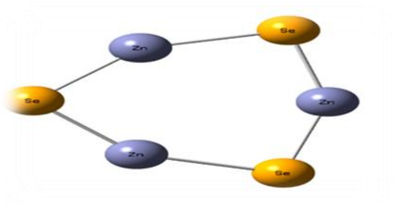

Figure 1. Using basis set 6-311G**, the DFT approach optimized the structures of (Zn_3Se_3).

Calculations were performed on the compounds' ionization potential (IP), which is the energy required to break the structural unit of the weakest electron attachment to the nucleus, Fermi level energy (Ef), and energy of bandgap ($E\boldsymbol{g}$). Electron energy is the energy generated when an electron is introduced to a gaseous atom, affinity (EA), and it may be calculated after determining the following equations to find the Lowest Unoccupied Molecular Orbital (LUMO) and Highest Occupied Molecular Orbital (HOMO) energies. [12, 13]. Electron extraction is more difficult at higher ionization energies.

.

$$E\boldsymbol{g} = ELUMO – EHOMO \quad (1)$$

$$IP = - EHOMO \quad (2)$$

$$EA= - ELUMO \quad (3)$$

$$Ef = (EHOM + ELUMO) / 2 \quad (4)$$

Moreover, the identities of the quantum molecules are (Cp, χ, η, S, and ω). Typically, these descriptors look like this: the following metrics are provided by [14, 15]: electronegativity (χ), which measures an atom's capacity to draw electrons into chemical bonds; Softness (s), global hardness (η), and electrophilicity index (ω). Bonds in a semiconductor, the energy that can be absorbed or released due to a change in the number of particles is called the ferry energy when the electron system is at absolute zero temperature. This energy is also known as the chemical potential (Eq.).

$$Cp = - \chi \quad (5)$$

$$\chi = IP+EA / 2 \quad (6)$$

$$\eta = IP−EA /2 \quad (7)$$

$$S = 1/ \eta \quad (9)$$

$$\omega = - \chi^2 / 2\eta \quad (10)$$

3. RESULTS and DISCUSSION

3.1 Vibrational Frequencies & FTIR spectra

The number of normal vibration modes of non-linear molecules can be computed using the equation ($3N^{-6}$), where N is the number of atoms. As a result, the six-atom Zn_3Se_3 molecule, twelve vibrational modes were found from the pattern's lowest frequency to its highest mode. These frequencies are shown in Table 1. In the range (290.94_291.62) cm^{-1}, the highest frequency modes are (11and 12).

Conversely, the DFT-B3LYP levels with the 6-311G** basis set were used to compute the IR spectra of the investigated structure in the region of 0–4000 cm^{-1}. Figure 2 depicts the Zn_3Se_3 FT-IR spectrum.

TABLE 1. The frequency range of Zn_3Se_3 's typical vibrational modes, in order of lowest to highest

No. Mode	Frequency/ cm^{-1}	Structure
MODE 1	61.27	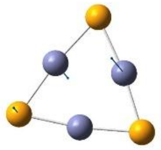
MODE2	61.35	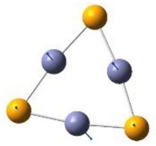
MODE3	85.42	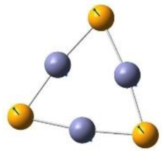
MODE4	85.42	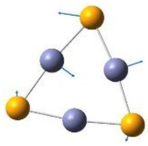
MODE5	93.55	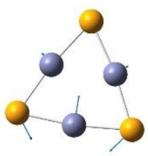
MODE6	152.67	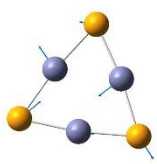
MODE7	169.10	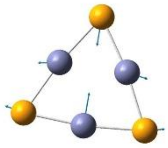
MODE8	169.64	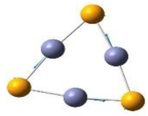
MODE9	174.18	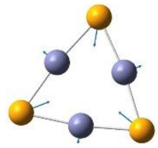
MODE10	271.59	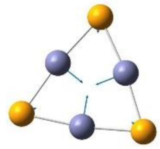
MODE11	290.94	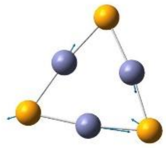
MODE12	291.62	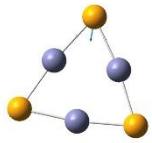

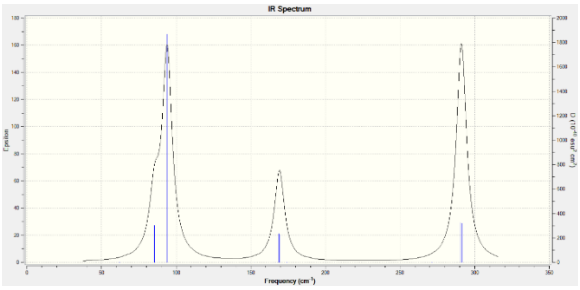

Figure 2. The FTIR spectrum for Zn3Se3

Additional peaks with signs at (1800, 800, and 1800) cm-1 correspond to the Zn_3Se_3 (DFT), ZnSe, and they are ascribed to the Zn-Se bond's stretching vibrations [16, 17].

3.2 Electronic Properties

A significant amount of complexity has been added to the model known as molecular orbital theory (MOTs), which addresses many different facets of orbital bonding, energy, chemical processes, and characterization. The highest occupied molecular orbitals (HOMOs), which have the highest energy, are those that have electrons occupying them. The second is known as the lowest energy unoccupied molecular orbital, or LUMO that is devoid of electrons. The DFT method with the 6-113G** basis set was used to calculate the values of the molecular orbitals for Zn3Se3 . The (1–10) Equations were used to a useful index of the interaction system which is the HOMO, LUMO, and HOMO-LUMO (Eg). It can be used to calculate the electronic characteristics IP, EA, Ef, Eg, Cp, χ, η, S, and ω. Zn_3Se_3 's electrical characteristics are shown in **Table 2**.

Figure 2 demonstrates the Zn_3Se_3 cluster's electronic properties and makes the HOMO and LUMO MOs for the molecules in question be clear. The energy gap (Eg) rises as more polymer is added, indicating that the Zn_3Se_3 particles are affected, strongly supporting the idea of quantum confinement, and the larger value for the band gap (the smallest nano particle diameter) [18].

Table 2. Demonstrates the electronic properties of Zn_3Se_3

Properties	**Zn3Se3 (DFT)**
E_{HOMO}	- 0.23784
E_{LUMO}	-0.19951
Ef **/ eV**	- 0.218675
Eg **/ eV**	0.03833
IP **/ eV**	0.23784
EA **/ eV**	0.19951
Cp **/ eV**	- 0.21867
χ **/ eV**	0.21867
η **/ eV**	0.01917
S **/ $(eV)^{-1}$**	52.164
ω **/ ev**	-1.247

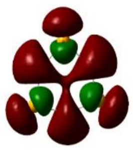

LUMO

Eg= 0.0383

Eg = ELUMO – EHOMO

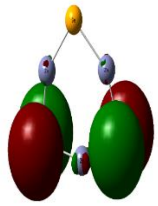

HOMO

Figure 2. Frontier molecular Zn3Se3 features: Eg and HOMO/LUMO orbitals

3.3 Molecular Electrostatic Potential

In order to assess the relationships and non-covalent interactions between molecules at a distance from one another and to look into repulsive or attractive interactions, density of the electron with charge, the molecular electrostatic potential (MEP) diagram, B3LYP calculations using basis set 6-311G(d,p), and nonlocalized dispersion among the structure's reactions were used [19]. Figure provided a description of these interaction zones for the molecule to depict three areas of contacts based on the electron density function. Blue zones illustrate the nature of hydrogen bonding. Green zones denote the Van der Waals bonding (VdW), while red areas represent repulsive interactions [20]. Moreover, the benefit of the molecular electrostatic potential scheme is a helpful instrument to look into how responsive the systems under study are to either nucleophilic or electrophilic assaults, depending on the charge distribution. The color-coded system for two regions is represented by the colored line in Fig. (4)'s upper border: the red and blue regions between -8.065×10^{-2} and 8.065×10^{-2}, and the Zn_3Se_3 cluster's range from -4.036×10-4 to 4.036×10^{-4}. The red-colored negative charge concentrations indicate the acceptor of an H-bonding molecule. In contrast, the second zone shows the donor of the H-bonding's positive charge densities in the blue ruler [21].

.

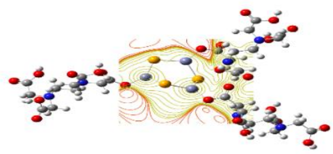

2D

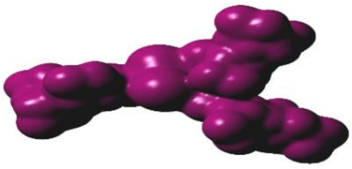

3D

Figure 4. Charge MEP is the Zn_3Se_3 surface surfaces diagram; MEP contour surface of Zn_3Se_3; densities distribution as color-coded ruler in top adage (red color for negative charge and blue for positive charge).

The top surface, however, will be the only one visible if all Zn_3Se_3 Plots of surfaces are made using every isosurface value. To view the surfaces of all the molecules under study, just draw the contours of each surface surrounding the molecule, as
the Zn_3Se_3 cluster illustrates in **Figure 4.**

4. CONCLUSION

Here is a bullet-point summary of the information:
-DFT Calculations: Density Functional Theory (DFT) calculations were performed using the 6-311G(d, p) basis set and the B3LYP hybrid functional.
- Zn_3Se_3 Cluster: structural and electronic properties of a Zn_3Se_3 cluster (three Zn and three Se atoms) were theoretically calculated.
- Comparison: the same DFT calculations were performed for another similar molecule for comparison. Spectral lines such as FTIR spectra were examined.
- Spectral Agreement: The active peaks in the theoretical and experimental FTIR spectra aligned well, confirming the accuracy of the calculations.
- Vibrational Modes: Twelve vibrational modes were observed for the Zn_3Se_3 molecule, within a frequency range of 0 cm^{-1}.
- Energy Gap (Eg): The HOMO-LUMO energy gap (Eg) was calculated. The energy gap increased from 4.031 eV to 4.459 eV after adding a polymer to the ZnSe cluster.
- Quantum Confinement: the findings support the quantum confinement effect, demonstrated by a higher band gap value and minimum nanoparticle diameter in line with experimental results.
- MEP Analysis: Molecular electrostatic potential (MEP), surface and contour diagrams, and estimated charge densities were calculated, showing nucleophilic and electrophilic attack points.

5. REFERENCES

1. Gel Gelu Bulo, the effete of deposition time on zinc selenide [ZnSe], thin films by chemical bath deposition technique. Master of science solid physics. October 2019 Hawassa Ethiopia
2. R. Rahimi, M. Solimannejad, Empowering hydrogen storage performance of B4C3 monolayer through decoration with lithium: A DFT study, Surfaces and Interfaces 29 (2022) 101723.
3. E.-W. Huang, W.-J. Lee, S.S. Singh, P. Kumar, C.-Y. Lee, T.-N. Lam, H.-H. Chin, B.-H. Lin, P.K. Liaw, Machine-learning and high-throughput studies for high-entropy materials, Materials Science and Engineering: R: Reports 147 (2022) 100645.
4. O.C. Adekoya, G.J. Adekoya, R.E. Sadiku, Y. Hamam, S.S. Ray, Density Functional Theory Interaction Study of a Polyethylene Glycol-Based Nanocomposite with Cephalexin Drug for the Elimination of Wound Infection, ACS Omega 7 (2022) 33808-33820.
5. B. Huang, O.A. von Lilienfeld, J.T. Krogel, A. Benali, Toward DMC Accuracy Across Chemical Space with Scalable Δ-QML, Journal of Chemical Theory and Computation 19 (2023) 1711-1721.
6. T. Alaa Hussein, N.M. Shiltagh, W. Kream Alaarage, R.R. Abbas, R.A. Jawad, A.H. Abo Nasria, Electronic and optical properties of the BN bilayer as gas sensor for CO2, SO2, and NO2 molecules: A DFT study, Results in Chemistry 5 (2023) 100978.
7. M. Hussein, H. Thjeel Al-Ogaili, Vibration Properties of ZnS nanostructure Wurtzoids: ADFT Study, Journal of Physics: Conference Series 1178 (2019) 012015.
8. M.T. Hussain, H. Thjeel Al-Ogaili, Study of geometrical and electronic properties of ZnS wurtzoids via DFT, Chalcogenide Letters 15 (2018) 523-528.
9. A.D. Becke, Density-functional thermochemistry. III. The role of exact exchange, The Journal of Chemical Physics 98 (1993) 5648-5652.
10. C. Lee, W. Yang, R.G. Parr, Development of the Colle-Salvetti correlation-energy formula into a functional of the electron density, Physical review. B, Condensed matter 37 (1988) 785-789.
11. M. Frisch, G. Trucks, H. Schlegel, G. Scuseria, M. Robb, J. Cheeseman, G. Scalmani, V. Barone, B. Mennucci, G. Petersson, H. Nakatsuji, M. Caricato, X. Li, H. Hratchian, A. Izmaylov, J. Bloino, G. Zheng, J. Sonnenberg, M. Hada, D. Fox, Gaussian 09, (2009).
12. V. Parey, M.V. Jyothirmai, E.M. Kumar, B. Saha, N.K. Gaur, R. Thapa, Homonuclear B2/B3 doped carbon allotropes as a universal gas sensor: Possibility of CO oxidation and CO2 hydrogenation, Carbon 143 (2019) 38-50.
13. Y. Huang, C. Rong, R. Zhang, S. Liu, Evaluating frontier orbital energy and HOMO/LUMO gap with descriptors from density functional reactivity theory, Journal of molecular modeling 23 (2017) 3.
14. G.B. Kaufman, Inorganic chemistry: principles of structure and reactivity, 4th ed. (Huheey, James E.; Keiter, Ellen A.; Keiter, Richard L.), Journal of Chemical Education 70 (1993) A279.
15. F. De Proft, P. Geerlings, Conceptual and Computational DFT in the Study of Aromaticity, Chemical Reviews 101 (2001) 1451-1464.
16. H. Yang, P.H. Holloway, B.R. Ratna, Photoluminescent and electroluminescent properties of Mn-doped ZnS nanocrystals, Journal of Applied Physics 93 (2003) 586-592.
17. S.G. Nanaki, G.Z. Kyzas, A. Tzereme, M. Papageorgiou, M. Kostoglou, D.N. Bikiaris, D.A. Lambropoulou, Synthesis and characterization of modified carrageenan microparticles for the removal of pharmaceuticals from aqueous solutions, Colloids and Surfaces B: Biointerfaces 127 (2015) 256-265.
18. R.N. Bhargava, D. Gallagher, X. Hong, A. Nurmikko, Optical properties of manganese-doped nanocrystals of ZnS, Physical Review Letters 72 (1994) 416-419.

19. of therapeutic potential of graphitic carbon nitride (g-C3N4) as a new drug delivery system for carboplatin to treat cancer, Journal of Molecular Liquids 331 (2021) 115607.
20. O. Noureddine, N. Issaoui, M. Medimagh, O. Al-Dossary, H. Marouani, Quantum chemical studies on molecular structure, AIM, ELF, RDG and antiviral activities of hybrid hydroxychloroquine in the treatment of COVID-19: Molecular docking and DFT calculations, Journal of King Saud University - Science 33 (2021) 101334.
21. O.C. Adekoya, G.J. Adekoya, E.R. Sadiku, Y. Hamam, S.S. Ray, Application of DFT Calculations in Designing Polymer-Based Drug Delivery Systems: An Overview, Pharmaceutics 14 (2022) 1972

.

Arabic Abstract

تم تصميم عتبات طاقة الألفة المنخفضة بدقة في التكوينات الهندسية الجزيئية لمجموعة Zn_3Se_3 . تم فحص الخصائص الهيكلية والإلكترونية لمركب Zn_3Se_3 باستخدام نظرية الكثافة الوظيفية (حسابات DFT/B3LYP باستخدام مجموعة الأساس 6-113p ,G (d). وتم فحص ترددات الوضع الاهتزازي الشامل بشكل منهجي باستخدام توزيع الطاقة المحتمل كأساس للتحليل. تم حساب فجوة نطاق الطاقة (E_g) لمركب Zn_3Se_3 ورسمها باستخدام المدارات الجزيئية العليا المشغولة والمنخفضة غير المشغولة (HOMO&LUMO). بالإضافة إلى ذلك، تم تحديد الإمكانات الكهروستاتيكية الجزيئية على السطح وتم تحديد مخطط كفاف لـ Zn_3S_3، إلى جانب الخصائص الإلكترونية. من الهياكل المذكورة، بما في ذلك جهد التأين (IP) والألفة الإلكترونية (EA) وعامل الإلكترون (Ef) والسعة الحرارية المولارية (Cp) والكهرسلبية (χ) والصلابة العامة (η) والنعومة (S) ومؤشر الكهروفيلية (ω).

Pure Sciences International Journal of kerbala

Year: 2025 Volume : 2 Issue : 5 ISSN: 6188-2789 Print 3005 -2394 Online

2025, Volume 2, Issues 5 PSIJK 18-26

Pure Sciences International Journal of Kerbala

Journal Homepage:https://journals.uokerbala.edu.iq/index.php/psijk

Removal of Pollution with Methyl Orange Dye Waste Water by Using Novel Graft Nano Co-polymer

Ali F A. Al -Ameri[1]. Khawla Ibrahim Abd[2]. Bahaa K. Al-Ghanimi[3*]. Zeyad Tareq Habeeb[4].

[1,3] *Ministry of Education, General Directorate of Education Karbala, Karbala. Iraq*
[2] *College of Veterinary Medicine, University of Kerbala, Karbala. Iraq.*
[3] *Department of Anesthesia and Critical Care, Al-Taff University College*
[4] *Department of Chemistry, College of Education for Pure Sciences, University of Kerbala, Karbala, Iraq.*

P A P E R I N F O

Paper history:
Received: 23 September 2024
Accepted: 9 October 2024
Published: 31 March 2025

Keywords:
Co-polymers, methyl orange, pollutions, Synthesis of graft PTGM nanoparticles

A B S T R A C T

The grafted nanocopolymers were synthesized via an esterification process, where the first step was to generate a linear copolymer by reacting terephthalic acid with glycerol. Then, a certain amount of maleic anhydride was added to the resulting linear copolymer solution to obtain the grafted PTGM nanoparticles. The prepared nanopolymers were characterized using FT-IR spectroscopy, ^{1}H-NMR, and atomic force microscopy (AFM). The average particle height was 8.3 nm and was exposed to three different temperatures (298, 308, and 318 K). Four different concentrations (1, 3, 5, and 7 ppm) of the nanocopolymers were examined and it was evident that they play a vital role in the adsorption process. The experimental results showed that the average surface area of this nanopolymer for adsorption of dye (methyl orange) decreased with increasing temperature, indicating that the process is endothermic. It was also observed that the highly efficient nanocopolymers were able to successfully remove (methyl orange) from aqueous solutions.

NOMENCLATURE			
DMSO	DiMethyl SulfOxide	Log	Logarithm
PTGM	Poly(Terphthalic acid-CO-Glycol-G-Maleic anhydride)	N	Number of malls
Wt	weight	g	gram
Vsol	Volume solvent	ppm	part pear million
Co	The concentration at zero	nm	nanomater
Ce	The concentration at equilibrium	Temp.	Temperature
Qe	The amount of adsorbate substance	N	The adsorption intensity
Eq.	equation	Kf	The adsorption amplitude
K	Kalvin	R_2	Reagen
mL	milliliter	λ	Wave length
AFM	Atomic force Microscope	Conc.	Concentration

1. INTRODUCTION

Nanomaterials are materials with a limited size range (1-100)nm[1, 2]. Controlling the size and shape at the nanoscale allows for the characterization, design, installation and utilization of materials, systems and devices [3, 4]. Pollution is one of the greatest concerns. Pollutants should be removed as much as possible, since they pose a threat to humans, health and aquatic organisms, and are the most significant water pollutants (dyes, organic compounds, heavy metals, pharmaceuticals and anything that affects or changes the natural properties of water). Industrial dyes are common in many modern fields including the dyeing of fabric, hair, leather, paper, food and cosmetics[5]. Many toxic and deadly dyes are consumed by 2% of the wastewater produced, which is similar to the amount produced by

*Corresponding Author Institutional Email:
bahaaghanimi.bg@gmail.com (Ali F A. Al -Ameri)

painting, and another 10% is used for textile coloring. Water (universal solvent) increases their susceptibility[6, 7]. Since dyes have a strong affinity for water, and are more difficult to remove via traditional methods, one of the most significant methods is the adsorption method on the surface of nanopolymers. Many toxic components in water systems, including many scientists, tend to utilize nanomaterials, larger and more effective adsorbents to create new and effective materials because the particles in question have a different interaction with each other than when they are naturally sized [8]. Our research also showed the capacity of poly (terephthalic acid-glycerol-G-maleic anhydride) toads to successfully adsorb dyes. Nanopolymers were found to be effective[9]for the purpose of eliminating pollutants.

2. MATERIALS and METHODS

Terephthalic acid, glycerin maleic anhydride, and other chemicals were used. All chemicals used in this work were of analytical grade procured from E. Merck Ltd.

2. 1. Synthesis of Graft PTGM Nanoparticles

The nanoparticles consist of terephthalic acid and glycerol in a ratio of 2:1 (200 mL, 2.0 mol) terephthalic acid and (50 mL, 2.0 mol) DMSO. A temperature-sensitive cup is integrated into the vessel. The mixture is heated to 40 degrees Celsius with a magnetic stirrer and then (92 g, 1.0 mol) Glycerol is incorporated into the mixture. Next, heat the mixture to 120 degrees Celsius and then add 25 ml of xylene to the vessel in 2 drop increments until the water from the esterification process is expelled and the vessel is only marginally heated. After the 80-minutes incubation at 145 degrees Celsius, the temperature will be decreased because the water no longer facilitates the generation of nanopolymers. The proposed equation would then state that the reaction vessel should be decreased to around 50 degrees Celsius. This is evident in the figure. The original formula for linear polymer creation (1).

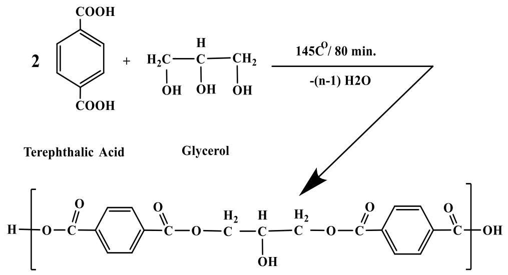

Equation 1. The initial stage of linear polymer synthesis.

In the second step, the anhydride maleic (0.5 mol, 49 g) was solving in 10 mL DMSO, heated to 40 °C and added it to the mixture (created in the first step). The beaker was gradually heated to 90 degrees Celsius, and then xylene was added in small doses. (2 drops per batch to remove water) until no more water came out after 40 mins at 105 °C. This was used to produce PTGM nanoparticles. The reaction flask was allowed to cool to room temperature and then cold distilled water was added to the resulting suspension after 6 h. The suspension was then allowed to settle overnight as shown in Eq. (2) and then filtered, washed with distilled water and dried..

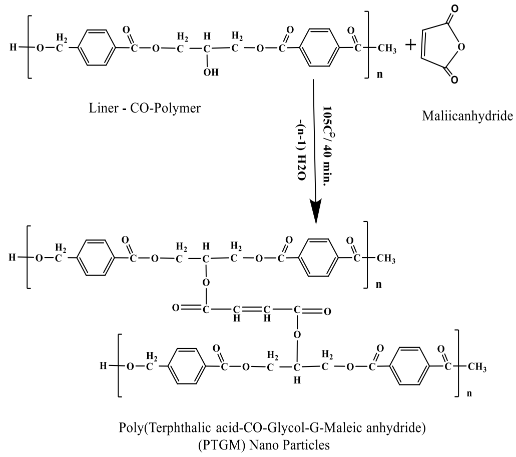

Equation 2. The second stage of the synthesis of graft PTGM nanoparticles

2. 2. Polymer Purification

Since the nanopolymers may be contaminated with trace amounts of unreacted solvent or monomers, they must be filtered. After separation, the synthesized nanopolymers are dissolved and precipitated using an appropriate solvent. According to the recommended protocol, a concentration of 5% is added while continuing to "stir" vigorously [10]. The polymer and solvent are miscible with the non-solvent. Once the solid polymer is formed, it is separated from the solution. To enhance the purity of the polymer, repeat the melting and re-emplacement process 3 times [11]. After cleaning, the nanopolymers are prepared for use. The new synthetic polymers are heated to 57 degrees Celsius and kept in a desiccator with a vacuum for processing and diagnostic testing [12].

2. 3. Adsorption Behavior of Grafted Nanopolymers

The process of adsorption of the new polymers onto dyes was studied to produce solutions containing Methyl orange dye (active ingredient). This was achieved by first preparing a solution of the dye in water (0.5 g) and then diluting it to 1000 mL to achieve a concentration of 500 ppm. From this concentrated solution, dilution solutions with concentrations of 1, 3, 5, and 7 ppm were prepared, all by taking an appropriate volume of the concentrated solution and then diluting it with 100 mL of water. The vials containing the solution consisting of the surface-adsorbed nanopolymer and the surface-adsorbed dye were left for 60 minutes and their absorbance was measured after 60 minutes. The solution came from a vibrator set at a temperature of 298K. Samples were then taken and the absorption of the solution was determined by observing the changes in the visible and ultraviolet spectra as time progressed. After determining the amount of dye (Methyl orange) adsorbed on the surface of the new polymer material, the following equation was established[13].

$Qe = (Co\text{-}Ce) * \frac{Vsol}{Wt}$	(3)

3. DISCUSSION and RESULTS

Nanopolymers were created through an esterification process and studied usingFT-IR, ^{1}H-NMR, and AFM. The first step is demonstrated in Figure 1: The spectrum of the linear copolymer's FT-IR is demonstrated in Figure 1. The spectrum has a strong, broad band at 3,423 cm^{-1} caused by the presence of OH in the copolymer, and a weak band at approximately 2902 cm-1 caused by the -OH of the carboxylic acid. Additionally, the band at around 2902 cm-$^{-1}$ is attributed to the -OH acid. The composition of CH sp3 and sp2 is 2544 and 2654 cm^{-1}, respectively, and the spectrum exhibits a strong association with the OC band of the ester band at around 1,726 cm^{-1}. The spectrum exhibits weak and sharp bands at 1597 cm^{-1} – 1158 cm^{-1} [14].The spectrum shows weak, but distinct bands between 1597 and 1158 cm^{-1} and a band between 1284 and 1259 cm^{-1} due to the C=C system of the benzene ring. Van states that the esterification of the oil (CO) is responsible for these bands. The spectrum is in agreement with the pattern of the linear copolymer that was proposed in the first step.

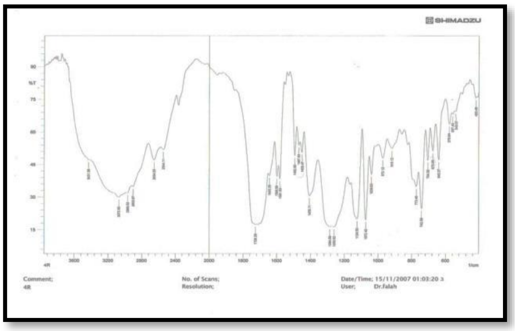

Figure 1. FTIR linear copolymer

Figure 2, ^{1}H-NMR spectrum shows the signal of the carboxylic acid group protons at 13.24 ppm and counts of each proton in the aromatic ring in the range of 7.53 - 8.10 ppm, while the signal is located at 6.27 - 6.46 ppm. The four methylene protons in the copolymer structure appear, the methyl protons double at 4.24-4.50 ppm, and the triplet signal from the alcohol protons appears at 3.44ppm. Our polymer was confirmed by this spectrum[5].

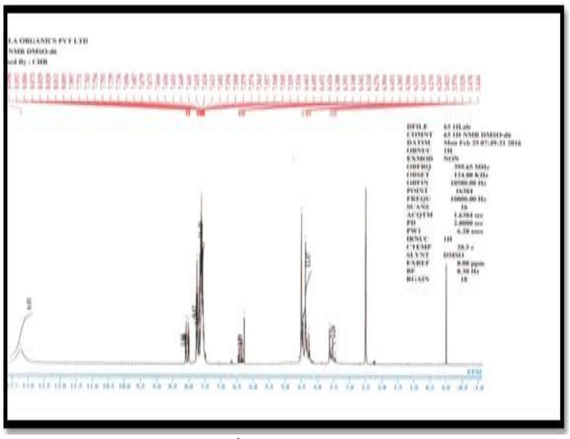

Figure 2. The ^{1}H-NMR spectrum of linear copolymer The individualized second stage polymer was created by second step infrared spectroscopy. **Figure 3** depicts the FT-IR spectrum of the copolymer, which exhibits numerous broad bands at 3550 cm^{-1} for alcohol -OH as well as aliphatic CH, aromatic C=H and Olefins. = CH at 3140 cm^{-1} and 3050 cm^{-1}, respectively, plus a strong, sharp band in place (1740 cm^{-1}) that is associated with the ester bond (C=O), a band inside of it that is linked with (CO) ester, and, based on the spectrum's composition.It can be deduced that the processed polymer has a structural composition similar to that proposed in the proposed structure[15, 16].

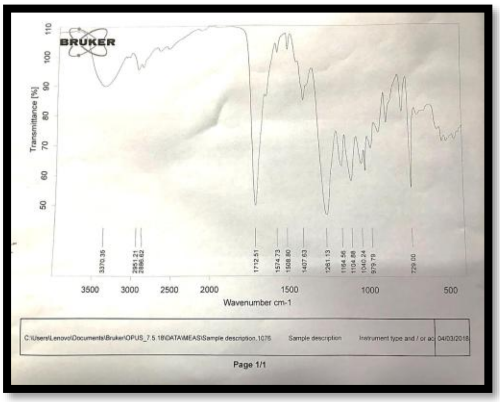

Figure 3. Graft co- polymer's FT-IR spectra

Figure 4, The ^{1}H-NMR spectrum demonstrates that DMSO has a signal at 2.5 ppm, multiple signals in the 3.5-4.8 ppm range, which are associated with the [CH2-OC = O, -CH = CH-] group, protons that have a chemical composition similar to that of aromaticity, as well as protons which are connected with the carboxylic acid. These protons are considered to have a single signal at 12.77 ppm...

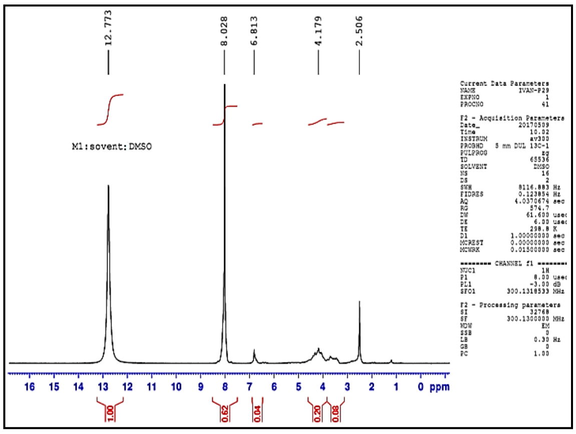

Figure 4. Graft spectrum of polymer ^{1}H-NMR

The prepared polymer was assessed using the first method of atomic force microscopy (AFM) for melting. From **Figure 5a,b,c,** the outer surface of the linear copolymer particles is demonstrated. The results revealed average roughness of the linear polymeric surface is 1.19nm, and the square root is 1.37nm, which implies that the darkness of the surface's roughness is dependent on the nanoparticles. Its consistency, regularity of the crystal system, average height and surface area of the particle are all demonstrated in **Figure 5A**, all of which are 4.80. **Table 1.** considers the overall percentage and various ratios of the common linear size of nanoparticles. The results demonstrate that the molecular width of the linear nanoparticles is 94.09, and **Figure 6**. demonstrates the different concentrations of the copolymer's linear particles in different sizes. The results demonstrate that these polymers are copolymeric nanoparticles, as illustrated below: Yin's Fig. (5A,B,C) The exterior of a building comprised of linear copolymer particles..

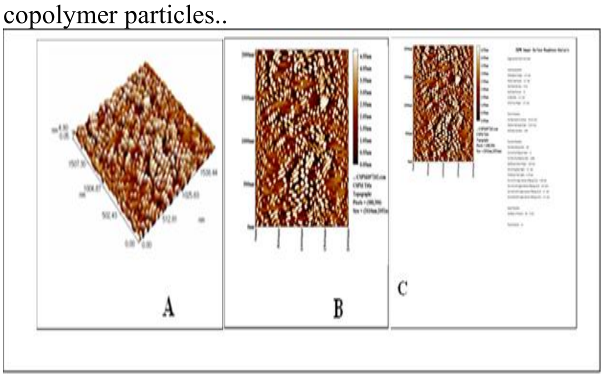

Figure 5. (A, B and C) The outer surface of the linear copolymer nanoparticle.

TABLE 1. The total rate of the particle sizes of the linear co-polymer nanoparticle and the different proportions of these volumes

Sample:1	**Code: Sample Code**
Line No.: lineno	Grain No.:139
Instrument: CSPM	Date:2018-04-23
Avg. Diameter: 94.09 nm	<=10% Diameter:75.00 nm
<=50% Diameter: 90.00 nm	<=90% Diameter:115.00 nm

Diameter (nm) <	**Volume (%)**	**Cumulation (%)**	**Diameter (nm) <**	**Volume (%)**	**Cumulation (%)**	**Diameter (nm) <**	**Volume (%)**	**Cumulation (%)**
75.0	7.19	7.19	100.0	8.63	68.35	125	1.44	93.53
80.0	12.95	20.14	105.0	7.19	75.54	130.	5.76	99.28
85.0	16.55	36.69	110.0	7.19	82.73	145	0.72	100.00
90.0	11.51	48.20	115.0	5.04	87.77			
95.0	11.51	59.71	120.0	4.32	92.09			

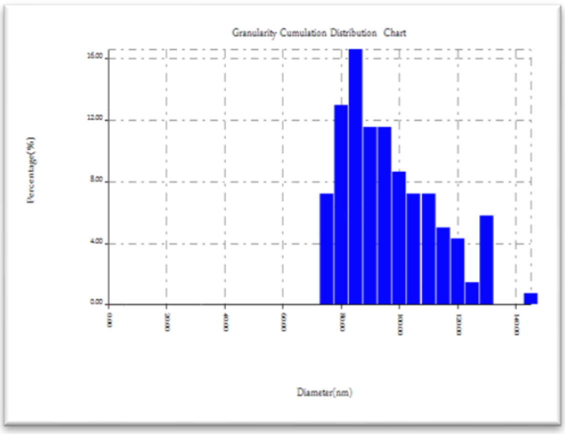

Figure 6. The diameters of linear co-polymer nanoparticles are distributed in varied ratios.

The particle size of the second smaller copolymer was determined using a two-steps method that involved the use of atomic force microscopy (AFM). This indicates that the size of the dark particles has a significant impact on the particles' roughness. The common crystal structure and consistent surface composition are demonstrated in Figure 7a. Table (2) calculates the average size of the copolymer nanoparticles as a whole and various percentages of this size. The results show that the molecular size of the copolymer grafted nanoparticles is 74.39nm. Figure (8) illustrates the distribution of different ratios of particle size of the copolymeric nanoparticles.

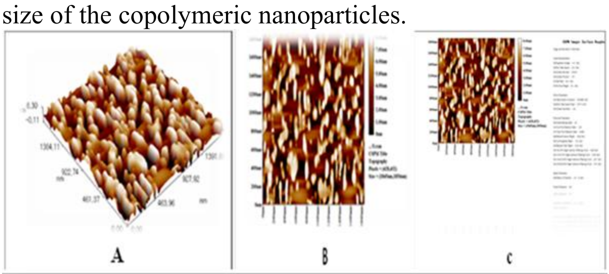

Figure 7. (A,B,C): Atomic force microscopy image of the grafted polymer showing the outer surface of the copolymer nanoparticle and some of its properties.

TABLE 2. The average rate of graft copolymer's particle sizes and the various percentages of these volumes.

Sample:1	**Code: Sample Code**
Line No.: lineno	Grain No.:208
Instrument: CSPM	Date:2019-05-31
Avg. Diameter: 74.39 nm	<=10% Diameter:0.00 nm
<=50% Diameter: 70.00 nm	<=90% Diameter:95.00 nm

Diameter (nm) <	**Volume (%)**	**Cumulation (%)**	**Diameter (nm) <**	**Volume (%)**	**Cumulation (%)**	**Diameter (nm) <**	**Volume (%)**	**Cumulation (%)**
55.00	10.58	10.58	85.00	7.69	75.96	115.0	1.44	98.56
60.00	12.98	23.56	90.00	6.73	82.69	120.0	0.48	99.04
65.00	10.10	33.65	95.00	4.81	87.50	125.0	0.48	99.52
70.00	12.50	46.15	100.0	4.33	91.83	140.0	0.48	100.00
75.00	7.21	53.37	105.0	2.88	94.71			
80.00	14.90	68.27	110.0	2.40	97.12			

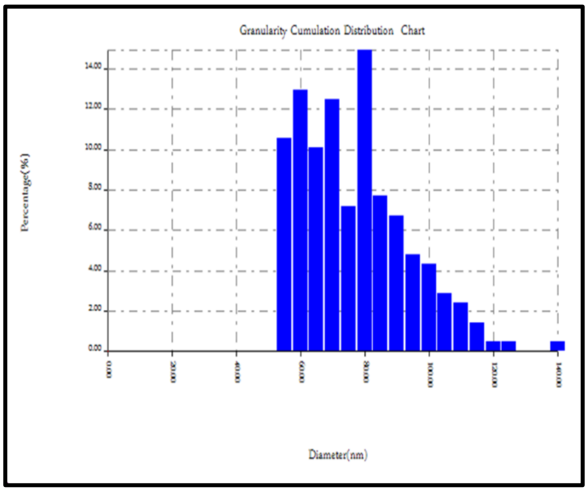

Figure 8. Distribution of the different ratios of the sizes of the graft co- polymer nanoparticles.

3. 1. Adsorption of Methyl orange

The titration graph is a representation of the relationship between absorption and concentration via a graph that is shown in Figure (10). Four different concentrations (1, 3, 5 and 7 ppm) of the (methyl orange dye) solution employed in the study were engaged to differentiate them. The absorption at these concentrations was recorded at their greatest wavelength as clarified in Figure 9 (max. = 418 nm).

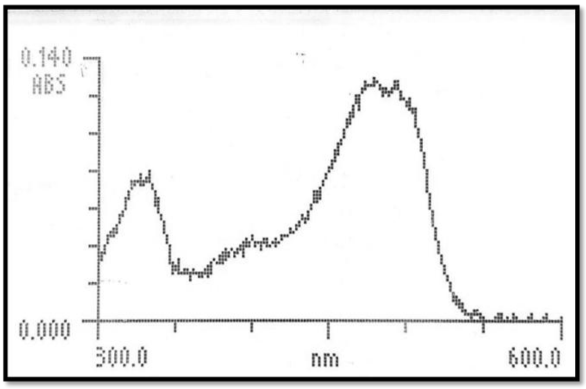

Figure 9. Maximum wavelength (λ max) for the (Methyl orange)

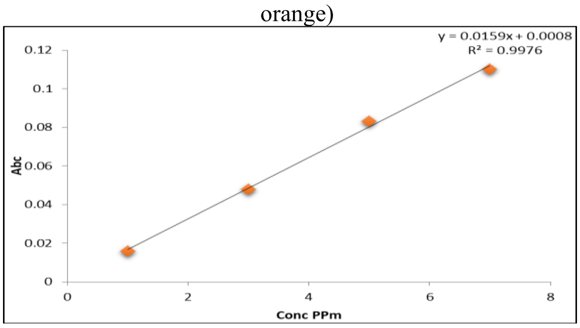

Figure 10. The calibration curve between absorption and concentration of methyl orange dye.

The effect of temperature on dye adsorption (methyl orange dye) on the surface of freshly prepared PTGM nanoparticles in the temperature range [298-308-318 K] is shown in Table 3. The data show that authors observed that the amount of orange G adsorbed on the surface of grafted PTGM particles decreased as the temperature increased [12]. The procedure is temperature-supporting. As the temperature increases, any physical association (requiring a low temperature) [17] decreases the rate of particle diffusion on the surface of PTGM nanoparticles [18]. This implies that there is a procedure by which the particles that are adsorbed by the layer are separated from it and reenter the liquid state [13]. as revealed in Figure 11.

TABLE 3. Effect of temperature on adsorption of methyl orange dye.

Conc.	**298K**		**308K**		**310K**	
	Ce	**Qe**	**Ce**	**Qe**	**Ce**	**Qe**
1	0.2641	0.7359	0.1383	0.8617	0.0754	0.9246
3	0.6415	2.3585	0.3899	2.6101	0.2012	2.7988
5	0.8301	4.1699	0.5157	4.4843	0.2641	4.4834
7	0.9559	6.0441	0.6415	6.3585	0.3270	6.6730

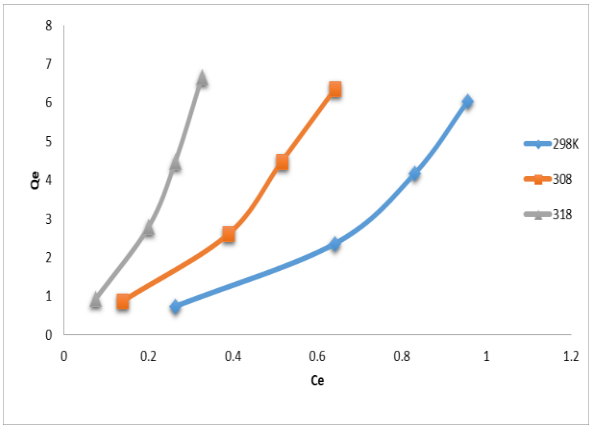

Figure 11. The effect of temperature on the polymer at concentrations (1, 3,5 and 7 ppm) and temperatures (298, 308 and 318)K.

3.2. Adsorption Isotherms

The association of the dye (Methyl orange) with the nanocopolymer was investigated, and the isotherms of relationship were determined. At a temperature of 298 K, as demonstrated in Figure (12), this demonstrates that the surface of the adsorbent is not uniform and that the general shape of the isotherm according to Giles' classification is similar to the Frendelsh principle of type S1 [19, 20].

TABLE 4. adsorption of methyl orange on the roof of the nano copolymer at a temperature of 298K.

Temp.	Conc. (ppm)	Ce	Qe
298K	1	0.2641	0.7359
	3	0.6415	2.3585
	5	0.8301	4.1699
	6	0.9559	6.0441
	7	0.2641	0.7359

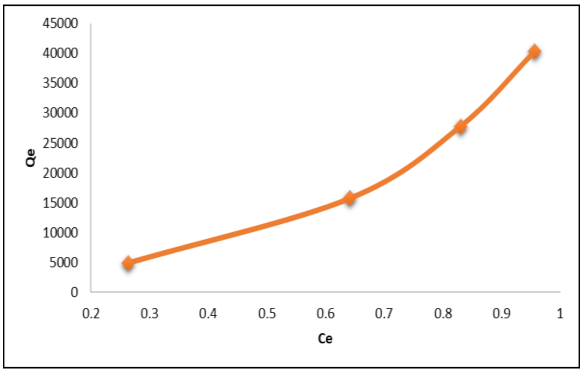

Figure 12. Adsorption isotherm methyl orange dye on the roof of graft co-polymer.

3.2. Freundlich's Adsorption Equation

The Freundlich equation is one of the most significant equations used to describe the attachment of substances to different surfaces. Many equations exist. The Freundlich equation for adsorption is one of the most significant isotherms, and its expression is as follows [21, 22]:

$$Qe = Kf * \frac{Cel}{n} \tag{4}$$

When entering the logarithm on the equation No. (4), the equation becomes as shown in Equation No. (5) and through it the adsorption data of the dyes were processed according to the following linear equation of the logarithmic Freundlich equation[23, 24]:

$$LogQe = Log\ Kf + \left(\frac{1}{n}\right) Log\ Ce \tag{5}$$

Ce: the equilibrium concentration of the adsorbent in (mg/L). Qe: the amount of adsorbent at the equilibrium (mg/g). Kf and n are isothermal constants that represent the amplitude and density of adsorption, respectively. Table (5) and Figure (13) determine the degree to which disperse red 1 coating is adsorbed on the surface of the newly created nanopolymer using the Freundlich equation. If ore connect Log Qe with Log Ce, we will get a direct line as illustrated below..

TABLE 5. adsorption of Methyl orange dye on the roof of a synthetic graft co-polymer at 298 K (By applying the Freundlich equation).

	298K		308K		318K	
Con.	LogCe-	LogQe	LogCe-	LogQe	LogCe-	LogQe
1	0.5782	-0.1331	0.8591	-0.0646	1.1226	-0.0344
3	0.1982	0.3726	0.409	0.4166	0.6963	0.4468
5	0.0808	0.6201	0.2876	0.6516	0.5782	0.6754
7	0.0195	0.78133	0.1928	0.8033	0.4854	0.8243

TABLE 6. Freundlich constant value of adsorbed on roof of graft co-polymer at (298K)

Temp.	-N	Kf	R2
298K	0.7566	284315.1486	0.9866
308K	0.7003	82186.4080	0.9725
318K	0.6282	43641.5332	0.9574

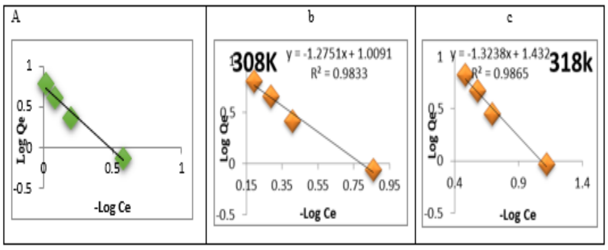

Figure 13. The Freundlich isothermal absorbs the methyl orange dye on the surface of the new graft co-polymer at a) 298 K, b) 308 K, c) 318 K.

4. CONCIUSION

This new nano-doped copolymer was synthesized by reacting terephthalic acid with glycerol to form a linear copolymer and adding malic anhydride in the first step. This is how the nano-doped copolymer was prepared. Our study showed that the nano-grafted copolymer was very effective in removing dyes and pollutants at a temperature of 25 degrees and neutral acid by adsorbing the effective methyl orange dye on the adsorbent surface. It has a crystalline structure.

5. REFERENCES

1. Z. N. Jawad, K. I. Abd, B. K. AL-Ghanimi, and M. N. Al-Baiati, "Using A Novel Nano Chitosan-Ampicillin Drug to Study the Effective Range of Drug Level Outside the Affected Cells," *HIV Nursing,* vol. 23, no. 2, pp. 953–956-953–956, 2023.
2. K. T. Rashid, H. M. Alayan, A. E. Mahdi, M. N. Al-Baiati, H. S. Majdi, I. K. Salih, J. M. Ali, and Q. F. Alsalhy, "Novel water-soluble poly (terephthalic-co-glycerol-g-fumaric acid) copolymer nanoparticles harnessed as pore formers for polyethersulfone membrane modification: permeability–selectivity tradeoff Manipulation," *Water,* vol. 14, no. 9, pp. 1507, 2022.
3. S. Hassan, and B. A. Ganai, "Deciphering the recent trends in pesticide bioremediation using genome editing and multi-omics approaches: A review," *World Journal of Microbiology and Biotechnology,* vol. 39, no. 6, pp. 151, 2023.
4. B. K. AL-Ghanimi, Z. N. Jawad, and M. N. Al-Baiati, "Study of the Effective Range of Drug Level Using a Nano Chitosan-Mefenamic Acid," *HIV Nursing,* vol. 23, no. 2, pp. 260–263-260–263, 2023.
5. [5] S. Bayda, M. Adeel, T. Tuccinardi, M. Cordani, and F. Rizzolio, "The history of nanoscience and nanotechnology: from chemical–physical applications to nanomedicine," *Molecules,* vol. 25, no. 1, pp. 112, 2019.
6. T. Shindhal, P. Rakholiya, S. Varjani, A. Pandey, H. H. Ngo, W. Guo, H. Y. Ng, and M. J. Taherzadeh, "A critical review on advances in the practices and perspectives for the treatment of dye industry wastewater," *Bioengineered,* vol. 12, no. 1, pp. 70-87, 2021.
7. D. Banerjee, "Water pollution and human health," 2017.
8. M. Sajid, M. K. Nazal, N. Baig, and A. M. Osman, "Removal of heavy metals and organic pollutants from water using dendritic polymers based adsorbents: a critical review," *Separation and Purification Technology,* vol. 191, pp. 400-423, 2018.
9. C. I. Idumah, "Recently emerging advancements in polymeric nanogel nanoarchitectures for drug delivery applications," *International Journal of Polymeric Materials and Polymeric Biomaterials,* vol. 73, no. 2, pp. 104-116, 2024.
10. Q. Lei, J. Zhao, F. He, X. Zhao, and J. Yin, "Preparation of Poly (Ionic Liquid) Microbeads via Cooling-Assisted Phase Separation Method," *Macromolecular Rapid Communications,* vol. 42, no. 17, pp. 2100275, 2021.
11. A. F. Hasan, M. M. Kareem, and M. N. Al-Baiati, "Synthesis a novel nano co-polymer and using as carrier drug system," *International Journal of Pharmaceutical Research,* vol. 12, no. 4, pp. 850-589, 2020.
12. H. E. Salman, and N. J. Hussein, "Synthesis of zinc-aluminum layered double hydroxides and application of adsorption for nitrate from water." p. 012070.
13. K. G. Akpomie, F. A. Dawodu, and K. O. Adebowale, "Mechanism on the sorption of heavy metals from binary-solution by a low cost montmorillonite and its desorption potential," *Alexandria Engineering Journal,* vol. 54, no. 3, pp. 757-767, 2015.
14. N. Boukabcha, A. Benmohammed, M. H. M. Belhachemi, M. Goudjil, S. Yahiaoui, Y. Megrouss, A. Djafri, N. Khelloul, Z. D. Benyehlou, and A. Djafri, "Spectral investigation, TD-DFT study, Hirshfeld surface analysis, NCI-RDG, HOMO-LUMO, chemical reactivity and NLO properties of 1-(4-fluorobenzyl)-5-bromolindolin-2, 3-dione," *Journal of Molecular Structure,* vol. 1285, pp. 135492, 2023.
15. M. N. Bahjat AL-Baiati, "Synthesis of new Corrosion Inhibitor from Nano-Polymer and study its adsorption on carbon steel at different Temperatures," *Egyptian Journal of Chemistry,* vol. 65, no. 11, pp. 691-705, 2022.
16. H. M. Awwad, A. F. Alkaim, and M. N. Al-Baiati, "Adsorption of Maxilon Blue (GRL) from Aqueous Solutions by using a novel nano-composite polymer." p. 012095.
17. S. N. Shankar, D. R. Dinakaran, D. K. Chandran, G. Mantha, B. Srinivasan, and U. P. N. Kannaian, "Adsorption kinetics, equilibrium and thermodynamics of a textile dye V5BN by a natural nanocomplex material: Clinoptilolite," *Energy Nexus,* vol. 10, pp. 100197, 2023.
18. A. A. Jalil, S. Triwahyono, S. H. Adam, N. D. Rahim, M. A. A. Aziz, N. H. H. Hairom, N. A. M. Razali, M. A. Abidin, and M. K. A. Mohamadiah, "Adsorption of methyl orange from aqueous solution onto calcined Lapindo volcanic mud," *Journal of Hazardous Materials,* vol. 181, no. 1-3, pp. 755-762, 2010.
19. C. H. Giles, D. Smith, and A. Huitson, "A general treatment and classification of the solute adsorption isotherm. I. Theoretical," *Journal of colloid and interface science,* vol. 47, no. 3, pp. 755-765, 1974.
20. H. M. Awwad, A. M. Aljeboree, M. N. Al-Baiati, and A. F. Alkaim, "Synthesis and Characterization of Nano-composite co-polymer: Adsorption and Removal Studies of vitamin B12 from Aqueous Solutions." p. 012057.
21. S. Gita, A. Hussan, and T. Choudhury, "Impact of textile dyes waste on aquatic environments and its treatment," *Environ. Ecol,* vol. 35, no. 3C, pp. 2349-2353, 2017.
22. Z. M. Shaker, H. I. Salman, and M. N. AL-Baiati, "Removal of reactive yellow 145 dye pollutant from wastewater by using a nano surface."
23. A. R. Khudhair, S. T. H. Sherazi, and M. N. Al-Baiati, "Adsorption of methylene blue from aqueous solutions by using a novel nano co-polymer."
24. A. Ashour, M. Kareem, and M. N. Al-Baiati, "Improving Asphalt Binder Properties Using Recycled Polyethylene Terephthalate and Natural Liquid Rubber." p. 012107.

Arabic Abstract

تم تصنيع البوليمرات النانوية المطعمة من خلال عملية الأسترة، حيث كانت الخطوة الأولى هي تحضير بوليمر مشترك خطي عن طريق تفاعل حمض التريفثاليك مع الجلسرين. بعد ذلك، تمت إضافة كمية معينة من أنهيدريد المالئيك إلى محلول البوليمر الخطي الناتج للحصول على جسيمات PTGM النانوية المطعمة. تم تشخيص وتشخيص البوليمرات النانوية باستخدام التحليل الطيفي FT-IR، ^{1}H-NMR، ومجهر القوة الذرية (AFM). كان متوسط ارتفاع الجسيمات 8.3 نانومتر وتعرض لثلاث درجات حرارة مختلفة (298، 308، و318 كلفن). تمت دراسة أربعة تراكيز مختلفة (1، 3، 5، و 7 جزء في المليون) من صبغة (الميثيل البرتقالي) ومن الواضح أنها تلعب دوراً حيوياً في عملية الامتزاز. أظهرت النتائج التجريبية أن امتزاز صبغة (الميثيل البرتقالي) انخفاض في متوسط مساحة السطح والسبب في ذلك انه امتز البوليمر النانوي عدد كبير من الجزيئات مع زيادة درجة الحرارة، مما يدل على أن العملية ماصة للحرارة. ولوحظ أيضًا أن البوليمرات النانوية عالية الفعالية نجحت في إزالة صبغة الميثيل البرتقالي من المحاليل المائية.

Pure Sciences International Journal of kerbala

Year: 2025 Volume : 2 Issue : 5 ISSN: 6188-2789 Print 3005 -2394 Online

2025, Volume 2, Issues 5 PSIJK 27-31

Pure Sciences International Journal of Kerbala
Journal Homepage:https://journals.uokerbala.edu.iq/index.php/psijk

Histochemical study for Effect of *Asparagus officinalis L.* roots extract on ovarian histology in female rat with Polycystic Ovary Syndrome

Farah Jawad Al-masoudi [1*], Ashwaq Kathum Obeid [2], Alaa Hussein Al-Safy [3]

[1] *Biomedical engineering Department / College of engineering / Kerbala University / Karbala / Iraq.*
[2,3] *Biology Department / College of Education for pure sciences / Kerbala University / Karbala / Iraq.*

P A P E R I N F O

Received: 23 September 2024
Accepted: 31 December 2024
Published: 31 March 2025

Keywords:
PCOS, asparagus officinalis L., collagen fibers, Trichrome stain, ovarian histology

A B S T R A C T

Polycystic ovarian syndrome (PCOS) is characterized by several symptoms, such as hirsutism hyperandrogenism, amenorrhea, anovulation, sterility, as well as metabolic and endocrine disorders. This study was conducted to evaluate the efficacy of an extract from the roots of *Asparagus officinalis L.* in treating female rats with induced polycystic ovarian syndrome. In this study, the impact of 400mg/kg of *asparagus officinalis L.* roots extract on the polycystic ovarian syndrome was examined over a period of 28 days in order to scrutinize the effects of asparagus officinalis L. roots extract on letrozole-induced polycystic ovary syndrome.
Thirty female albino rats were chosen. They were divided into five groups. Group 1 Control, Group 2 asparagus officinal is Extract 400 mg/ kg for 28 days, Group 3 is the PCOS inducer. Rats were given letrozole (1 mg/kg) orally for 28 days in a 0.5% Carboxy-Methylcellulose (CMC) solution. Group 4 is a treatment group in which the animals were dosed with letrozole for 28 days. After that, they were dosed with asparagus root extract for another 28 days, and Group 5 is the preventive group, which received asparagus root extract for 28 days. Then, it was dosed with letrozole for the same period. The Trichrome stain showed results low in stroma and collagen fibers of the structure ovaries in all groups, including control except the PCOS group that indicates a high presence of collagen. In addition to the number of primary, antral, and graphene follicles increased considerably. The treatment and preventative groups showed fewer cystic follicles than the PCOS group. The findings reveal decrease in collagen fibers by asparagus root extract. Therefore, it speeds up oogenesis and early cell divisions.

1. INTRODUCTION

Chronic anovulation, hyperinsulinemia [1], and elevated androgen levels are all factors in PCOS, a group of reproductive problems that primarily affect women. [2] This illness affects the metabolic and endocrine systems,[3] but its underlying etiology is still unknown. [4,5] It is the predominant cause of female anovulatory infertility. [6], an increase in ovarian volume, follicle collecting, and a lack of corpus luteum. [7,8]. Several therapeutic medicines, including metformin [9,10,11], glucocorticoids, aromatase inhibitors, and clomiphene citrate, have been recommended for the treatment of the PCOS. [12,13,14]. However, a number of negative effects, such as nausea, vaginal bleeding, and abdominal pain, are associated with these medications. [15,16]. Therefore, people prefer herbal remedies to the pharmaceuticals mentioned above for treatment of the PCOS. [17,18,19]. In reality, *asparagus officinalis L.* (AR) is a food crop that has been farmed for its therapeutic properties by a number of ancient cultures. As a result, the crop has a long and interesting history. It is also a valuable plant because of its medicinal and nutraceutical properties. [20]. *asparagus officinalis L.* has been used to treat cardiac issues, palpitations, dyspnea, and toothaches. Saponins, one of its main constituents, are essential for the anti-tumor action and lowering the risk of diseases including obesity, diarrhea, and constipation. [21]. *asparagus officinalis L.* roots have diuretic and potent cardiac sedative diuretic and powerful cardiac sedative effects are present in A. officinalis roots. [22,23]. This study was conducted to evaluate the efficacy of an extract from the roots of Asparagus officinalis L. in treating female rats with induced polycystic ovarian syndrome.

*Corresponding Author Institutional Email:
farah.j@uokerbala.edu.iq (Farah Jawad Al-masoudi)

2. MATERIALS AND METHODS

2.1. Experimental Animals

In this experiment, thirty female adult albino rats were employed weighing 180-230 g. They were bought at the pharmacy college Karbala University and they were kept in breeding cages with meticulous care. The rats were divided equally into five groups, with six rats (n=7/group), to guarantee statistical significance and fairness. Group 1 Normal Control, Group 2 Animals were received *asparagus officinalis* roots extract 400 mg/ kg up to 28 days, Group 3 animals with induced the PCOS by letrozole up to 28 days, Group 4 is a treatment group in which the animals were dosed with letrozole up to 28 days, Afterwards, they were dosed with asparagus root extract up to another 28 days, and Group 5 is the preventive group, which received asparagus roots extract for 28 days. Then, it was dosed with letrozole for the same period.

2.2. Induction the pcos and prepare asparagus officinalis l. extract

To induce PCOS, rats were given letrozole (1 mg/kg bw) orally up to 28 days in a 0.5% Carboxy-Methylcellulose (CMC) solution. [24]. However, the roots were procured from Iraqi markets and fully dried in a laboratory before being pulverized into powder, The resultant powder was mixed with 70% ethyl alcohol for 24 hours at room temperature to produce a solid extract, after filtering, the mixture was dried for 48 hours. The 400 mg/kg concentration of the solid extract was then diluted in 1 cc of distilled water. The solutions were kept in a refrigerator until use [25].

2.3. Histological Study

After 24 hours from the last day of the experiment, rats were given a 3-5 minute chloroform-soaked cotton sedation. Ovaries were dissected, then fixed by 10% formalin for 48 hours, and processed as tissue before being employed in study.

2.4. Statistical Analysis

For the presentation of the results, standard error of the mean (SEM) is employed. ANOVA is a comparison of statistical variances between groups. P 0.05 served as the threshold for statistical significance.

3. RESULTS and DISCUSSION

The Masson’s trichrome stain showed results low in stroma and collagen fibers of the structure ovaries in all groups, including the control one **Figure 1,2,4,5** except the PCOS group that indicates a presence of fibrosis. **Figure 3**. Due to the absence of corpus luteum and antral follicles, the mean number of primary follicles in the PCOS group fell in comparison to control and other groups, whereas the mean number of cystic follicles in the PCOS group increased considerably in comparison to other groups. While corpus luteum and antral follicle counts significantly increased in the treatment and prevention groups, the average number of cystic follicles sharply fell in both. Additionally, there was a rise in the quantity of ovarian follicles in the group consuming Asparagus roots extract **TABLE 1.** Letrozole, an aromatase inhibitor, was administered to female Wistar rats in the study to induce polycystic ovarian syndrome. [26]. The collagen fiber density in the control group and the other groups that received 400 mg of Asparagus root extract decreased, according to the results of histological sections stained in trichrome. In contrast, with including the asparagus group without cyst formation, the therapeutic group and the preventive group, compared with the cyst formation group, which was characterized by fibrosis around the cystic follicles and the stroma. The strong staining in the ovarian cortex is also attributed to an increase in the theca externa layer because it is composed of collagen fibers, which led to its deposition in the ovarian cortex [27].

When ovarian follicles grow and develop, the connective tissue's constituents, particularly the forms of collagen around them, go through significant modifications [28].PCOS is characterized by abnormal collagen synthesis and increased ovarian stroma volume and density [29].In this case, the ovary is characterized by an increase in androgen production in the ovary with a thickness of the tunica albuginea and the appearance of fibrous ligaments in the ovarian cortex consisting of many cystic vesicles [30]. Additionally, the extract from asparagus roots contained a variety of amino acids, vitamins, minerals, and estrogenic compounds that promoted follicle growth and maturation and decreased fibrosis. [31] Such substances as quercetin, tryptophan, and arginine, [32] which function as intermediary factors to activate the activity of hormones, also regulate the action of hormones. Granulosa cells also help ovarian follicles differentiate and expand by secreting estrogen, which controls its activity and thins the integumentary layer [20,33].

These results agree with those from the preceding studies [34,35,36]. The results of histopathological measurements in the group of animals treated with letrozole in which polycystic ovaries were induced showed a significant decrease ($P<0.05$) in the numbers of ovarian follicles and corpus luteum and a significant increase ($P<0.05$) in the number of cystic follicles. It is an aromatase inhibitor, which negatively affects hormone levels, thus leading to interruption of ovulation and infertility of the ovary [37]. The table also offered a significant increase ($P<0.05$) in the total number of ovarian follicles and the corpus luteum and a significant decrease ($P<0.05$) in the number of cystic follicles for the groups treated with asparagus ovarian,The reason for this increase is due to the properties of the asparagus root extract from the effective and biologically active compounds, as quercetin promotes the growth of ovarian follicles [38], and arginine and aspartic acid participate in the formation and maturation of eggs due to the stimulatory ability in the response of the pituitary gland that releases gonadal hormones [39,40]. Conclutoin asparagus showed helpful effects in letrozole induced pcos in female wistar rats. Its effect was comparable to that of clomiphene citrate, most widely used treatment for ovulation induction in pcos condition. These results suggest that asparagus roots may be a potential natural supplement for promoting the health of female reproductive systems. It is a relevant article and participate in genuine remedies for problems in this sector generally.

TABLE 1. The influence of *asparagus officinalis L.* on ovarian follicle numbers in adult female rats.

Parameters	control	Asperges	PCOS	Treatment	preventive
Primodial F.	5.3 ± 0.21^{b}	6.5 ± 0.22^{a}	1.84 ± 0.26^{e}	4.6 ± 0.20^{c}	3.67 ± 0.21^{d}
Primary F.	4.33 ± 0.21^{b}	5.5 ± 0.22^{a}	1.33 ± 0.21^{e}	3.66 ± 0.21^{c}	2.67 ± 0.21^{d}
Secondary F.	3.3 ± 0.21^{b}	4.6 ± 0.21^{a}	0.67 ± 0.21^{e}	2.8 ± 0.17^{bc}	1.67 ± 0.21^{d}
Graphain F.	2.5 ± 0.22^{b}	3.5 ± 0.22^{a}	0.50 ± 0.22^{e}	1.83 ± 0.17^{c}	1.17 ± 0.17^{d}
Corpus L	4.5 ± 0.22^{b}	5.66 ± 0.21^{a}	0.33 ± 0.21^{e}	3.83 ± 0.17^{c}	2.83 ± 0.17^{d}
Cysts F.	0 ± 0.00^{d}	0 ± 0.00^{d}	5.83 ± 0.31^{a}	1.66 ± 0.33^{c}	3.50 ± 0.34^{b}

The values are displayed as mean ±SD, values in the same column with different letters, statistically significant (P <0.05)

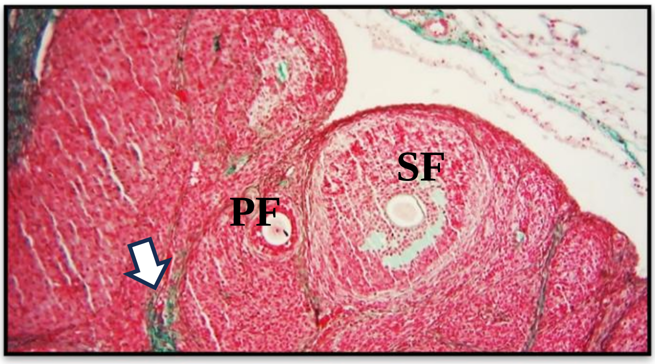

Figure 1. Histological section in ovaries in control group Shows less of stroma (arrow)secondary follicle (SF), Primary follicle (PF) (masson trichrome stain X10).

Figure 2. Histological section in ovaries in asparagus group Shows graafian follicle (GF), corpus luteum (CL) (masson trichrome stain X10).

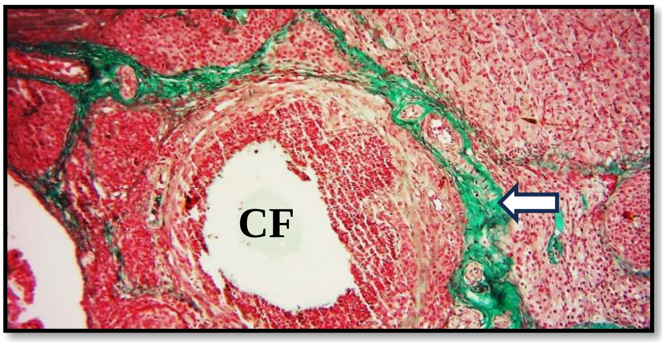

Figure 3. Histological section in ovaries in PCOS group Shows aggregation of stroma plenty (collagen fibers) (arrow), Cysts follicle (CF) (masson trichrome stain X10).

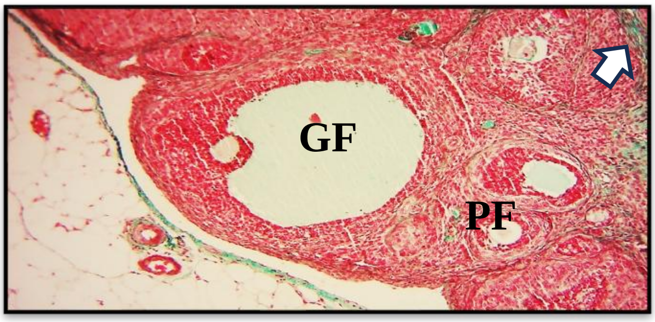

Figure 4. Histological section in ovaries in treated group with asparagus Shows less of stroma (collagen fibers) (arrow), graafian follicle (GF), Primary follicle (PF) (masson trichrome stain X10).

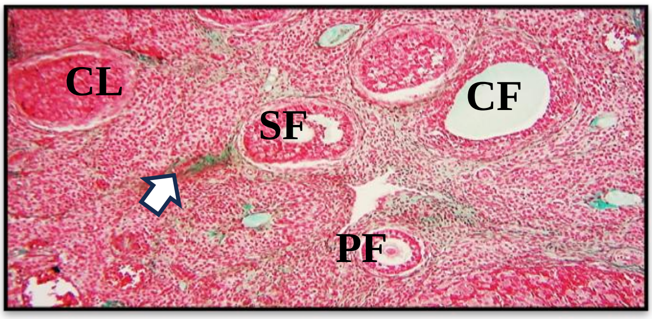

Figure 5. Histological section in ovaries in preventive group Shows less of stroma (collagen fibers) (arrow), secondary follicle (SF), Primary follicle (PF), corpus luteum (CL) , Cysts follicle (CF) (masson trichrome stain X10).

4.REFERENCES

1. Hassan, M. F., Jawad, M. A., & Al-yasiry, R. Z. Does Insulin Resistance (IR) Have an Impact on The Reproductive and Fertility Potential in Polycystic Ovary Syndrome (PCOS) Women?. Maaen Journal for Medical Sciences, 2(1), (2023). 3.
2. Ali, M. M., Ghazi, W., & Abboud, A. H. Prevalence of anovulation in subfertile women in Kerbala 2012, a descriptive cross-sectional study. Al-Kufa University Journal for Biology, 6(2):(2014).
3. Talib, Z. R., Hassan, A. H., Jawad, H. J., & AbdulWahid, H. H. (2023). EVALUATION CHANGES OF GHERLIN AND LEPTIN ON POLYCYSTIC OVARY SYNDROME IN IRAQ. Ann. For. Res, 66(1), (2023): 1322-1331..
4. Zehravi, M., Maqbool, M., & Ara, I. Polycystic ovary syndrome and infertility: an update. International journal of adolescent medicine and health, 34.2,(2022): 1-9.
5. Al-Tu'ma, F., HadiFarhan, N., & Al-Safi, W. G. Association between fat mass and obesity Geners9939609 polymorphism with PCOS women in Iraqi population. Ijppr. Human, 5.1(2015): 62-72.
6. Nirav, O. R. "Current Management on PCOS (Polysystic Ovary syndrome)." Stein-LeventhalSyndrome, Investigation in Gynecology Research and womens Health (2017): 46-28.
7. Kadhim, S. M., Al-Fartusie, F. S., & Klichkhanov, N. K. Evaluation of Adiponectin and Hepcidin with some Biochemical Parameters in Sera of Women with Polycystic Ovary Syndrome. Al-Mustansiriyah Journal of Science, 34.1(2023):52-57.
8. Marbut, M. M., Awwad, N. Y., Yousif, M. N., & Ahmed, M. S. Hormonal assessment in women with polycystic ovary syndrome in Tikrit city. Journal of Madenat Alelem University College, 11(1),(2019):1-9.
9. Hussein, M. R., Ouda, M. H., Abdulwahid, H. H., & Abo Al-Maali, H. M. Association of genetic polymorphism of LKB/STK11 with therapeutic response of metformin in women with polycystic ovary syndrome. Eur J Mol Clin Med, 7(3),(2021): 539-552.
10. Hussein, M. R., Ouda, M. H., HM, A. A. M., & Abdulwahid, H. H. EFFECT OF GENETIC POLYMORPHISM OF LKB/STK11 WITH THERAPEUTIC RESPONSE TO METFORMIN IN POLYCYSTIC OVARY SYNDROME WOMEN IN KERBALA PROVINCE. Biochemical & Cellular Archives, 20(2).(2020).
11. Mohammad Al-Khafaje, M. Comparison between The Efficacy of Combined Metformin–Letrazole with Metformin–Clomiphene Citrate in Polycystic Ovarian Syndrome. Kerbala Journal of Medicine, 9(2),(2016), 2462-2469.
12. Al-Hasnawi, N. K., Hadi, D., Alnasrawi, T. H., & Althabet, Z. A. Study the effect of Kisspeptin 1 on polycystic ovarian syndrome PCOS and obesity in Iraqi women patients. In AIP Conference Proceedings (Vol. 2787, No. 1). AIP Publishing.(2023).
13. AL-Ma'aroof, S. F. M., Ahmed, M. M., & Mansor, N. H. Studying the effect of ovulation stimulation by using clomiphene citrate on serum level of tumor necrosis factor alpha and interleukin-1ß in sub-fertile women in Holy Kerbala Province. J Contemp Med Sci| Vol, 2(6),(2016): 59-62.
14. Manna, M. J., Jabur, M. S., Alsabah, A. S., & Baqir, L. S. A Review on new drugs for treatment of Polycystic Ovarian Syndrome. Karbala Journal of Pharmaceutical Sciences, 1(21):(2023).
15. Mohammad Al-Khafaje, M. Comparison between The Efficacy of Combined Metformin–Letrazole with Metformin–Clomiphene Citrate in Polycystic Ovarian Syndrome. Kerbala Journal of Medicine, 9(2),(2016), 2462-2469.
16. Pachiappan, S., Matheswaran, S., Saravanan, P. P., & Muthusamy, G. Medicinal plants for polycystic ovary syndrome: A review of phytomedicine research. Int J Herb Med, 5(2), (2017):78-80.
17. Hamza, A. H., AlBishri, W. M., & Alfaris, M. H. Effect of Vitex agnus-castus plant extract on polycystic ovary syndrome complications in experimental rat model. Asian Pacific Journal of Reproduction, 8(2), (2019):63-69.
18. Al-masoudi, F. J., & Jawad, A. K. Promising histological and functional effects of asparagus officinalis L. roots extract on letrozole induced polycystic ovary syndrome in female rat. Journal of Survey in Fisheries Sciences, 10(3S),(2023):4786-4792.
19. Alkalby, J., & Hamzah, F.Ameliorative effect of fenugreek on sex hormones in polycystic ovary syndrome female rats induced by letrozole. Kufa Journal For Veterinary Medical Sciences, 8(2), (2017):24-32.
20. Calcaterra, V., Verduci, E., Cena, H., Magenes, V. C., Todisco, C. F., Tenuta, E., ... & Zuccotti, G. Polycystic ovary syndrome in insulin-resistant adolescents with obesity: the role of nutrition therapy and food supplements as a strategy to protect fertility. Nutrients, 13(6), (2021):1848.
21. Mahood, R. A. H. Effects of Pimpinella anisum oil extract on some biochemical parameters in mice experimentally induced for human polycystic ovary syndrome. Journal of Biotechnology Research Center, 6(2), (2012): 67-73.
22. Lee, J. W., Lee, J. H., Yu, I. H., Gorinstein, S., Bae, J. H., & Ku, Y. G. Bioactive compounds, antioxidant and binding activities and spear yield of Asparagus officinalis L. Plant foods for human nutrition, 69, (2014): 175-181.
23. Abedi, H. A., Jahromi, H. K., Sadeghi, N., Amjadi, S. P., & Jahromi, Z. K. Evaluating the effect of aqueous extract of the roots of native edible asparagus in Iran (Asparagus officinalis L) on the concentration of liver factors in male rats treated with cadmium chloride. Journal of Fundamental and Applied Sciences, 8(4), (2016): 2008-2022.
24. Motoki, S., Tang, T., Taguchi, T., Kato, A., Ikeura, H., & Maeda, T. Distribution of rutin and protodioscin in different tissue parts of asparagus (Asparagus officinalis L.). HortScience, 54(11), (2019):1921-1924.
25. Wang, M. X., Yin, Q., & Xu, X.A rat model of polycystic ovary syndrome with insulin resistance induced by letrozole combined with high fat diet. Medical science monitor: international medical journal of experimental and clinical research, 26, (2020): e922136-1.
26. Hosseinkhani, A., Asadi, N., Pasalar, M., & Zarshenas, M. M. Traditional Persian medicine and management of metabolic dysfunction in polycystic ovary syndrome. Journal of traditional and complementary medicine, 8(1), (2018), 17-23.
27. Jashni, H. K., Jahromi, H. K., Ranjbary, A. G., Jahromi, Z. K., & Kherameh, Z. K. Effects of aqueous extract from Asparagus officinalis L. roots on hypothalamic-pituitary-gonadal axis hormone levels and the number of ovarian follicles in adult rats. International Journal of Reproductive BioMedicine, 14(2), (2016): 75.
28. Tamadon, A., Hu, W., Cui, P., Ma, T., Tong, X., Zhang, F., ... & Feng, Y. How to choose the suitable animal model of polycystic ovary syndrome?. Traditional Medicine and Modern Medicine, 1(02), (2018):95-113.
29. Vlieghe, H., Leonel, E. C., Asiabi, P., & Amorim, C. A. The characterization and therapeutic applications of ovarian theca cells: An update. Life sciences, 317, (2023), 121479.
30. Auersperg, N., Maines-Bandiera, S. L., Dyck, H. G., & Kruk, P. A. Characterization of cultured human ovarian surface epithelial cells: phenotypic plasticity and premalignant changes. Laboratory investigation; a journal of technical methods and pathology, 71(4),(1994): 510-518.

31. Clément, F., Monniaux, D., Thalabard, J. C., & Claude, D. Contribution of a mathematical modelling approach to the understanding of the ovarian function. Comptes rendus. Biologies, 325(4), (2002): 473-485.
32. Papachroni, K. K., Piperi, C., Levidou, G., Korkolopoulou, P., Pawelczyk, L., Diamanti-Kandarakis, E., & Papavassiliou, A. G. Lysyl oxidase interacts with AGE signalling to modulate collagen synthesis in polycystic ovarian tissue. Journal of cellular and molecular medicine, 14(10), (2010): 2460-2469.
33. Guo, Q., Wang, N., Liu, H., Li, Z., Lu, L., & Wang, C. The bioactive compounds and biological functions of Asparagus officinalis L.–A review. Journal of Functional Foods, 65, (2020):103727.
34. Cuiling, L., Wei, Y., Zhaoyuan, H., & Yixun, L. Granulosa cell proliferation differentiation and its role in follicular development. Chinese Science Bulletin, 50,(2005): 2665-2671.
35. Alam, M. H., & Miyano, T. Interaction between growing oocytes and granulosa cells in vitro. Reproductive medicine and biology, 19(1), (2020): 13-23.
36. Badawi, A. M., Ebrahim, N. A., Ahmed, S. B., Hassan, A. A., & Khaled, D. M. The possible protective effect of Bougainvillea spectabilis leaves extract on estradiol valerate-induced polycystic ovary syndrome in rats (biochemical and histological study). European Journal of Anatomy, 22(6), (2018): 461-9.
37. Sapmaz, T., Sevgin, K., Topkaraoglu, S., Tekayev, M., Gumuskaya, F., Efendic, F., ... & Irkorucu, O. Propolis protects ovarian follicular reserve and maintains the ovary against polycystic ovary syndrome (PCOS) by attenuating degeneration of zona pellucida and fibrous tissue. Biochemical and Biophysical Research Communications, 636, (2022), 97-103.
38. Ullah, A., Jahan, S., Razak, S., Pirzada, M., Ullah, H., Almajwal, A., ... & Afsar, T. Protective effects of GABA against metabolic and reproductive disturbances in letrozole induced polycystic ovarian syndrome in rats. Journal of Ovarian Research, 10, (2017), 1-8.
39. Pourhoseini, S. A., Mahmoudinia, M., Najafi, M. N., & Kamyabi, F. The effect of phytoestrogens (Cimicifuga racemosa) in combination with clomiphene in ovulation induction in women with polycystic ovarian syndrome: A clinical trial study. Avicenna Journal of Phytomedicine, 12(1), (2022): 8.
40. Krishna, M. B., Joseph, A., Thomas, P. L., Dsilva, B., Pillai, S. M., & Laloraya, M. (2018). Impaired arginine metabolism coupled to a defective redox conduit contributes to low plasma nitric oxide in polycystic ovary syndrome. Cellular Physiology and Biochemistry, 43(5),(2018): 1880-1892.

Arabic Abstract

متلازمة المبيض متعدد الكيسات (PCOS) لها عدة أعراض مثل كثرة الشعر، فرط الأندروجين، انقطاع الطمث، انعدام الاباضة والعقم بالإضافة إلى الاضطرابات الأيضية واضطربات الغدد الصم. تهدف الدراسة الحالية تقييم فعالية مستخلص من جذور نبات الهليون في علاج إناث الفئران المستحث بها متلازمة تكيس المبايض. في هذه البحث، تم دراسة تأثير 400 ملغم / كغم من مستخلص جذور نبات الهليون على متلازمة تكيس المبايض لمدة 28 يومًا من أجل فحص تأثيرات مستخلص جذور نبات الهليون على متلازمة تكيس المبايض المستحثة بالليتروزول. قسمت ثلاثين أنثى من فئران الالبينو إلى خمس مجموعات،المجموعة الأولى 1 هي مجموعة التحكم ، المجموعة الثانية 2 جرعت بمستخلص جذور الهليون 400 مجم/كجم لمدة 28 يوم، المجموعة الثالثة 3 هي المجموعة المستحث فيها متلازمة تكيس المبايض ولتحفيز متلازمة تكيس المبايض، تم إعطاء الفئران ليتروزول (1 مجم/كجم) عن طريق الفم لمدة 28 يومًا في محلول 0.5٪ كربوكسي ميثيل سلولوز (CMC).، المجموعة الرابعة 4 هي مجموعة علاجية تم تجريع الحيوانات باللتريزول لمدة 28 يوم بعدها جرعت لمستخلص جذور الهليون لمدة 28 يوم اخرى اما المجموعة الخامسة 5 هي المجموعة الوقائية مستخلص جذور الهليون لمدة 28 وبعدها تم التجريع بالليتريزول لنفس المدة . أظهرت نتائج ملون التميز الثلاثية الألوان قلة في ألياف السدى والكولاجين في التركيب النسجي للمبايض في جميع المجموعات، بما في ذلك المجموعة الضابطة باستثناء مجموعة متلازمة تكيس المبايض التي تشير إلى وجود نسبة عالية من الكولاجين، بالإضافة إلى زيادة عدد الجريبات الأولية ،الثانوية (الغارية) والحويصلة جراف بشكل كبير. أظهرت المجموعة العلاجية والوقائية عددًا أقل من الجريبات المتكيسة مقارنة بمجموعة متلازمة تكيس المبايض كما تظهر النتائج انخفاضًا في ألياف الكولاجين في المجموعة التي جرعت بمستخلص جذور الهليون حيث انه يعمل على تسريع عملية تكوين البويضات والانقسامات المبكرة للخلايا.

Pure Sciences International Journal of kerbala
PSIJK
Year: 2025 Volume : 2 Issue : 5 ISSN: 6188-2789 Print 3005 -2394 Online

2025 ,Volume 2 , Issues 5 PSIJK 32-39

Pure Sciences International Journal of Kerbala
Journal Homepage:https://journals.uokerbala.edu.iq/index.php/psijk

Investigation the Cytotoxic Effect of Erythromycin and the Potential Protective Role of Vitamin C in Male White Rats

Hatem Karim Jassab[1 *], Ali Mohammed Hussein Kazim[2], Alaa Ramthan Hussein[3]

[1,2] Babel Education Directorate/ Kutha Education Department/ Babylon/ Iraq.
[3]Thi-Qar Education Directorate/ Al-Rifai Education Department/ Thi-Qar/ Iraq.

P A P E R I N F O

Received: 23 September 2024
Accepted: 7 January 2025
Published: 31 March 2025

Keywords:
Erythromycin, Weights, Chromosomal Aberration, Vitamin C, DNA Damage

A B S T R A C T

The study aimed to demonstrate the side effects of certain drugs currently used as antibiotics. The research examined the effects of erythromycin at both the cellular and molecular levels, as well as the potential protective role of vitamin C. A total of 25 male white rats *Mus musculus* were used in the experiment for 14 days**.** The study was conducted in the laboratory of the College of Science University of Babylon in May 2024 **.**The animals were divided into five groups, with five rats in each group. The first group was the control group, while the second and third groups received the drug at concentrations of (15, 30) mg/kg, respectively, as treatment groups. The fourth and fifth groups were dosed with the drug at the aforementioned concentrations along with vitamin C at a concentration of (100) mg/kg as protective groups.

The results of the experiment showed structural abnormalities in chromosomes, including deletions in the treated groups (G2, G3), specifically in dicentric chromosomes. Additionally, breaks and ring chromosomes were observed in the treated groups compared to the control group. However, the results of the protective groups (G4, G5) showed a significant reduction in the rates of these abnormalities. The results also indicated a significant decrease in the proportion of non-fragmented DNA, and a significant increase in the mean DNA fragmentation was recorded in groups (G2, G3), while no such observation was made in groups (G4, G5). High DNA fragmentation was found only in group (G3), which received a concentration of (30) mg/kg, but this was not observed in the other experimental groups**.**

1. INTRODUCTION

Erythromycin a drug from the macrolide group, is characterized by its broad-spectrum effect against bacteria and is considered more effective than penicillin. Therefore, it is used in the treatment of many infections [1]. Erythromycin is part of a large therapeutic group composed of more than 13 compounds or drugs that were first extracted over six decades ago in the 1950s. However, it quickly showed many drawbacks, including side effects for patients, poor solubility in water (H_2O), and instability in gastric acids, all of which lead to reduced bioavailability and limited therapeutic effectiveness [2]. Despite the side effects associated with erythromycin treatment, such as nausea, abdominal cramps, and hepatotoxicity, among others, it is still used in pharmacies. However, these drawbacks have limited its oral use [3]. Many studies and research have been conducted on erythromycin to overcome these disadvantages, eventually leading to modifications in the chemical structure of the drug for safer use and increased effectiveness against microbial infections [4]. The use of dietary supplements in alternative medicine as adjuvants to chemical drugs aims to reduce side effects on the body or enhance their effectiveness. One of the compounds used alongside certain drugs, including erythromycin, is vitamin C [5]. Vitamin C, also known as ascorbic acid, is a water-soluble vitamin found in fresh foods, particularly citrus fruits and vegetables. It is important for the body's functions and for protecting the mucous membranes in the respiratory tract, shielding them from infections and microbial inflammation. It was discovered in the early 20th century [6]. Vitamin C acts as a cofactor or substrate for many neurotransmitters and enzymes, participates in collagen synthesis, serves as an antioxidant, protects the

*Corresponding Author Email:
hhkk65130@gmail.com (Hatem Karim Jassab)

heart from stress, and improves iron absorption in the intestines [7]. Vitamin C is a micronutrient with multiple roles, particularly in electron donation. It is a powerful natural antioxidant and an enzyme cofactor, contributing to the body's immune system and acting as a protective agent against the toxicity of many compounds and drugs used today. Vitamin C accumulates in immune phagocytic cells, which helps increase ROS (reactive oxygen species) in immune complexes, thus killing microbes. Additionally, vitamin C plays a role in regulating gene expression [8].

The comet assay, also known as the single-cell gel electrophoresis (SCGE) test, is a tool used to detect any damage or degradation of DNA molecules. It is also employed in assessing the effects of certain substances at the genetic level. This test is considered one of the most versatile, rapid, and accurate methods for obtaining results. It is a highly sensitive and fast-responding technique for detecting single and double-strand breaks in DNA, which are caused by various physical and chemical factors in eukaryotic cells [9].

2. MATERIALS AND METHODS

2.1. Experimental Animals

A total of 25 male white rats *Mus musculus* were used in the experiment, with ages ranging between 10-12 weeks and weights ranging from 215-265 grams. The rats were fed a diet consisting of a mixture of various grains, supplemented with powdered milk.

2.2. Experimental Design

The rats were divided into five groups as follows:

1. First Group (Control Group): Consisted of 5 rats, which were given a saline solution at a concentration of 0.5 ml.
2. Second Group (Therapeutic Group): Consisted of 5 rats, which were given erythromycin at a concentration of 15 mg/kg.
3. Third Group (Therapeutic Group): Consisted of 5 rats, which were orally administered erythromycin at a concentration of 30 mg/kg.
4. Fourth Group (Protective Group): Consisted of 5 rats, which were given erythromycin at a concentration of 15 mg/kg along with vitamin C at a concentration of 100 mg/kg.
5. Fifth Group (Protective Group): Consisted of 5 rats, which were given erythromycin at a concentration of 30 mg/kg along with vitamin C at a concentration of 100 mg/kg.

The concentrations for the drug and the vitamin were determined as follows:

- The dosage of vitamin C was calculated based on a previous reference [10].
- The dosage of erythromycin was determined according to pharmacokinetic data [11]. The experiment lasted for two weeks.

2.3 Sample Collection

The rats were Animal sacrificing , and a blood sample of 5 ml was collected via cardiac puncture for testing. The blood was placed in specialized tubes and centrifuged at 4000 rpm to separate the serum, which was then stored at 4°C. Afterward, the animals were dissected to collect bone marrow samples from the femur and sternum for genetic testing.

2.4 Tests

1- Comet Assay

The comet assay was used to measure DNA damage using the OX Select Comet Assay kit. All required reagents and materials were prepared in advance, including comet agarose gel (Comet LM Agarose), Green Stain Solution, antifade solution, alkaline unwinding solution, and electrophoresis buffer for the assay. The procedure was carried out according to the steps outlined in a reference [12]. A ready-made software program on the computer was used to perform the necessary calculations for each sample [13].

2- Chromosomal aberration test

Slides were prepared after carefully dissecting the animal. After preparation, the slides were stained with a 2% methylene blue solution for 12 minutes. The slides were examined using an oil immersion lens [14], and non-dividing cells were counted according to the mitotic index using the following formula:

$$\text{Mitotic Index (MI)}=\frac{Number\ of\ Dividing\ Cells}{Total\ Number\ of\ Cells} \times 100$$

2.5 The Statistical Analysis

The statistical analysis of the experiment was conducted according to the completely randomized design to study the effect of the drug efficacy and the protective role of Vitamin C in male white mice using the tow-way analysis variance and LSD test for significant difference to show the significance of the difference between the arithmetic means of the experimental variables. All statistical analyses were conducted using the ready statistical program 25. SPSS.V.

3. RESULTS

3.1 Effect Of Erythromycin And The Protective Role Of Vitamin C On Chromosomal Aberration Rate

The results shown in **Table 1** indicate a significant increase ($P<0.05$) in the appearance of chromosomes that experienced deletions in the third group, which was administered erythromycin at a concentration of 30 mg/kg, compared to the control group. In contrast, the fifth, fourth, and second groups did not show a significant difference in chromosomal deletion. The results also revealed a significant increase in the presence of dicentric chromosomes, especially in the third group compared to the first (control) group, while no significant differences (p>0.05) were observed in the second, fourth, and fifth groups regarding dicentric chromosomes. There was a noticeable increase in the occurrence of acentric chromosomes in the therapeutic group that received erythromycin at a concentration of 30 mg/kg. However, the fourth and fifth protective groups were not affected by the drug, while the second group, which received 15 mg/kg, showed a lower rate of acentric chromosomes compared to the third group and the control.

When observing **TABLE 1**, the fourth, second, and fifth groups did not show significant differences in the appearance of ring chromosomes compared to the control group.Yet, the therapeutic third group recorded significant differences in the appearance of ring chromosomes at a probability level of (p<0.05) compared to the control group. The results showed the presence of chromosome breaks in the therapeutic groups that received erythromycin at both concentrations (30 and 15 mg/kg) compared to the protective and control groups. **Table 1** indicated a statistical difference in the overall chromosomal abnormalities between the first (control), second, and third groups. In contrast, no significant differences were observed in the fourth and fifth protective groups when compared to the control.

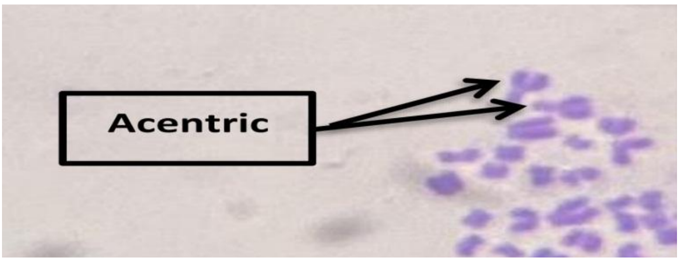

Figure 1. Acentric chromosome in metaphase of bone marrow cells in white mice of the second treatment group (magnification 1000x)

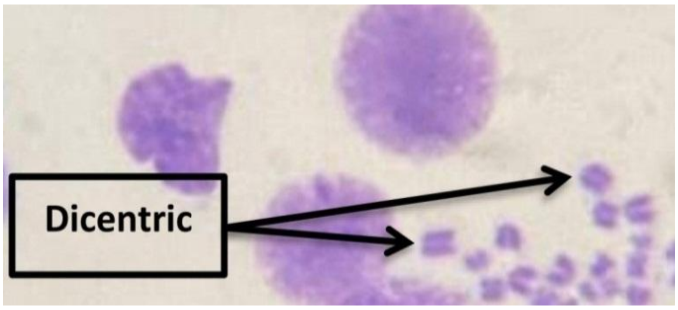

. **Figure 2**. Dicentric chromosome in metaphase of bone marrow cells in white mice of the therd treatment group (magnification 1000x)

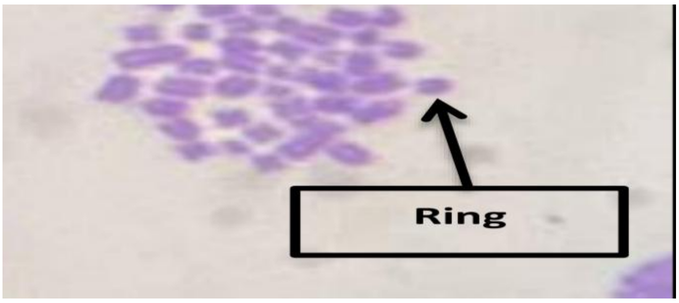

. **Figure 3.** Ring chromosome in metaphase of bone marrow cells in white mice of the therd treatment group (magnification 1000x)

TABLE 1. Effect of Erythromycin and The Protective Role of Vitamin C on Chromosomal Aberration Rate

Groups	**Deleted Chromosome Percentage**	**Dicentric Chromosome Percentage**	**Acentric Chromosomes**	**Ring Chromosome**	**Broken Chromosomes**	**Total Aberrations**
Control Group(G1)	B 0.191±0.0826	B 0.250±0.047	BC 0.070±0.385	B 0.0790+0.066	C 0.168+0.059	C 1.09+0.157
Erythromycin G2(15mg/kg)	AB 0.320+0.871	B 0.299+0.073	AB 0.429+0.122	B 0.181+0.105	B 0.263+0.076	B 1.095+0.157
Erythromycin G3(30mg/kg)	A 0.328+0.162	A 0.604+0.108	A 0.521+0.212	A 0.308+0.104	A 0.320+0.821	A 2.015+0.372
Vitamin C G4(100mg/kg) Erythromycin 15mg/kg	B 0.282+0.091	B 0.0.372+0.142	C 0.312+0.086	B 0.231+0.048	C 0.175+0.041	C 1.056+0.308
Vitamin C G5 (100mg/kg) Erythromycin 30mg/kg	B 0.221+0.209	B 0.432+0.082	BC 0.452+0.021	B 0.105+0.082	C 0.176+0.072	BC 0.782+0,112
p-value	0.018	0.011	0.007	0.001	0.002	0.004
LSD	**0.236**	**0.138**	**0.134**	**0.208**	**0.098**	**0.363**

3.2 Effect Of Erythromycin And The Protective Role Of Vitamin C On Dna Damage Rates

The results in **Table 2** show a significant decrease in the percentage of intact DNA in the treatment groups (G2 and G3), whether the erythromycin concentration was 15 mg/kg or 30 mg/kg. Meanwhile, the results of the groups that received vitamin C along with the drug as a protective factor showed a significant decrease in the percentage of fragmented DNA compared to the second and third groups, and the control group. Table (2) indicates a significant increase in the average DNA fragmentation in the groups that received the drug alone (15 mg/kg and 30 mg/kg). In contrast, no significant differences were observed in the average DNA fragmentation in the two protective groups compared to the control group when the animals were given both the vitamin and the drug together. The results of **Table 2** showed no significant difference in the high DNA strand breakage rates in groups G2, G4, and G5 compared to the control. However, a significant difference in DNA strand breakage was observed in the third group, which received the drug at a concentration of 30 mg/kg, compared to the control group.

TABLE 2. Effect of Erythromycin and the protective role of Vitamin C on DNA damage rates

Groups	Unbroken DNA	low DNA breakage	moderate DNA breakage	High DNA breakage
Control Group(G1)	A 50.062±3.321	A 40.113±3.923	D 6.449±0.982	C 6.023±1.217
Erythromycin G2(15mg/kg)	C 39.732±40.032	B 36.321±2.821	B 12.926±2.821	A 13.331±1.298
Erythromycin G3(30mg/kg)	D 36.682±1.802	B 35.706±1.382	A 17.023±2.621	A 14.092±0.872
Vitamin C G4(100mg/kg) Erythromycin 15mg/kg	B 45.492±0.802	A 41.728±0.662	D 8.023±1.203	C 7.231±0.931
Vitamin C G4(100mg/kg) Erythromycin 30mg/kg	C 42.807±1.682	A 37.992±1.348	C 11.122±1.601	B 9.235±0.786
p-value	0.001	0.002	0.003	0.001
LSD	**3.162**	**2.742**	**2.523**	**5.982**

4. DISCUSSION

The Effect of Erythromycin and the Protective Role of Vitamin C on Chromosomal Aberration Rates. The results of the experiments indicated cytotoxicity due to erythromycin, particularly in groups two and three, which received the drug alone at concentrations of 15 and 30 mg/kg. This outcome is consistent with findings from study [15], which reported that erythromycin caused chromosomal aberrations, with a significant increase in structural deviations in human lymphocyte chromosomes. Additionally, study [16] highlighted growing concerns regarding the drug's impact on embryos in pregnant women, particularly in the form of structural abnormalities in sister chromatids. These abnormalities serve as an indicator of genetic safety after exposure to the drug during pregnancy, especially given that fetal and neonatal cells are sensitive to teratogenic effects. A study [17] conducted on pregnant mice treated with erythromycin (a macrolide family drug) at various doses during late pregnancy revealed a reduction in cell proliferation, changes in the morphology of fetal testes, and deviations in cellular functions. Exposure to different concentrations of orally administered erythromycin poses a risk to epithelial cells in the intestine, as study [18] demonstrated that drug accumulation in food at certain concentrations affects the permeability of the intestinal epithelial layer. Acute exposure increased cytotoxicity and caused changes in embryonic gene expression related to the production of adhesion proteins, suggesting that these gene expression alterations are associated with the drug's immune activation and compensatory mechanisms in the intestinal epithelium.

The results of the study showed that the protective groups, which received vitamin C along with the drug, produced outcomes different from those of the second and third therapeutic groups. Statistical analyses revealed no significant differences in chromosomal abnormalities, aligning with study [19], which highlighted the protective role of vitamin C in reducing structural DNA damage caused by the genotoxic and cytotoxic effects of erythromycin. Moreover, study [20] demonstrated a reduction in chromosomal structural damage when vitamin C was used as a protective agent alongside macrolide treatments. Study [21] mentioned that vitamin C enhances the efficacy of enzymes involved in DNA methylation, thereby maintaining genome stability due to its antioxidant properties and its role in promoting the activity of the TET enzyme family. These enzymes, with the assistance of vitamin C, help regulate and demethylate harmful methylation, ensuring genomic stability.

The Effect of Erythromycin and the Protective Role of Vitamin C on DNA Damage Rates

Our current study noticed a significant increase in DNA fragmentation rates, particularly in groups two and three, which received erythromycin alone without vitamin C. These results are consistent with study [22], which showed that the drug causes genotoxicity resulting in DNA fragmentation, especially in conjunction with strong oxidative agents and cellular degeneration. This effect is attributed to intracellular reactions that lead to chromatin condensation and ultimately programmed cell death. Additionally, the drug has mitochondrial toxic effects due to increased oxidative stress and DNA fragmentation in epithelial and fibroblast cells [23]. Study [24] highlighted the drug toxicity of macrolides, specifically clarithromycin (a member of the macrolide family), and its inhibitory effect on CYP3A5 (a genetic variant in humans responsible for metabolizing drugs and related molecules in the body). In some volunteers who took the drug orally, results showed inhibition of the gene expression studied due to drug accumulation after the treatment period. In a study conducted by [25], mice were administered telithromycin, and the comet assay revealed DNA damage in lymphocytes and structural harm to the DNA, confirming the genotoxicity of these drugs. The current study results indicate that vitamin C acts as a protective agent against DNA damage caused by erythromycin, as noted in study [26]. This study highlighted the vitamin's role in preventing partial DNA fragmentation by directly reducing the damage caused by ROS molecules, which can harm proteins and DNA in cellular environments. Comet assay analyses revealed no significant differences in DNA damage between the groups receiving both the drug and vitamin C when compared to the control group. This finding aligns with study [27], which emphasized vitamin C's protective role against DNA damage from harmful mutations due to its antioxidant properties and its ability to neutralize free radicals causing oxidative stress.

5. CONCLUSIONS

Erythromycin affects the structural integrity of chromosomes, with its impact varying according to the doses administered. Combining erythromycin with Vitamin C can mitigate its side effects on chromosomal structures. The drug induces DNA damage by causing fragmentation of the double-stranded DNA. Vitamin C exhibits a protective effect, safeguarding DNA from structural aberrations induced by erythromycin. A dose of 30 mg/kg of erythromycin administered to mice results in the most pronounced genetic effects.

6.REFERENCES

1. Ning Q.; Wang D.; An J.; Ding Q.; Huang Z.; Zou Y.; Wu F.; You J.; Combined effects of nanosized polystyrene and erythromycin on bacterial growth and resistance mutations in Escherichia coli. *Journal of Hazardous Materials*. 15 (422), (2022),126858.
2. Platon, V.M.; Dragoi, B.; and Marin, L.; Erythromycin formulations—a journey to advanced drug delivery. *Pharmaceutics*, 14(10), (2022), 2180.
3. Farzam, K.; Nessel, T.A.; and Quick, J.; Erythromycin. In StatPearls [Internet]. *StatPearls Publishing*. (2023).
4. Cyphert, E.L.; Wallat, J.D.; Pokorski, J.K; and Von Recum, H.A.; Erythromycin modification that improves its acidic stability while optimizing it for local drug delivery. *Antibiotics*, 6(2), (2017), 11.
5. El Shahawy, M. S.; El Metwaly, I.; and Shady, Z. M.; Value of supplementing vitamin C to the triple therapy on the eradication rates of Helicobacter pylori infection. *Advances in Digestive Medicine*, 7(3), (2020), 124-131.
6. Granger, M.; and Eck, P.; Dietary vitamin C in human health. *Advances in food and nutrition research*, 83, (2018), 281-310.
7. Lykkesfeldt, J.; On the effect of vitamin C intake on human health: How to (mis) interprete the clinical evidence. *Redox biology*, 34, (2020),101532.
8. Carr, A.C.; and Maggini, S.; Vitamin C and immune function. *Nutrients*, 9(11), (2017), 1211.
9. Azqueta, A.; Ladeira, C.; Giovannelli, L.; Boutet-Robinet, E.; Bonassi, S.; Neri, M.; Gajski, G., Duthie, S.; Del Bo, C.; Riso, P.; and Koppen, G.; Application of the comet assay in human biomonitoring: An hCOMET perspective. *Mutation Research/Reviews in Mutation Research*, 783, (2020),108288.
10. Ahmad, R.M.; AL-Hubaity, A.Y.; and Alazow, N.S.; The role of Vitamin C on the structural changes of male Albino rats kidney induced by tramadol. Annals of the College of Medicine, *Mosul*, 41(1), (2019), 57-62.

11. Atli, O.; Ilgin, S.; Altuntas, H.; and Burukoglu, D.; Evaluation of azithromycin induced cardiotoxicity in rats. *International journal of clinical and experimental medicine*, 8(3), (2015), 3681.
12. De Boeck, M.; Touil, N.; De Visscher, G.; Vande, P. A.; and Kirsch-Volders, M.; Validation and implementation of an internal standard in comet assay analysis. *Mutation Research/Genetic Toxicology and Environmental Mutagenesis*, 469(2), (2000),181-197.
13. Olive, P.L.; Banáth, J.P.; and Durand, R.E.; Heterogeneity in radiation-induced DNA damage and repair in tumor and normal cells measured using the" comet" assay. *Radiation research*, 122(1), (1990), 86-94.
14. Tolliver, D.K.; and Robbins, L.W.; Techniques in karyology: The bone marrow extraction method. In: Goldman, C.A. (Eds.), Tested studies for laboratory teaching. Volume 12. Proceedings of the 12th Workshop/Conference of the Association for Biology Laboratory Education (ABLE), (1991), 69–74.
15. Sahoqi, M.; and Kareema M. W.; Applications in Design and Laboratory Analysis. Dar Al-Hikma for Printing and Publishing, University of Mosul, Iraq. (1991).
16. Djordjević, K. M.; Arsenijević, S. N.; Milošević-Djordjević, O. M.; Marinković, D. M.; and Grujičić, D. V.; Pharmacotherapy During Pregnancy and Its Association with Genome Instability in Mother and Fetus. *Kragujevac Journal of Science*, 45, (2023).
17. Kong, Z.; Zhu, L.; Liu, Y.; Chen, G.; Jiang, T., and Wang, H.; Effects of azithromycin exposure during pregnancy at different stages, doses and courses on testicular development in fetal mice. *Biomedicine & Pharmacotherapy*, 170, (2024), 116063.
18. Hao, H.; Gokulan, K.; Piñeiro, S.A.; Williams, K.M.; Yuan, Z.; Cerniglia, C.E.; and Khare, S.; Effects of acute and chronic exposure to residual level erythromycin on human intestinal epithelium cell permeability and cytotoxicity. *Microorganisms*, 7(9), (2019), 325.
19. Dutta, J.; Modulatory Effects of Vitamin C on Enrofloxacin Induced Chromosome Damage and AgNOR Counts in Chick Bone Marrow Nuclei. *Toxicology International*, 25(3), (2018), 1-6.
20. Abasova, O. Y.; Reutova, N. V.; Sycheva, L. P.; and Chernysheva, E. A.; Studies of Antimutagenic Effects of Vitamins A and C in Humans. *Bulletin of Experimental Biology and Medicine*, 154(5), (2013), 649–653.
21. Brabson, J. P.; Leesang, T.; Mohammad, S.; and Cimmino, L.; Epigenetic regulation of genomic stability by vitamin C. *Frontiers in genetics*, 12, (2021), 675780.
22. Kandila, A. M.; Farrag, A. R. H.; Hassan, B. N.; and I S, D. E. E; Histological Study and DNA Changes in the Kidneys of Rat Fetuses Maternally Treated with Clarithromycin. *The Egyptian Journal of Hospital Medicine*, 61(1), (2015), 575-590.
23. Jiang, X.; Baucom, C.; and Elliott, R. L.; Mitochondrial toxicity of azithromycin results in aerobic glycolysis and DNA damage of human mammary epithelia and fibroblasts. *Antibiotics*, 8(3), (2019), 110.
24. Pinto, A. G., Wang, Y. H., Chalasani, N., Skaar, T., Kolwankar, D.; Gorski, J. C.; and Hall, S. D.; Inhibition of human intestinal wall metabolism by macrolide antibiotics: effect of clarithromycin on cytochrome P450 3A4/5 activity and expression. *Clinical Pharmacology & Therapeutics*, 77(3), (2005), 178-188.
25. Maletić, J.; Đelić, N.; Radaković, M.; Maletić, M.; Lakić, N.; Kukolj, V.; and Stanimirović, Z.; Evaluation of DNA damage in rat lymphocytes exposed to tulathromycin in vitro. *Genetika*, 47(1), (2015), 339-348.
26. Du, J.: Cullen, J. J.; and Buettner, G. R.; Ascorbic acid: chemistry, biology and the treatment of cancer. *Biochimica et Biophysica Acta (BBA)- Reviews on Cancer*, 1826(2), (2012), 443-457.
27. Lutsenko, E. A.; Cárcamo, J. M.; and Golde, D. W.; Vitamin C prevents DNA mutation induced by oxidative stress. *Journal of Biological Chemistry*, 277(19), (2002), 16895-16899.

Arabic Abstract

هدفت الدراسة إلى بيان التأثير المحتمل لبعض أنواع العقاقير المستخدمة حالياً كمضادات حيوية. تناول البحث الآثار الجانبية التي يسببها عقار الإريثرومايسين على المستويين الخلوي والجزيئي، ودور فيتامين C كعامل وقائي محتمل. استخدمت في التجربة ذكور الفئران البيضاء لمدة 14 يومًا، قُسمت الحيوانات إلى خمس مجموعات بواقع 5 فئران في كل مجموعة. المجموعة الأولى كانت مجموعة السيطرة، بينما تلقت المجموعتان الثانية والثالثة العقار بتركيز (15، 30) mg/kg على التوالي كمجموعات علاجية. أما المجموعتان الرابعة والخامسة فقد جُرعتا بالعقار بتركيز المذكور مع فيتامين C بتركيز (100) mg/kg كمجموعات وقائية. أظهرت نتائج التجربة حدوث تشوهات تركيبية في الكروموسومات تمثلت بوجود حذف (Deletion) في المجموعتين العلاجيتين (G2، G3) في الكروموسومات ذات مركزين (Dicentric)، بالإضافة إلى ظهور تكسر وكروموسوم حلقي (Ring) في المجموعات العلاجية مقارنة مع مجموعة السيطرة. بينما سجلت نتائج المجموعتين الوقائيتين (G4، G5) انخفاضًا معنويًا في نسب حدوث التشوهات المذكورة. بينت النتائج انخفاضًا معنويًا في نسب الـ DNA غير المتكسر، وسجلت أيضًا ارتفاعًا ذا قيمة معنوية في متوسط تكسر الـ DNA للمجموعتين (G2، G3)، بينما في المجموعتين (G4، G5) لم يُلاحظ ذلك. وُجد أن هناك تكسرًا عاليًا في الحمض النووي للمجموعة (G3) فقط التي جرعت بتركيز (30) mg/kg، ولم يُلاحظ هذا في باقي المجموعات التجريبية.

Pure Sciences International Journal of kerbala

Year: 2025 Volume : 2 Issue : 5 ISSN: 6188-2789 Print 3005 -2394 Online

2025 ,Volume 2 , Issues 5 PSIJK 40-44

Pure Sciences International Journal of Kerbala
Journal Homepage:https://journals.uokerbala.edu.iq/index.php/psijk

Estimation of Interleukin 6 and Tumor Necrosis Factor in Pfizer Covid Vaccinated Case

Radhia Hussain Fadel[1*], Mohemed Fleeh Dareef[2], Salah Mehdi[3]

[1]Medical microbiology/Pathological Analysis Dept.- College of health and medical technology/Kufa / Al-Furat Al-Awsat technical university-31003 . [2] Medical microbiology/Pathological Analysis Dept.- College of health and medical technology/Baghdad / Medical technical university [3]Medical microbiology/Pathological Analysis Dept.- College of health and medical technology/Baghdad / Medical technical university.

P A P E R I N F O

Received: 16 October 2024
Accepted: 27 October 2024
Published: 31 March 2025

Keywords:
Pfizer vaccine, IL-6, TNF-α

A B S T R A C T

Background: Pfizer vaccine, which is a nucleoside-modified mRNA vaccine against coronavirus disease 2019 (COVID-19) is one of the first mRNA products to be approved by the Food and Drug Administration (FDA) and the European Medicines Agency (EMA).
Aim of the study: The aim of this study is to study the impact of Pfizer vaccine on the levels of interlukin-6 (IL-6) and tumor necrosis factor alpha (TNF-α) after 3 months and 6 months of vaccination with Pfizer vaccine.
Materials and methods: The study was done during the period from May /2022 to September / 2022). A case-control study involved 150 subjects who were divided into three groups (each group included 50 subjects). The first group included (50) vaccinated group 3 months after second dose of Pfizer vaccine, and the second group included (50) vaccinated group 6 month after second dose of Pfizer vaccine. The third group was the control group which included (50) healthy unvaccinated subjects. Serum levels of IL-6 and TNF-α were estimated by ELISA technique. Results: The results showed that the mean levels of TNF-α among male participants (after 3 months of vaccination, after 6 months of vaccinations, and in the control group) were (65.40, 47.34, and 9.45), respectively, with highly significant differences between the three groups ($p<0.01$). The results showed that the mean levels of TNF-α among female participants (after 3 months of vaccination, after 6 months of vaccinations, and the control group) were (67.50, 48.74, and 9.06), respectively, with highly significant differences between the three groups ($p<0.01$). In addition, the results showed that the mean levels of IL-6 among male participants (after 3 months of vaccination, after 6 months of vaccinations, and the control group) were (81.36, 101.88, and 51.26), respectively, with highly significant differences between the three groups ($p<0.01$). The results showed that the mean levels of IL-6 among female participants (after 3 months of vaccination, after 6 months of vaccinations, and the control group) were (83.05, 98.03, and 52.07), respectively, with highly significant differences between the three groups ($p<0.01$). Conclusion: Pfizer vaccine was shown to have significant impacts on IL-6 and TNF-α levels among vaccinated individuals.

1. INTRODUCTION

The coronavirus disease 2019 (COVID-19) pandemic is caused by severe acute respiratory syndrome coronavirus 2 (SARS-CoV-2). Most infected individuals with mild symptoms spontaneously recover, but SARS-CoV-2 infection can result in a severe acute respiratory illness requiring mechanical ventilation with ~1% mortality [1]. To induce immunity and reduce the severity of SARS-CoV-2 infection, several categories of vaccines have been developed [2].

The primary goal of vaccination is to induce innate immunity and protective adaptive immunity against SARS-CoV-2 in the form of antibodies and specific T-cell responses [3]. Pfizer and the German biotechnology business (BioNTech) collaborated to create a COVID-19 vaccination utilizing messenger RNA (mRNA) technology. The Pfizer-BioNTech COVID-19 vaccine was created quickly in reaction to the worldwide pandemic brought on by the new coronavirus, SARS-CoV-2 [4]. IL-6 is known to be produced early in the immune response and is involved in the activation of innate immune cells, such as neutrophils and macrophages. It helps to promote inflammation and coordinate the initial response to infections. In the context of COVID-19 vaccines, IL-6 production may be induced by the vaccine as a part of the innate immune response to the viral antigens in the vaccine [5].

*Corresponding Author Institutional Email: cauth.@uokerbala.edu.iq (Radhia Hussain Fadel)

Tumor necrosis factor-alpha (TNF-α) is a secretory protein produced by various immune cells, including macrophages, T cells, and natural killer (NK) cells [6]. TNF-α plays a critical role in the immune response and inflammation. It is involved in the regulation of immune cell activation, proliferation, and apoptosis, as well as in the induction of other inflammatory cytokines [7].

2. MATERIALS and METHODS

The current case-control study included (150) participants who were divided into three groups (each group included 50 subjects). The first group included (50) vaccinated group 3 months after second dose of Pfizer vaccine, and the second group included (50) vaccinated group 6 month after second dose of Pfizer vaccine. The third group was the control group which included (50) healthy unvaccinated subjects. This study was conducted during the period from May /2022 to September / 2022). Venous blood samples were taken from all participants and put in gel tubes to clot for 20-30 minutes, then centrifuged to obtain serum samples. ELISA kits were used to in vitro quantitative determination of Human (IL-6) and (TNF-α) concentrations in serum.

Statistical analysis: The experimental results were performed according to the graph pad prism version 8 where Tukey multiple comparisons were done. One and two-way (ANOVA) was preformed to investigate the significance of differences between groups. The values were expressed as (mean±standard errors) of mean (SEM) and P value<0.01 was considered statistically significant.

3. RESULTS

The results in **TABLE 1** showed that the mean levels of TNF-α among male participants (after 3 months of vaccination, after 6 months of vaccinations, and in the control group) were (65.40, 47.34, and 9.45), respectively, with highly significant differences (HS) between the three groups (p<0.01). The results showed that the mean levels of TNF-α among female participants (after 3 months of vaccination, after 6 months of vaccinations, and the control group) were (67.50, 48.74, and 9.06), respectively, with highly significant differences (HS) between the three groups (p<0.01).

Table 1. Mean TNF-α levels among the study group

Mean TNF-α level (pg/ml)	After 3 months vaccination	After 6 months vaccination	Controls	p-value
Males	65.40	47.34	9.45	P<0.01 (HS)
Females	67.50	48.74	9.06	P<0.01 (HS)

The mean levels of (IL-6) among male participants (after 3 months of vaccination, after 6 months of vaccinations, and in the control group) were (81.36, 101.88, and 51.26), respectively, with highly significant differences (HS) between the three groups (p<0.01). The results showed that the mean levels of IL-6 among female participants (after 3 months of vaccination, after 6 months of vaccinations, and the control group) were (83.05, 98.05, and 52.05), respectively, with highly significant differences (HS) between the three groups (p<0.01), as shown in **TABLE 2.**

Table 2. Mean IL-6 levels among the study group

Mean IL-6 level (pg/ml)	After 3 months vaccination	After 6 months vaccination	Controls	p-value
Males	81.36	101.88	51.26	P<0.01 (HS)
Females	83.05	98.05	52.05	P<0.01 (HS)

4. DISCUSSION

Results showed that the mean levels of TNF-α and IL-6 were significantly higher in the two vaccinated groups (after 3 months and after 6 months) when compared to their levels in the control group for both males and females. The mean levels of TNF-α was higher in females than males after 3 and 6 months of vaccination, but without significant differences. The mean levels of IL-6 was higher in females than males after 3 of vaccination, and was higher in males than females after 6 months of vaccination, but without significant differences.

In one study, no differences were instead revealed for sex, with male and female showing a comparable antibody titer 1 month after vaccination, and similar levels of antibody decay. Literature in this regard is still conflicting, reporting in some cases a higher initial antibody level in women compared to men [8], while others showed no differences due to sex [9]

The S1 subunit of the Spike protein in the vaccine produces an endothelial lesion that is amplified by simultaneous exposure to the inflammatory cytokine TNF-α and the male hormone dihydrotestosterone [10]. This condition of endothelial lesion, amplified by simultaneous exposure to TNF-α and androgens, may allow us to resolve some controversies. There is growing evidence that suggests that males have a higher risk of outcomes in the case of myocarditis [11], despite the fact that they are able to suppress the production of pro-inflammatory cytokines (IL-1β, IL-6 and TNF-α) and increasing the production of anti-inflammatory cytokines [12]. Since the effects of testosterone may be different under normal physiological conditions and in pathological states [13], in the presence of an endothelial lesion and/or myocarditis these effects may be different from the physiological conditions .

In our study, TNF-α was significantly higher among the two vaccinated groups compared to the controls, and was higher in the 3 months group compared to the 6 months group. mRNA vaccines have been developed by Moderna and Pfizer-BioNTech. A cutting-edge technique called RNA and DNA vaccines employs genetically modified RNA or DNA produce a protein that safely elicits an immune response [14].

However, in one study, no significant difference in serum levels of TNF-α was detected 7 days and up to 1 month after full vaccination, which might result from specific cohort characteristics and timing of sampling [15].

Biochemical studies revealed that Spike protein triggers inflammation via activation of the NF-κB pathway and the induction of pro-inflammatory cytokines, such as IL-6, TNF-α, and IL-1β [10]. After the first dose of the BNT162b2 vaccine, the human organism produces systemic inflammation which is accompanied by the upregulation of TNF-α and IL-6 after the second dose [11]. Another study reported that serum TNF-α levels did not increase after the first dose but increased significantly after the second dose. It follows that after the second dose of the vaccine, there are markedly increased concentrations of TNF-α in the serum, already only after the first day following the second vaccine dose. Finally, there would be a significant linear correlation between the levels of pro-inflammatory cytokine TNF-α and the degree of symptoms (systemic scores) occurring one day after the second dose of the BNT162b2 vaccine. For these authors, these data suggest that pro-inflammatory cytokine (TNF-α) was produced in response to the BNT162b2 vaccination, especially after the second dose [12].

In our study, IL-6 was significantly higher among the two vaccinated groups compared to the controls, and was higher in the 3 months group compared to the 6 months group .This finding agreed with [13] who found that post-vaccination PASC-like symptoms were associated with an inflammatory profile with statistically significant elevations in IL-6.

Patients with COVID-19 have significantly higher concentrations of inflammatory mediators than healthy controls [14]. Elevated concentrations of IL-6 and persistent inflammation can also last for months and might be related to the development of post-COVID-19 conditions [15]. A study presented by Karimabad et al., 2021 [16] for the coronary artery disease patients were found increase in the levels of IL-6 after second vaccination with a BNT162b2 mRNA (Pfizer/BioNTech) vaccine at day 2, and this study agreed with our finding of increased levels of IL-6 after 2nd dose of Pfizer vaccine but at (20-30) days, and this confirm the association of IL-6 with the vaccination and will be resulting in antibody development. Our study on the circulating levels of cytokines implies that cytokine modulation could be a biomarker for effective vaccination and antibody generation, and the role of these cytokines upon vaccination became more apparent after the 2nd vaccination [17].

IL-6 plays a crucial role to induce lymphocytic apoptosis that leads to the development of lymphopaenia in COVID-19 patients [18,19]. The high level of IL6 significantly downregulates the expression of human leukocyte D antigen (HLA-DR) that substantially impairs lymphocyte function, along with the depletion of CD4+ lymphocytes, CD19+ lymphocytes and natural killer (NK) cells. In addition, IL6 is considered to have an impact in the severity of COVID-19 patients, which is significantly associated with adverse clinical outcomes [20,21,22].

The severe clinical evolution of COVID-19 was related to an exacerbated host immune response, called hyperinflammatory syndrome, which occurs due to the action of the immune system in response to infection through the release of inflammatory cytokines, a phenomenon known as cytokine storm [23]. Among the main cytokines related to the clinical severity of SARS-Cov-2 infection is IL-6, which promotes a highly specific reaction of adaptive immunity by stimulating CD8+ T and B cells, which also favors the survival of phagocytic neutrophils. However, there is tissue damage by deregulation of the extracellular matrix and by attraction of pro-inflammatory macrophages and neutrophils to the tissues [24].

5. REFERENCES

1. Al-Kufaishi AMA, Al-Hasnawi MAJ, Al-Musawi NJT. Evaluation of Bradykinin and Leukotriene B4 and D4 in Serum of Patients with COVID-19: A Case Control Study. Med J Babylon. 2024;21(Suppl 1):S154–8.
2. Forni G, Mantovani A. COVID-19 vaccines: where we stand and challenges ahead. Cell Death Differ. 2021;28(2):626–39.
3. 3.Al-Mamouri SRK, Al-Kufaishi AMA. Evaluation of total antioxidant capacity and total oxidant status in patients with COVID-19. J Pharm Negat Results. 2022;13(4):125–9.
4. Li, D., Liu, C., Li, Y., Tenchov, R., Sasso, J. M., Zhang, D., & Zhou, Q. (2023). Messenger RNA-based therapeutics and vaccines: what's beyond COVID-19?. ACS Pharmacology & Translational Science, 6(7), 943-969.
5. Moore, J. B., & June, C. H. (2020). Cytokine release syndrome in severe COVID-19. Science, 368(6490), 473-474.
6. Hirano, T., & Murakami, M. (2020). COVID-19: a new virus, but a familiar receptor and cytokine release syndrome. Immunity, 52(5), 731-733.

7. Diao, B., Wang, C., Tan, Y., Chen, X., Liu, Y., Ning, L., ... & Chen, Y. (2020). Reduction and functional exhaustion of T cells in patients with coronavirus disease 2019 (COVID-19). Frontiers in immunology, 827.
8. Shrotri M., Navaratnam A.M.D., Nguyen V., Byrne T., Geismar C., Fragaszy E., et al. Virus Watch Collaborative, Spike-antibody waning after second dose of BNT162b2 or ChAdOx1. Lancet Lond. Engl. 2021;398(10298):385–387.
9. Padoan A., Dall'Olmo L., Rocca F.D., Barbaro F., Cosma C., Basso D., et al. Antibody response to first and second dose of BNT162b2 in a cohort of characterized healthcare workers. Clin. Chim. Acta. 2021;519:60–63.
10. Kumar, N.; Zuo, Y.; Yalavarthi, S.; Hunker, K.L.; Knight, J.S.; Kanthi Y. SARS-CoV-2 Spike Protein S1-Mediated Endothelial Injury and Pro-Inflammatory State Is Amplified by Dihydrotestosterone and Prevented by Mineralocorticoid Antagonism. Viruses 2021, 13, 2209.
11. Barcena, M.L.; Jeuthe, S.; Niehues, M.H.; Pozdniakova, S.; Haritonow, N.; Kühl, A.A.; Sex-Specific Differences of the Inflammatory State in Experimental Autoimmune Myocarditis. Front. Immunol. 2021, 12, 686384.
12. Fairweather, D.; Petri, M.A.; Coronado, M.J.; Cooper, L.T. Autoimmune heart disease: Role of sex hormones and autoantibodies in disease pathogenesis. Expert. Rev. Clin. Immunol. 2012, 8, 269–284.
13. Diaconu, R.; Donoiu, I.; Mirea, O.; Bălşeanu, T.A. Testosterone, cardiomyopathies, and heart failure: A narrative review. Asian J. Androl. 2021, 23, 348–356.
14. Mascellino, M. T., di Timoteo, F., de Angelis, M., & Oliva, A. (2021). Overview of the main anti-sars-cov-2 vaccines: Mechanism of action, efficacy and safety. In Infection and Drug Resistance (Vol. 14, pp. 3459–3476). Dove Medical Press Ltd.
15. Cavic, M., Nesic, A., Mirjacic Martinovic, K. et al. Detection of humoral and cellular immune response to anti-SARS-CoV-2 BNT162b2 vaccine in breastfeeding women and naïve and previously infected individuals. Sci Rep 13, 6271 (2023.(
16. Karimabad, M.N., Kounis, N.G., Hassanshahi, G., Hassanshahi, F., Mplani, V., Koniari, I. 2021. The Involvement of CXC Motif Chemokine Ligand 10 (CXCL10) and Its Related Chemokines in the Pathogenesis of Coronary Artery Disease and in the COVID-19 Vaccination: A Narrative Review. Vaccines, 9(11), p.1224.
17. Saleh, R. H., Mohammed, H. Q., & Al-badri, S. A. F. A.-badri. (2022). Comparative study of IL- 2, IL-6 levels for recovered COVID-19 patients and vaccinated participants. International Journal of Health Sciences, 6(S1), 13274≤13283.
18. Abbasifard, M. , & Khorramdelazad, H. (2020). The bio-mission of interleukin-6 in the pathogenesis of COVID-19: A brief look at potential therapeutic tactics. Life sciences, 257, 118097.
19. Tan, L. , Wang, Q. , Zhang, D. , Ding, J. , Huang, Q. , Tang, Y. Q. , & Miao, H. (2020). Lymphopenia predicts disease severity of COVID-19: A descriptive and predictive study. Signal Transduction and Targeted Therapy, 5(1), 1–3.
20. Chen, X. , Zhao, B. , Qu, Y. , Chen, Y. , Xiong, J. , Feng, Y. (2020). Detectable serum severe acute respiratory syndrome coronavirus 2 viral load (RNAemia) is closely correlated with drastically elevated interleukin 6 level in critically ill patients with coronavirus disease 2019. Clinical Infectious Diseases, 71(8), 1937–1942.
21. Gong, J. , Dong, H. , Xia, Q.-S. , Huang, Z. , Wang, D. , Zhao, Y. , et al. (2020). Correlation analysis between disease severity and inflammation-related parameters in patients with COVID-19: A retrospective study. BMC Infectious Diseases, 20(1), 1–7.
22. Liu, X. , Wang, H. , Shi, S. , & Xiao, J. (2021). Association between IL-6 and severe disease and mortality in COVID-19 disease: a systematic review and meta-analysis. Postgraduate Medical Journal, 98(1165), 871–879. doi: 10.1136/postgradmedj-2021-139939.
23. Elahi R, Karami P, Heidary AH, Esmaeilzadeh A. An updated overview of recent advances, challenges, and clinical considerations of IL-6 signaling blockade in severe coronavirus disease 2019 (COVID-19). Int Immunopharmacol 2022;105:108536.
24. Gubernatorova EO, Gorshkova EA, Polinova AI, Drutskaya MS. IL-6: relevance for immunopathology of SARS-CoV-2. Cytokine Growth Factor Rev 2020;53:13–24.

Arabic Abstract

الاختلافات بين المجموعات الثلاث (ع <0.01). أظهرت النتائج أن متوسط مستويات TNF-α بين الإناث المشاركات (بعد 3 أشهر من التطعيم، بعد 6 أشهر من التطعيمات، والمجموعة الضابطة) بلغ (67.50، 48.74، 9.06)، على التوالي، مع وجود فروق ذات دلالة إحصائية كبيرة بين المجموعات الثلاث (P<0.01). بالإضافة إلى ذلك، أظهرت النتائج أن متوسط مستويات الإنترلوكين 6 بين المشاركين الذكور (بعد 3 أشهر من التطعيم، وبعد 6 أشهر من التطعيمات، والمجموعة الضابطة) بلغ (81.36، 101.88، 51.26)، على التوالي، مع وجود فروق ذات دلالة إحصائية كبيرة بين المجموعات الثلاث (P<0.01). أظهرت النتائج أن متوسط مستويات الإنترلوكين 6 بين الإناث المشاركات (بعد 3 أشهر من التطعيم، بعد 6 أشهر من التطعيمات، والمجموعة الضابطة) بلغ (83.05، 98.03، 52.07)، على التوالي، مع وجود فروق ذات دلالة إحصائية كبيرة بين المجموعات الثلاث (P<0.01). الاستنتاج: تبين أن لقاح فايزر له تأثيرات كبيرة على مستويات IL-6 وTNF-α بين الأفراد الملقحين.

Pure Sciences International Journal of kerbala

Year: 2025 Volume : 2 Issue : 5 ISSN: 6188-2789 Print 3005 -2394 Online

2025 ,Volume 2 , Issues 5 PSIJK 45-54

Pure Sciences International Journal of Kerbala

Journal Homepage:https://journals.uokerbala.edu.iq/index.php/psijk

A Novel Numerical Method for Resolving the Time-Fractional Equation of Advection, Diffusion, and Reaction

Mohammed Hamza Mohammed

Ministry of Education, Holy Karbala Education Directorate

P A P E R I N F O

Paper history:
Received: 28 October 2024
Accepted: 8 December 2024
Published: 31 March 2025

Keywords:
Fractional Differential Equations - Numerical Method-Advection-Diffusion-Reaction Equations - Time Fractional Equations - Numerical Solution - Novel Methodology - Mathematical Modeling - Computational Efficiency - Fractional Calculus.

A B S T R A C T

This study used Lie transformations to provide both numerical and analytical answers for the partial reaction-diffusion-adhesion equations for both time and space. If the balances allowed via the goal calculations permit the determination of Lie transformations, then we can reduce slight fractional variance calculations to normal variance calculations containing fractions. We suggest a different approach to find the numerical and analytical answers beginning from the numerical and analytical answers in the spatio-temporal fractal adhesion-diffusion-interaction model. Recent findings on the adhesion-diffusion interaction equation were obtained by the authors. Separate adhesion-diffusion reaction equations for partial temporal and spatial variables were presented.
The excellent accuracy of the suggested approach makes it a useful instrument for solving a Wide category of fractional differential equation problems. The numerical results show its effectiveness and applicability.

1. Introduction

Due to its numerous applications in a variety of disciplines, including science, engineering, and economics, fractional-order differential equations (FDEs) have attracted a great deal of attention from scholars in recent years. Within the paradigm of fractional calculus, these equations are essential to comprehending phenomena such as transport in porous media and groundwater contamination. Fractional-order systems are nonlocal, and their memory effect has drawn attention due to its special properties and consequences for system behavior. Engineers working on real-world problems favor fractional-order systems over traditional integer-order systems because of their distinct qualities. The accurate representations of nonlinear events provided by fractional differential equations encourage researchers to create numerical techniques for efficiently solving these kinds of equations. Consequently, a multitude of analytical and numerical techniques have been developed, such as variational iterative techniques, homotopy analysis techniques, Wavelet operational techniques, and domain decomposition techniques. Furthermore, numerous numerical methods have been developed to solve various kinds of fractional diffusion equations, highlighting the continuous attempts to improve the comprehension and solution of these intricate systems. As an extension of Fibonacci numbers, the focus has recently switched to Fibonacci polynomials, providing a new angle on the field of polynomials. It is not difficult to produce these polynomials using recurrence relations, and it is only recently that their importance in the field of polynomials has become apparent. Numerous approaches utilizing Fibonacci polynomials have surfaced. These include the approach put forth by Koc et al. [1] in 2013 to address ordinary boundary value problems, the matrix method by Abd-Elhameed and Youssri [2] in 2016 to address generalized pantograph equations, and the Fibonacci operational method by Koc et al. [1] in 2013 to address FDEs. Bessel's operational matrix, Legendre operational matrix, and Chebyshev operational matrix are some of the operational matrices that have been produced recently in the field of fractional-order partial differential equations (FPDEs). Notably, Fibonacci polynomials' operational matrix has proven to be more accurate than orthogonal polynomials', and because of its effectiveness in managing a high number of zeros, it has also been shown to greatly reduce computing time. When solving Fibonacci polynomials-based FPDEs, the novel method

*Corresponding Author Institutional Email:
mohammed1995676@gmail.com (Mohammed Hamza Mohammed)

of approximating a variable's integer-order power independently of its fractional power has demonstrated to produce accurate derivative computations. Fibonacci polynomials provide more accurate solutions for FPDEs than orthogonal polynomials, even at lower degrees, demonstrating their scientific significance over other approaches.

Turning our attention to the vital role that water plays in supporting life, just a small amount of the Earth's surface is actually readily accessible as fresh water, despite the fact that water covers a vast portion of its surface. Water contamination can result from pollution from a variety of sources, affecting both surface and groundwater sources. Whereas groundwater contamination is caused by the seepage of artificial materials such as oil, gasoline, road salt, chemicals, fertilizers, and pesticides, which can have a negative impact on water quality. surface water pollution is usually caused by wastewater discharge. In order to solve the difficulties of solving time-fractional equations involving advection, diffusion, and reaction in such contaminated water systems, a unique numerical method has been presented. This method shows promise for addressing environmental issues. One basic mathematical model that is widely used in scientific and engineering sectors for computer simulations is the advection-reaction-diffusion equation (ARDE). It is used in many different domains, including chemical reactions, mass and energy movement, global weather prediction, and oil reservoir simulations. Molecular diffusion is the process by which solute molecules diffuse across a fluid. This happens when solute molecules randomly collide with fluid molecules, causing a flux from areas of higher concentration to areas of lower concentration. The advective term describes the bulk migration of solute particles in the direction of fluid flow at a rate equal to the fluid velocity. In addition to advective transport, molecular diffusion is another way that the solute spreads in porous media. Bear and Bachmat [3] state that the tortuosity of the medium and the diffusion coefficient of the particular solute in water determine the coefficient of molecular diffusion in an isotropic media. Interestingly, the rate of molecular diffusion advances even in the absence of fluid movement and is independent of groundwater velocity.

Many models and techniques have been developed over time to address the problem of groundwater contamination. To illustrate the transfer of contamination in biological, chemical, and radioactive processes, Younes [4] presented the Eulerian Lagrangian localized adjoint approach with a moving grid in 2005 for resolving nonlinear ARDE in one dimension. An analytical solution to an advection-diffusion equation with variable coefficients characterizing solute transport in porous media was given by Ahmed et al. [5]. Guerrero et al. [6] developed a method in 2009 to get analytic solutions for multi-species contamination transport controlled by sequential fractional-order equations in finite mediums by using traditional integral transform techniques. Enhancing the understanding and solution of complex dynamics related to advection, diffusion and interaction processes. The main goal of this work was by developing a new numerical approach to the nonlinear fractional ordering of ARDE spacetime:

$$\frac{d^{\alpha}u(x,t)}{dt^{\alpha}} = u(x,t)\frac{d^{\beta}u(x,t)}{dt^{\beta}} - v\frac{du(x,t)}{dx} + ku(x,t) \qquad (1)$$
$$0 \le x \le 1, 0 < \alpha \le 1, 1 < \beta \le 2$$

with initial and boundary conditions as

$$u(x,0) = \psi_1(x), 0 \le x \le 1 \qquad (2)$$

$$u(0,t) = \psi_2(t), t > 0 \qquad (3)$$

$$u(1,t) = \psi_3(t), (t)t > 0 \qquad (4)$$

The equation u(x, t), where the parameters A and ß stand for the corresponding fractional-order derivatives of time and space, represents the solute concentration in the fluid at position x and time t. The variable v represents the fluid's constant velocity in the x-direction, and the symbol k stands for the coefficient of the source/sink term, which is responsible for the solute's production or loss in the system. Moreover, the known functions Ψ1(x), Ψ2(t), and Ψ 3(t) indicate the initial distribution of solute concentration and the concentration at the medium's border points at any given time t. The fractional-order advection-reaction-diffusion equation (ARDE) is reduced to the standard ARDE with a nonlinear diffusion term when A = 1 and ß = 2. In the fluid domain, the solute concentration rises when this nonlinear diffusive factor is added in comparison to the linear diffusion equation. The diffusive term's positive exponent of u(x, t) causes slower diffusion rates than what is expected from a conventional linear diffusion scenario, which raises the fluid's solute concentration. In porous media systems, the contrast between slow and fast diffusion processes is highly relevant. Consequently, in comparison to a linear model, the existence of a nonlinear element in the diffusivity component is significant from a physical standpoint. This feature has motivated academics to work on nonlinear fractional-order porous media issues, highlighting how crucial it is to handle these kinds of difficulties in system dynamics.

The above-mentioned attributes and factors have spurred the creation of a new numerical technique intended to efficiently solve the time-fractional equation including the system's advection, diffusion, and reaction processes.

While solving Eq. (1), we have concentrated on using Dirichlet boundary conditions in our study.However, one can also employ well-posed and ill-posed Neumann and Cauchy boundary conditions for this purpose. In their research, Deng et al. [7] have thoroughly investigated the well-posedness of fractional diffusion models with various boundary conditions. Three types of spectrum methods—the collocation, Galerkin, and Tau methods—have reportedly been used to solve two-dimensional problems numerically in the literature.

By applying the chosen spectral approach to the solution, which is stated as a series of polynomials, such as ∑aijØiØj, where Ø is a set of polynomials, the coefficients are obtained using spectral methods. The residues corresponding to partial differential equations (PDEs) in the collocation method must be zero at specified collocation points. Applying boundary conditions comes first in the Tau technique, which expands the residual function into a polynomial series. The Galerkin technique first selects basis functions that meet the initial and boundary criteria, and then it verifies that the residual is orthogonal to the selected basis functions.

In this work, we have attempted to solve the space-time fractional-order advection-reaction-diffusion problem, Eq. (1), by the use of its operational matrices and the Fibonacci collocation approach. Using example figures that correspond to particular circumstances, the effect of the reaction term on the solution profile under various parametric values of 'a' and 'ß'—which take into account the existence or absence of the advection term—is explained.

2. TF-ADR and SF-ADR MODEL SOLUTIONS

We obtained fractional ordinary differential equations by trans\forming the original models (1) and (3) in [14, 15, 16, 17] by means of Lie homologies. The original equations can be solved using the answers to these simplified equations. The FracSym package [18, 19, 20, 21], implemented in MAPLE, was used to find the Lie point symmetries. For fractional differential equations based on fractional Riemann-Liouville derivatives, this approach automatically finds symmetries. With the help of this suggested approach, answers that could be difficult to find by directly integrating the original model can be found.

Fractional partial differential equations (FPDEs) are often solved analytically or numerically in the literature. As an alternative to integrating an FPDE, We were able to solve a first-order ordinary differential equation at a low computational cost because it requires a simple initial condition. We summarize the main conclusions from [14, 15, 16, 17] in this section, to help identify solutions for the TF-ADR and SF-ADR simulations.

Based on the paper “A New Mathematical Process for Resolving the Fractional Time Equation of Advection, Diffusion and Reaction” the introduction to the chapter “Solutions to TF-ADR and SF-ADR Prototypes” has been rewritten in English.

2.1 The Model of Time Fraction

The infinitesimal Eq. (5) representing Lie symmetries accepted by the TF-ADR equation has been studied in [22].

$$\xi 1 = 0\ \xi 2 = a1,\ \eta = \chi(t, x) + a2\ u, \qquad (5)$$

Meanng:

(\xi_1 = 0, \xi_2 = a_1) :

(\xi_1): This usually corresponds to the coefficient of the time variable ((t)) in a transformation. In this case, (\xi_1 = 0) indicates that there is no dependency on time in the symmetry or transformation being analyzed.

(\xi_2): This typically represents the coefficient of the spatial variable ((x)) in the transformation or symmetry. Here, (\xi_2 = a_1) means that the spatial variable (x) depends linearly on a parameter (a_1), which could be a scaling factor or a parameter related to the transformation.

\ )eta = \chi(t, x) + a_2 u:(

(\eta): This variable typically represents the transformed or modified dependent variable (for example, in a PDE or transformation context, it could be (u(t, x)), the primary variable of interest).

(\chi(t, x)): This is a function of the independent variables (t) (time) and (x) (space). It serves as a general term or a function that depends on the independent variables.

(u): This often refers to the solution or dependent variable in, say, a PDE. Scaling (u) by (a_2) means that (u) gets multiplied by a constant (or parameter) (a_2).

The expression (\eta = \chi(t, x) + a_2 u) combines the effect of (\chi(t, x)) and (u), showing that (\eta) incorporates both a general component ((\chi)) based on (t) and (x), and a contribution from (u), scaled by the parameter (a_2).

When the constraint is satisfied by the function

φ = φ(t, x).

$$\begin{aligned} d_t^\alpha X - k_1 d_{xx} X + k_2 d_x X + \alpha_1 d_x f(.;\alpha) \\ + d_u f(.;\alpha)(X + \alpha_2 u) - \alpha_2 f(.;\alpha) \\ = 0 \end{aligned} \qquad (6)$$

If we impose A1 = 1 we get the following lie point transformation

$T = t,\ U = u(t,x)e^{-\alpha_2 x} - \int e^{-\alpha_2 x} X(t,x)dx$ we (7)

obtain the solution by the transformation Eq. (12),

(8)

$$u(t,x,\alpha) = e^{\alpha_2 x}\left(U(t) + \int e^{-\alpha_2 x} X(t,x)dx\right)$$

And the source term by integration of Eq. (11), $f(.;\alpha) = e^{\alpha_2 x}(\emptyset(t,U) - \int e^{-\alpha_2 x}(d_t^\alpha X(t,x) - k_1 d_{xx} X(t,x) + k_2 d_x X(t,x))d_x)$ (9)

The resolution and foundation terminology of the TF-ADR system (taking (lect= k_1 A^2 - k_2) and (Θ (t, U)) being a random purpose of its arguments) are represented by (u(t, x; α))) and (f(t, x, u; α)), respectively.

Therefore, equation (1) can be reduced to the succeeding slight nonlinear regular variance calculation by using transformation (6) and the preceding form of (f(. ; α)).

$$D_T^\alpha U(T) - a_2 \leftthreetimes U(T) + \emptyset\big(T, U(T)\big) = 0 (10)$$

By choosing an arbitrary function (Θ (T, U(T))) which modifies the basis terminology (f (t, x, u; α)) and the solution modules set via (6) the solution of equation (15) is defined.

In the particular scenario where (Ø (T, U(T)) = Ø *(T) + C_2U(T)), Ordinary fractional differential equation (15) can be expressed as:

$$D_T^\alpha U(T) + (c_2 - a_2 \leftthreetimes)U(T) + \emptyset^*(T) = 0 (10)$$

And under non-vanishing initial conditions

$$[D_T^{\alpha-1} U(T)]_{T=0} = b_1 \qquad (11)$$

Its precise solution, found in [8], is expressed in terms of the Mittag Leffler purpose,

$$U(T) = b_1 T^{a-1} E_{a,a}\big((a_2 \leftthreetimes - c_2)T^a\big) - \int_0^T (T-S)^{a-1} E_{a,a}\big((a_2 \leftthreetimes - c_2)(T-S)^a\big)\emptyset^*(S)dS \qquad (12)$$

Were

$$E_{a,a}(t) = \sum_{k=0}^{\infty} \frac{t^k}{\mathcal{T}(a(k+1)}$$

And the basis terminology is given by

$f(.;a) = c_2 u + k_1 d_x X(t,x) + e^{\alpha_2 x}\big(\emptyset^*(t) - \int e^{-\alpha_2 x}\big(c_2 X(t,x) + d_t^a X(t,x) - \leftthreetimes d_x X(t,x)\big)dx\big)$ (13)

2.2 The Space Fractional Model

Specifically, the following SF–ADR equation (3) infinitesimals were found in [9]

ξ1 = ˜A1, ξ2 = 0, η = ˜χ(t, x) + ˜a2u

everywhere the parameters ˜a1 and ˜A2 and the function ˜χ = ˜χ(t, x) satisfy the restraint

$d_t\tilde{X} - k_1 d_{xx}^{\beta+1}\tilde{X} + k_2 d_x \tilde{X} + \tilde{a}_1 d_t f(.;\beta) + \big(\tilde{X} + \tilde{a}_2 u\big)d_u f(.;\beta) - \tilde{a}_2 f(.;\beta) = 0$ (14)

We obtain the following transformation through the assumed symmetries ˜A1 = 1

$$X = x, \qquad V = u(t,x)e^{-\widetilde{a_2}t} - \int e^{-\widetilde{a_2}t}\tilde{X}(t,x)dt \qquad (15)$$

Thus, we obtained the precise solution to the fractal space problem

$$u(t,x;\beta) = e^{\tilde{a}2t}\big(V(x) + \int e^{-\tilde{a}2t}\tilde{X}(t,x)dt\big) \qquad (16)$$

and, by

$$f(.;\beta) = e^{-\tilde{a}2t}\Big(\tilde{\emptyset}(x,V) - \int e^{-\tilde{a}2t}\big(d_t\tilde{X}(t,x) - k_1 d_x^{\beta+1}\tilde{X}(t,x) + k_2 d_x \tilde{X}(t,x)\big)dt\Big) \qquad (17)$$

We can set (u(t, x; β)) and (f(t, x, u; β))) as the resolution and basis term of the SF-ADR system, using a stochastic function for its parameters as (φ (x, V)).

The SF-ADR equation (3) has also been simplified to the fractional ordinary differential equation through the transformation in equation (15) and the preceding formulation of (f(. ; β)):

$$-k_1 D_X^{\beta+1}V(X) + k_2 D_X V(X) + \tilde{\emptyset}\big(X, X(X)\big) + \tilde{a}_2 V(X) = 0 \qquad (18)$$

The solution of equation (24), which can be customized with the right choice of ˜χ = ˜χ (t, x), defines the random-roles φ (X, V(X)). This, in line, determines the categories of solutions and the basis terminology (f(t, x, u; β))

In particular, setting

$$\tilde{\emptyset}\big(X, V(X)\big) = -k_1 D_X \emptyset^{**}(X) - \tilde{a}_2 V(X) \qquad (19)$$

we get

$$\boldsymbol{D_X^{\beta}V(X)} - \boldsymbol{\frac{k_2}{k_1}V(X)} + \emptyset^{**}\boldsymbol{(X)} = 0 \quad (20)$$

Whose precise answer, with respect to non-vanishing boundary conditions

$$\left[D_X^{\beta-1}V(X)\right]_{X=0} = \tilde{b}_1$$

is the following

$$V(X) = \tilde{b}_1 X^{\beta-1} E_{\beta,\beta}\left(\frac{k_2}{k_1}X^{\beta}\right) - \int_0^X (X - S)^{\beta-1} E_{\beta,\beta}\left(\frac{k_2}{k_1}(X-S)^{\beta}\right)\emptyset^{**}(S)dS \quad (21)$$

Where

$$E_{\beta,\beta}(x) = \sum_{k=0}^{\infty} \frac{x^k}{\mathcal{T}(\beta(k+1))}$$

is the Mittag Leffler function [8] and the source terminology states.

$$f(\cdot;\beta) = -\tilde{a}_2 u$$
$$-e^{\tilde{a}2t}\left(k_1\emptyset_x^{**}(x) + \int e^{-\tilde{a}2t}\left(-\tilde{a}_2\tilde{X} + d_t\tilde{X}(t,x) - k_1 d_x^{\beta+1}\tilde{X}(t,x) + k_2 d_x\tilde{X}(t,x)\right)dt\right) \quad (22)$$

We denote the resolution and the basis term for the SF–ADR system as u(t, x; β) and f(t, x, u; β), respectively, with φ (x, V) as a random-purpose of its arguments. The SF–ADR problem (3) was reduced to the subsequent slight regular variance calculation by using conversion (21) and the original form of (f.; β) Rewrite to suit the heading: A new computational technique for solving the time-fractional equation of advection, distribution, and response

$$-k_1 D_X^{\beta+1}V(X) + k_2 D_X V(X) + \tilde{\emptyset}\left(X, V(X)\right) + \tilde{a}_2 V(X) = 0 \quad (23)$$

Solving calculation (23), the solution is defined by choosing arbitrary functions φ˜ (X, V(X)) where with the appropriate selection of ˜ χ = ˜ χ (t, x) assigns the basis term f(t, x, u; β) and solution modules.

Specifically, rewrite to suit the heading: A novel numerical technique for solving the time fractional equation of diffusion, and reaction

$$\tilde{\emptyset}\left(X, V(X)\right) = -k_1 D_X \emptyset^{**}(X) - \tilde{a}_2 V(X) \quad (24)$$

we get

$$D_X^{\beta}V(X) - \frac{k_2}{k_1}V(X) + \emptyset^{**}(X) = 0$$

Whose precise answer, with respect to non-vanishing boundary conditions

$$\left[D_X^{\beta-1}V(X)\right]_{X=0} = \tilde{b_1} \quad (25)$$

is the following

$$V(X) = \tilde{b}_1 X^{\beta-1} E_{\beta,\beta}\left(\frac{k_2}{k_1}X^{\beta}\right) - \int_0^X (X - S)^{\beta-1} E_{\beta,\beta}\left(\frac{k_2}{k_1}(X-S)^{\beta}\right)\emptyset^{**}(S)dS \quad (26)$$

$$f(.;\beta) = -\tilde{a}_2 u$$
$$-e^{\tilde{a}_2 t}\left(k_1\emptyset_x^{**}(x) + \int e^{-\tilde{a}_2 t}(-\tilde{a}_2\tilde{X} + d_t\tilde{X}(t,x) - k_1 d_x^{\beta+1}\tilde{X}(t,x) + k_2 d_x\tilde{X}(t,x)\right)dt) \quad (26)$$

3. TIME and SPACE FRACTIONAL MODEL SOLUTIONS

This division examines the TSF–ADR equation's Lie symmetries

$$d_t^a u(t,x) - k_1 d_{xx}^{\beta+1}u(t,x) + k_2 d_x u(t,x) + f(t,x,u;a,\beta) = 0,\ 0 < a,\beta \le 1 \quad (27)$$

The infinitesimal generators listed below describe the Lie symmetries that are admitted by (27)

ξ1 = 0, ξ2 = 0, η = ¯ χ(t, x) + ¯ a2u (28)

Everywhere the constraint is satisfied by the purpose χ = ¯ χ(t, x)

$$d_t^a\bar{X} - k_1 d_{xx}^{\beta+1}\bar{X} + k_2 d_x\bar{X} + (\bar{X} + \bar{a}_2 u)d_u f(.;a,\beta) - \bar{a}_2 f(.;a,\beta) = 0 \quad (29)$$

The method described in [9] does not work since the symmetries recognized by equation (27) have infinitesimal (28) preventing the transformation that transforms the TSFADR equation into a fractional normal equation. Based on the data presented in the above section we present a substitute method to get the mathematical resolution. And the analytical prototypical of TSF-ADR.

Let us now examine u(t, x; α; β) as the resolution to the TSF–ADR equation provided by

$$u(t,x;a;\beta) = A\,u(t,x;a) + B\,u(t,x;\beta)$$

the solutions produced by the transformations (12) and (20) are combined linearly

$$u(t,x;a) = e^{a_2 x}U(t) + e^{a_2 x}\int e^{-a_2 x}X(t,x)dx$$

$$u(t,x;\beta) = \quad e^{\tilde{a}_2 t}V(x) + e^{\tilde{a}_2 t}\int e^{-\tilde{a}_2 t}X(t,x)dx \qquad (30)$$

where, we put χ = ˜ χ, consequently we take

$$u(t,x;a;\beta) = A\, e^{a_2 x}U(t) + A\, e^{a_2 x}\int e^{-a_2 x}X(t,x)dx + B\, e^{\tilde{a}_2 t}V(x) + B\, e^{\tilde{a}_2 t}\int e^{-\tilde{a}_2 t}X(t,x)dt \qquad (31)$$

where the solutions to the simplified equations (14) and (23), respectively, are U(t) and V (x)

We get that the resolution of the TSF-ADR prototypical when the basis terminology f(t, x, u; α; β) is a lined amalgamation of 2 roles (29)

$$\mathrm{f(t,x,u;\ \alpha;\ \beta)} = A f_1\mathrm{(t,x,u;\ \alpha;\ \beta)} + B f_2\mathrm{(t,x,u;\ \alpha;\ \beta)}$$

given by

$$(32)$$

$$f_1\mathrm{(t,x,u;\ \alpha;\ \beta)} = e^{a_2 x}\Big(\emptyset\big(t,U(t)\big) - \int e^{-a_2 x}\left(d_t^a X(t,x) + k_2 d_x X(t,x)\right)d_x\Big) + k_1 d_x^{\beta+1}\left(e^{a_2 x}\int e^{-a_2 x}X(t,x)dx\right) + k_1 a_2\left(a_2 e^{a_2 x} - x^{-\beta}E_{1,1} - \beta(a_2 x)\right)U(t)$$

$$f_2\mathrm{(t,x,u;\ \alpha;\ \beta)} = e^{\tilde{a}_2 t}\Big(\tilde{\emptyset}\big(x,V(x)\big) - \int e^{-\tilde{a}_2 t}\left(-k_1 d_x^{\beta+1}X(t,x) + k_2 X_x(t,x)\right)d_t\Big) - d_t^a\left(e^{\tilde{a}_2 t}\int e^{-\tilde{a}_2 t}X(t,x)dt\right) + \left(\tilde{a}_2 e^{\tilde{a}_2 t} - t^{-a}E_{1,1} - a(\tilde{a}_2 t)\right)V(x)$$

We observe that terms including β are smaller than f1(t, x, u; α, β) equals f (t, x, u; α) (14) and terms involving β are less than f2(t, x, u; α, β) equals f (t, x, u; β) (23). In fact, if c = 1, we have

$$f1\,(t,x,u;\ \alpha;\ \beta)|_{\beta=1} \quad (33)$$
$$= e^{a_2 x}\Big(\emptyset\big(t,U(t)\big) - \int e^{-a_2 x}\left(d_t^a X(t,x) + k_2 d_x X(t,x)\right)d_x\Big) - k_1\left(e^{a_2 x}\int e^{-a_2 x}\,d_{xx}X(t,x)dx\right)$$

and if α = 1

$$f2\,(t,x,u;\ \alpha;\ \beta)|_{\alpha=1}$$
$$= e^{\tilde{a}_2 t}\Big(\tilde{\emptyset}\big(x,V(x)\big) - \int e^{-\tilde{a}_2 t}\left(-k_1 d_x^{\beta+1}X(t,x) + k_2 X_x(t,x)\right)d_t\Big) - \left(e^{\tilde{a}_2 t}\int e^{-\tilde{a}_2 t}\,d_t X(t,x)dt\right)$$

Specifically, using the definitions in (2) and (4), for β = 1 and α = 1, $\partial^t_\alpha = \partial t$ and $\partial x^{\beta+1} = \partial_{xx}$, respectively. Next, we have

$$f_1(t,x,u,a,\beta)|\beta = 1 = f(t,x,u,a)$$
$$f_2(t,x,u,a,\beta)|a = 1 = f(t,x,u,\beta)$$

That is, we can use these resolutions to catch a solution for the TSF model. ADR, if f(t, x, u, α) and f(t, x, u, β) are the source terminologies for the resolutions of SF-ADR and TF-ADR which are known to us.

4. FROM the STANDARD ADR MODEL to the TSF-ADR MODEL

Appropriate assumptions were made for Any functions χ(t, x) , φ (x, V), φ (t, U) and based on the results from previous sections. As a result, a specific physical problem might be defined with an appropriate source term, enabling the extraction of the matching traditional ADR model as the TSFADR model's limit. Next, in order to obtain, we choose χ(t, x), and φ(t, U), φ˜ (x, V) in section

$$f(t,x,u;a)|_{a=1} = f(t,x,u;\beta)|_{\beta=1} = f(t,x,u) \quad (34)$$

so that the terms of the combination in linear form (31) fulfill the following as a result of (32)

$$f1(t,x,u;a,\beta)|_{a=1,\beta=1} = f(t,x,u)$$
$$f2(t,x,u;a,\beta)|_{a=1,\beta=1} = f(t,x,u)$$

Finally, we obtain assuming A + B = 1 (35)

$$f(t,x,u;a,\beta)|_{a=1,\beta=1} = f(t,x,u)$$

This means that the basis term of TSF-ADR is equivalent to the role f(t, x, u) of the conventional ADR system when α=1 and β= 1.

$$dt_u(t,x) - k_1 d_{xxu}(t,x) + k_2 d_{xu}(t,x) + f(t,x,u) = 0 \quad (36)$$

Considering that we do not recognize the exact formula of the resolution (29), (it is obtained through the set of linear solutions (30) for α = β = 1) and therefore we are unable to show the relationship amongst the resolution of the TSF-ADR prototypical and the resolution of the ADR system. In the subsequent analysis, we employ a numerical method to demonstrate that the TSF–ADR model's solution (29) has the same limit as the ADR model's solution.

5. THE NUMERICAL METHOD

Here, we provide the numerical outcomes of applying the suggested method to get TSF-ADR model answers that are connected to precise ADR model solutions. The method was presented in [10, 11], where a number of numerical tests were used to confirm the procedure's accuracy and efficiency with respect to the answers produced for the SF-ADR and TF-ADR models. Using the same methods in the current work, numerical solutions for the SF – ADR , TF – ADR models were derivedwhich allows mathematical resolutions of the TSF-ADR system to meet the required conditions (32).
We now provide a brief overview of the procedure. We begin by independently solving the two simplified equations (14) and (23). We apply transformations (12) and (20) to the numerical solutions we find satisfactory to develop estimated resolutions for the SF-ADR system (3) and the TF-ADR system (1). The two discovered numerical solutions are then combined to get the mathematical resolution for the TSF-ADR system (5), as mentioned (29). Finally, we show that when α → 1 and β → 1 the solutions of the TSF-ADR model typically agree with the ADR model.
We decided to examine Caputo's method, which contains the numeral-order results of the indefinite purposes in minimum time at their limit values, i.e. has the fundamental benefit of
having initial conditions similar to those of integer-order differential equations.
We go over how Caputo's fractional derivative is explained.

$$* D_T^a U(T) = \frac{1}{\mathcal{T}(1-a)} \int_0^T \frac{1}{(T-S)^a} \frac{d}{dS} U(S) dS \quad (37)$$

and its connection to the fractional derivative of Riemann-Liouville

$$* D_T^a U(T) = D_T^a \big(U(T) - U(0)\big), \qquad 0 < a < 1$$

U(0) is the starting point. The fractional time equation (15) can be expressed, based on the relationship amid the Riemann-Liouville and Caputo results, in the following way:

$$D_T^a U(T) + \frac{U(0)}{\mathcal{T}(1-a)T^a} - a_2 \leftthreetimes U(T) + \emptyset\big(T, U(T)\big) = 0 \quad 0 < a < 1 \quad (38)$$

The RL derivative and the Kabuto derivative are equal under homogeneous starting conditions, where the typical factor of the Kabuto derivatives is ∗DαT [8].
We also reformulated the fractional space equation (23) in terms of the Caputo resultant using the same assumptions

$$k_1^* D_X^{\beta+1} V(X) + \frac{V(0)}{\mathcal{T}(1-\beta)X^\beta} - k_2 D_X V(X) - \tilde{a}_2 V(X) - \tilde{\emptyset}\big(X, V(X)\big) = 0 \quad (39)$$

When it is not possible to determine the logical resolutions U(T) and V (X), a numerical method must be employed. In this instance, we offer a numerical scheme, the 2nd direction contained trapezoidal process (TR), It is frequently used to solve linear and nonlinear fractional ordinary differential equations as it is an oversimplification of the standard implied trapezoid technique on fractional ordinary differential equations (FODEs). See the papers [12, 13] for the technical specifics of the suggested approach. A nonlinear equation must be solved each time fractional ordinary differential equations are integrated using the numerical approach.Thus, a nonlinear equation solution methodology, such as the conventional Newton method, must be used.
One of the most widely used iterative methods is Newton's. It requires evaluating the Jacobian matrix at each iteration, which can be done analytically if the processing cost is too high. Alternatively, it can be computed numerically. It is analytically assessed for each example in this work, and numerical answers are achieved with an equal number of iterations. Using MatLab software, the suggested numerical technique is implemented on an Intel Core i5.
In order to test the suggested method, we appropriately select the arbitrary functions in the following. As a result, we can obtain analytical solutions and compare them with numerical solutions.

We set

$$\varphi(t,U) = \varphi * (t) + c_2 U(t)\tilde{\varphi}(x,V) = -k_1 D_x \varphi^{**}(x) - \tilde{a}_2 V(x) \quad (40)$$

for the analytical solution to equations (36) and (37) to be provided in Mittag-Leffler functions in terms (17) and (26). As a result, we also get the TSF-ADR equation's analytical solution (29) (5).
The presented numerical test results confirm the efficacy and dependability of the suggested technique based on the assessment of estimated and precise resolutions for a variety of grid facts and the fractional order standards of the results α and β, which showed a high degree of accuracy.

6. FRACTIONAL-ORDER ADVECTION REACTION DIFFUSION EQUATION SOLUTION FOR SPACE–TIME

The authors have attempted to use the suggested numerical technique in Sect. 5 after confirming its efficacy, efficiency, and correctness. The method will be used to solve the space-time fractional-order ARDE under the initial condition

u(x,0) = x(1-x)

and boundary conditions

u(0,t) = 0, u(1,t)=0

Now, to solve the ARDE using the proposed numerical method let us approximate u(x, t) by Fibonacci polynomial as

$$u(x,t) \cong \emptyset^T(x) C \emptyset(t) \quad (41)$$

Where

$$C = \begin{pmatrix} c_{11} & c_{12} & \cdots & \cdots & c_1 n + {}_1 \\ c_{21} & c_{22} & \cdots & \cdots & c_1 n + {}_1 \\ \vdots & \vdots & & \ddots & \vdots \\ cn_1 & cn_2 & & \cdots & cn + {}_1 n + {}_1 \end{pmatrix}_{(n+1)\times(n+1)}$$

$$\begin{aligned} R(x,t) &= t^{(-a)} \emptyset^T(x) C M^a \emptyset(t) \\ &- x^{-\beta} (\emptyset^T(x) C \emptyset(t)) (\emptyset^T(x) \left(M^\beta\right)^T C \emptyset(t) \\ &+ v\left(\emptyset^T(x)(M^1)^T C \emptyset(t)\right) - k(\emptyset^T(x) C \emptyset(t)) \end{aligned}$$

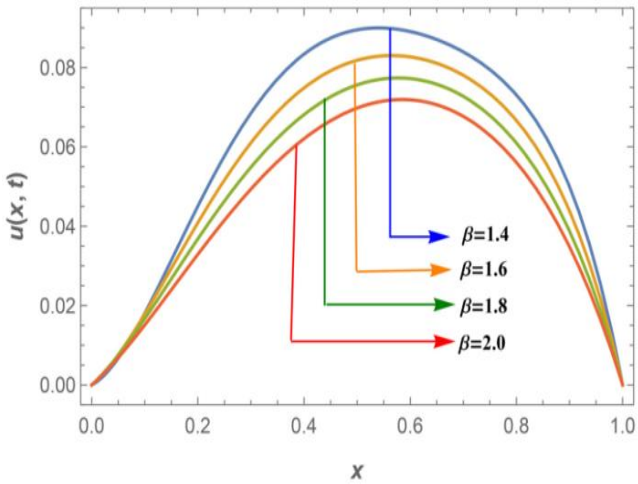

Figure 1. Variations of the conservative system's u(x, t) versus x at t = 0.6 when v = 0.2

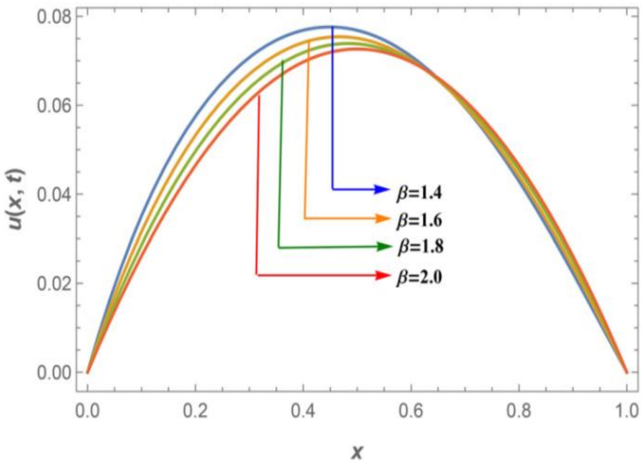

Figure 2. Variations of the conservative system's u(x, t) vs x at t = 0.6 for v = 0

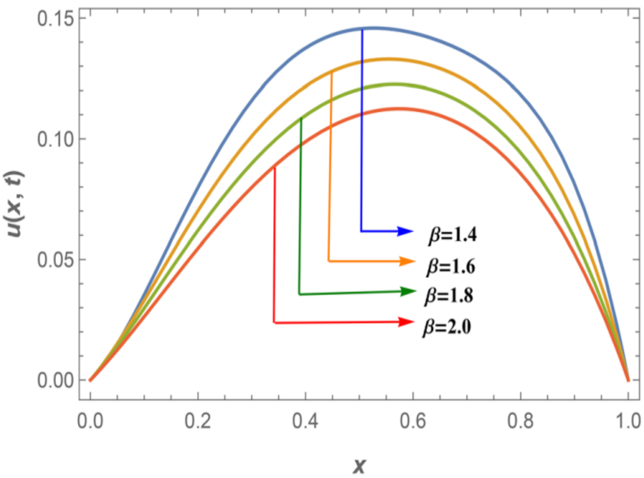

Figure 3. Variations of the nonconservative system's u(x, t) vs x at t = 0.6 for v = 0

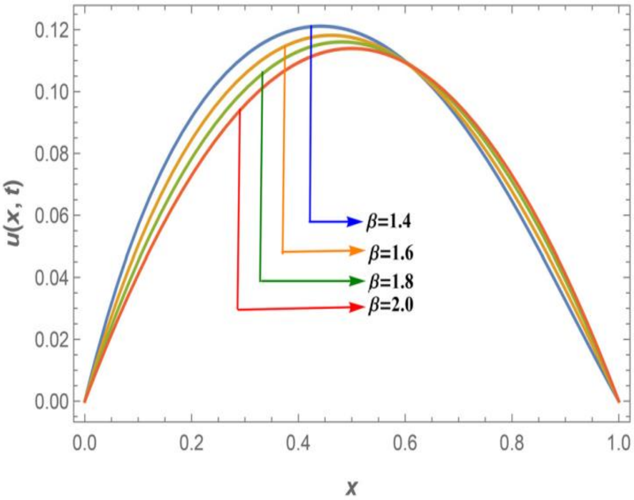

Figure 4. Variations of the nonconservative system's u(x, t) vs x at t = 0.6 for v = 0.2

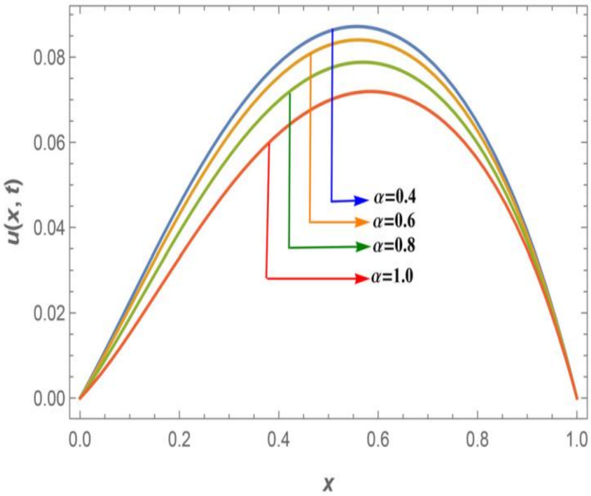

Figure 5. Variations of the conservative system's u(x, t) vs x at t = 0.6 for v = 0.2

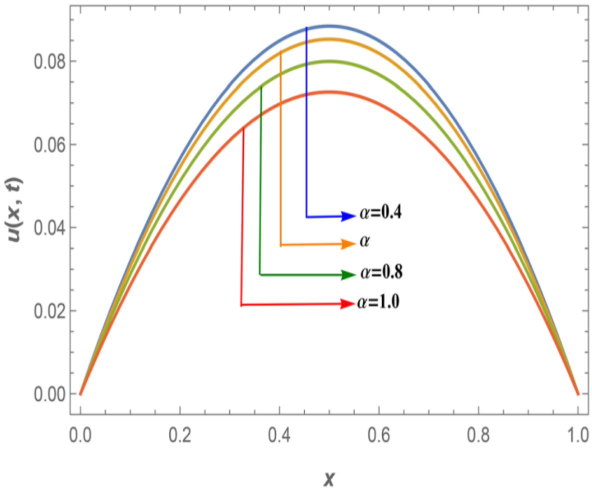

Figure 6. Variations of the conservative system's u(x, t) vs x at t = 0.6 for v = 0

h = 1, 2, 3,..n. To collocate the boundary conditions, x = 1 and t = 1 must be included in addition to these points. At last, we have an algebraic equation system of $(n+1)^2$ numbers of unknowns, which can be solved using Newton's method.
MATHEMATICA software is utilized to acquire numerical results for n = 7.

7. RESULTS and DISCUSSION

This section's Figs. 1–6 show the numerical solute concentration values in the presence and absence of advection and reaction terms, along with changes in the temporal parameter a while maintaining the spatial parameter b fixed, as well as changes in b for a fixed a.
In order to demonstrate the impact of the advection term, the changes of u(x, t) versus x at t = 0.6 are shown in Figs. 1-2 and 3–4 for the conservative system (k = 0) and the nonconservative system (k = 1), respectively, maintaining a = 1 and ß = 1.4(0.2) 2.0. It can be observed that in both systems when there is an advection term present, u(x, t) drops as b increases, but subsequently the converse happens.
Moreover, it is observed that in the case of a nonconservative system, the sink term (k = 1) causes damping. Once more, for both conservative and nonconservative systems, the solute concentration translations are easily observed with the fluid velocity (v = 0.2) and without any alteration to the curves' slopes.
The changes of u(x, t) for conservative and nonconservative systems, assuming ß = 1 and a = 0.4(0.2) 1.0, are depicted in Figures 5–6 with x at t = 0.6. The figures have resemblance to earlier instances, with the exception of variations in overshoots.

8. CONCLUSION

In this study, based on the outcomes of the SF-ADR and TF-ADR models, we describe a strategy for solving the TSF-ADR model. By bearing in mind the lined fusion of the resolutions of the SF-ADR and FT-ADR systems, we can then determine the model solutions.
We use a numerical method that is frequently used to solve lined and nonlinear models of small regular variance calculations. Mathematical testing and error exploration provide closeness classification as evidence of the correctness, efficacy and dependability of the recommended approach.

9. REFERENCES

1. Koc¸, A. B., C¸akmak, M., Kurnaz, A., and Uslu, K., 2013, “A New Fibonacci Type Collocation Procedure for Boundary Value Problems,” Adv. Differ. Equa- tions, 2013(1), p. 262.
2. Abd-Elhameed, W. M., and Youssri, Y. H., 2016, “A Novel Operational Matrix of Caputo Fractional Derivatives of Fibonacci Polynomials: Spectral Solutions of Fractional Differential Equations,” Entropy, 18(10), p. 345.
3. Bear, J., and Bachmat, Y., 1967, “A Generalized Theory on Hydrodynamic Dis-persion in Porous Media,” IASH Symposium on Artificial Recharge and Man- agement of Aquifers, Vol. 72, IASH Publ. Int. Union Geod. Geophys., Haifa, Israel, pp. 7–16.
4. Younes, A., 2005, “A Moving Grid Eulerian Lagrangian Localized Adjoint Method for Solving One-Dimensional Nonlinear Advection-Diffusion-Reaction Equations,” Transp. Porous Media, 60(2), pp. 241–250.
5. Ahmed, M., Zainab, Q. U. A., and Qamar, S., 2017, “Analysis of One-Dimensional Advection–Diffusion Model With Variable Coefficients Describing Solute Trans- port in a Porous Medium,” Transp. Porous Media, 118(3), pp. 327–344.
6. Guerrero, J. S. P., Skaggs, T. H., and Van Genuchten, M. T., 2009, “Analytical Solution for Multi-Species Contaminant Transport Subject to Sequential First-Order Decay Reactions in Finite Media,” Transp. Porous Media, 80(2), pp. 373–387.
7. Deng, W., Li, B., Tian, W., and Zhang, P., 2018, “Boundary Problems for the Fractional and Tempered Fractional Operators,” Multiscale Model. Simul., 16(1), pp. 125–149.
8. I. Podlubny. Fractional Differential Equations: an introduction to fracti- onal derivatives, fractional differential equations, some methods of their solution and some of their applications, Academic Press, San Diego, (1999).
9. A. Jannelli, M. Ruggieri and M. P. Speciale, Exact and Numerical Solutions of Time fractional Advection–diffusion Equation with a Nonlinear Source Term by means of the Lie Symmetries, Nonlinear Dynamics, (2018); doi: 10.1007/s11071-018-4074-8.
10. A. Jannelli, M. Ruggieri and M. P. Speciale, Analytical and Numerical Solutions of Fractional Type Advection-diffusion Equation, AIP Conference Proceedings 1863, 530005 (2017). doi: 10.1063/1.4992675.
11. A. Jannelli, M. Ruggieri and M. P. Speciale, Analytical and Numerical Solutions of Fractional Type Advection-diffusion Equation, AIP Conference Proceedings 1863, 530005 (2017). doi: 10.1063/1.4992675.
12. K. Diethelm. The Analysis of Fractional Differential Equations. Springer-Verlag Berlin Heidelberg, (2010).
13. R. Garrappa. Trapezoidal methods for fractional differential equations: Theoretical and computational aspects, Math. and Comput. in Simulation, 110, 96–112, (2015).
14. Heydari, Mohammad Hossein Et Al. “Numerical Treatment of The Space–Time Fractal–Fractional Model of Nonlinear Advection–Diffusion–Reaction Equation Through The Bernstein Polynomials.” Fractals (2020): 2040001.
15. Jannelli, Alessandra et al. “Numerical solutions of space-fractional advection-diffusion equations with nonlinear source term.” Applied Numerical Mathematics 155 (2019): 93-102.
16. Dwivedi, Kushal Dhar et al. “Numerical Solution of Nonlinear Space–Time Fractional-Order Advection–Reaction–Diffusion Equation.” Journal of Computational and Nonlinear Dynamics 15 (2020): n. pag.
17. Scotton, Jaque Willian Et Al. “Simulação Numérica Da Advecção-Difusão Unidimensional Empregando Um Modelo Com Derivadas Fracionárias.” (2020).
18. Jefferson, G. F. and John Carminati. “FracSym: Automated symbolic computation of Lie symmetries of fractional differential equations.” Comput. Phys. Commun. 185 (2014): 430-441.
19. Sethukumarasamy, K. et al. “On Lie Symmetry Analysis of Certain Coupled Fractional Ordinary Differential Equations.” Journal of Nonlinear Mathematical Physics (2021): n. pag.
20. Al-deiakeh, Rawya et al. “Lie symmetry analysis, explicit solutions, and conservation laws of the time-fractional Fisher equation in two-dimensional space.” Journal of Ocean Engineering and Science (2021): n. pag.
21. Singla, Komal and Rajesh Kumar Gupta. “Generalized Lie symmetry approach for fractional order systems of differential equations. III.” Journal of Mathematical Physics 58 (2017): 061501.
22. Fujita, Yasuhiro. “Integrodifferential Equation Which Interpolates The Heat Equation And The Wave Equation I(Martingales And Related Topics).” (1989).

Arabic Abstract

تم استخدام تحويلات نظرية لاي في هذه الدراسة لتوفير أجوبة رقمية وتحليلية على السواء لمعادلات التفاعل الجزئي - الانتشار - الالتصاق لكل من الزمان والمكان. و إذا كانت الأرصدة المسموح بها من خلال حسابات الهدف تسمح بتحديد تحويلات نظرية لاي، فهنا يمكننا خفض حسابات الفرق الكسرية الطفيفة إلى حسابات الفرق العادية التي تحتوي على الكسور. ونقترح نهجاً مختلفاً لإيجاد الإجابات العددية والتحليلية بدءاً من الإجابات العددية والتحليلية الموجودة في نموذج لفراكتل الزماني المكاني في تفاعل الالتصاق والانتشار. وبالنسبة للنتائج الأخيرة بشأن معادلة التفاعل بين الالتصاق والانتشار التي حصل عليها المؤلفون. فان معادلات تفاعلات التصاق ونشر منفصلة لمتغيرات وقتية ومكانية جزئية. والدقة الممتازة للنهج المقترح تجعله أداة مفيدة لحل فئة واسعة من مشاكل المعادلة التفاضلية الكسرية.
وتظهر النتائج العددية فعاليتها وامكانياتها وقابليتها للتطبيق

Pure Sciences International Journal of kerbala

PSIJK

Year: 2025 Volume : 2 Issue : 5 ISSN: 6188-2789 Print 3005 -2394 Online

2025, volume 2 , Issues 5 PSIJK 55-61

Pure Sciences International Journal of Kerbala
Journal Homepage:https://journals.uokerbala.edu.iq/index.php/psijk

On Pure Ideals: A Review

Mohammed Khalid Shahoodh*[1], Omare Kareem Ali[2], Montaser I. Adwan[3]

[1]Ministry of Education, General Directorate of Education in Ramadi, Anbar, Iraq
[2]Department of Applied Mathematics, College of Sciences, University of Anbar, Iraq
[3]Department of Mathematics, College of Education for Pure Sciences, University of Anbar, Iraq

P A P E R I N F O

Received: 11 November 2024
Accepted: 2 February 2025
Published: 31 March 2025

Keywords:
Pure ideals, Strongly Pure ideals, PIP-ring, PIGP-ring, MRGP-ring, Commutative ring.

A B S T R A C T

Ring theory is one of the branches of an abstract algebra. This field is the study of a mathematical system with two binary operations. In this branch, many articles have studied this algebraic structure and presented some new works. However, the concept of purity has been studied before more than 40 years ago, especially the relation between the pure ideal and some other ideals on the given ring. In this paper, we survey the important results that concern with pure ideals. Some different types of ideals have been discussed such as N-pure ideals, z-ideals, Π-pure ideals and strongly pure ideals. Moreover, some recent results based on the work of several researchers have been summarized. On the other hand, regarding these types of ideals, some questions have been presented. Furthermore, many important results about various types of rings which are based on the notion of pure ideals have been studied.

1. INTRODUCTION

An abstract algebra is one of the major branches in Mathematics. The name of algebra is mentioned in the book of the mathematician Muhammad ibn Musa al-Khwarizmi. An abstract algebra is a broader field, and this field is concerned with the study of algebraic structures and the relations between them. A number of articles have been reviewed in ring theory and others in group theory. In other words, some authors have been published their articles which concerned with specific topic in rings or groups. For instance, in 2005 Nicholson and Zhou in [1] presented such study in order to summarize the developments on the concept of clean rings. In their study, many results are presented for exchange ring (changing property), group rings, semi-boolean ring and the connection among C*-algebras and clean rings of continuous functions. In addition, they presented some results which concentrated on the strongly clean rings. Regarding these topics, they stated some questions, some of which have been answered and others are not. Furthermore, another study with different direction has been determined in [2]. This study was a survey on the strongly clean rings. Moreover, a brief survey paper on the rings generated by units has been presented in [3]. On the other hand, a short survey that emphasizes the theorems of Schur and Baer has been written in [4]. This study discussed some of the recent results that generalize these theorems. In this paper, we present a short survey on the notion of pure ideals with related concepts and discuss them in detail. The present paper is an attempt to provide some results that concerned pure ideals and their related concepts in a suitable way for everyone who has some basic information about this topic. According to our work, we are unable to find such study in the literature that has been published on this topic. Therefore, this study is conducted. Then, this study can be considered as a first step on this way and perhaps it will encourage others to provide and extend some works on this topic. The present article has been divided into two sections. In section two, we look at the pure ideals with some other types of ideals and the relations between them. In Section three, some types of rings based on the notion of pure ideals have been studied.

*Corresponding Author Institutional Email: moh861122@yahoo.com (Mohammed Khalid Shahoodh)

2. PURE IDEALS, Z-IDEALS, STRONGLY PURE IDEALS, N-PURE IDEALS, GP-IDEALS AND Π-PURE IDEALS

The study of pure ideals is going back to around fifty years ago. The references [5-8] are the first who worked on the concept of pure ideals. This concept has been developed and studied extensively by [9-12]. Many papers have tackled this notion by different ways. In this section, our attention has been paid to study the pure ideals with some other types of ideals and discussed the relation between them. As a starting point, an ideal ζ of Ṙ is said to be pure ideal (for short PI) if, for every $v \in \zeta$ there exist $u \in \zeta$ such that $v = vu$ or equivalence to, for any ideal ξ in Ṙ, we have $\zeta \cap \xi = \zeta\xi$ is hold. A paper by [13] studied this type of ideals in the ring of (bounded) real-valued, continues functions C(Γ) on the completely regular Hawsdorff space Γ. This way may give the connection between the functional analysis and an abstract algebra. An Artin-Rees property means, for every ideal $\zeta \in$ Ṙ there exist $n \in Z^+$ such that $\zeta^n \cap \xi \subseteq \zeta\xi$, then we say that ξ has Artin-Rees property. The author proved that, the sum of every two pure ideals is also pure ideal. This result can be generalized to a finite number of pure ideals. Besides, the author considered another type of ideals namely z-ideal. This ideal is defined as follows: an ideal ζ is said to be z-ideal if, for every $v \in \zeta$ there exist $\mathcal{H}_v$ (the intersection of all maximal ideals in the ring which containing v) such that $\mathcal{H}_v \subseteq \zeta$. Clearly, the pure ideals are z-ideals. But what about the convers?. In particular, when is every z-ideal is a pure ideal in the proposed ring C(Γ)?. It's clear that from the definition of pure ideal, every pure ideal in C(Γ) has Artin-Rees property. The author answered the mentioned question as follows: z-ideal in C(Γ) is pure ideal iff it has Artin-Rees property. Further, he characterized a space Γ in which every z-ideal of C(Γ) has Artin-Rees property. He proved the following statements are equivalent: (i) Every z-ideal of C(Γ) is pure, (ii) Γ is a P-space, and (iii) Every ideal of C(Γ) is pure.

Corollary 2.1 [13] Every z-ideal of C(Γ) has Artin-Rees property iff Γ is a P-space.

Corollary 2.2 [13] Every ideal of C(Γ) has Artin-Rees property iff Γ is a P-space.

Question 1: Is there a general presentation that can give the specific number of pure ideals and z-ideals in C(Γ)?.

On the other hand, in [14] it has been defined the right (left) strongly pure ideal as follows: An ideal ζ of Ṙ is strongly right (left) pure ideal (for short R(L)SPI), if $\forall v \in \zeta$ there exist a prime element $s \in \zeta$ in which $v = vs(v = sv)$. Clearly that every strongly pure ideal is a pure ideal but the convers need not to be true. Because, the prime element s in the ideal ζ is not always existed, for example in the ring of integers module 6, we have $(3) = \{0,3\}$ is a SPI of Z_6. However, $(2) = \{0,2,4\}$ is a PI of Z_6 but it's not SPI of Z_6. Because no prime element $s \in (2)$ in which $2 = 2 \cdot s$. Moreover, the author presented several properties of such types of ideals such as, if ζ is SPI of Ṙ, then $\xi\zeta = \xi \cap \zeta$ for every ideal ξ of Ṙ. Based on this result, it should be noted that SPI satisfying the Artin-Rees property. In other words, one can check through this direction, whether the connection between SPI and z-ideal is valid or not. Furthermore, the author proved any ideal generated by prime idempotent element is a SPI. Then, she generalized this property to a finite number of prime idempotent elements. The following proposition provided some necessary and sufficient conditions to get the SPI from PI.

Proposition 2.1 [14] Suppose Ṙ is a factorial ring with ζ be an ideal of Ṙ in which every non-zero and non-unit element of Ṙ is irreducible. Then, ζ is SPI iff ζ is PI.

Remarkably, the RSPI is not the left and the LSPI is not the right. This property has been checked in one direction by the same author. She presented a condition to get the RSPI from the LSPI. The condition which was given is to assume that Ṙ is a reduced ring. The mentioned result is given in the following proposition.

Proposition 2.2 [14] Suppose Ṙ is a reduced ring with ζ be any ideal of Ṙ. Then, ζ is a RSPI iff ζ is a LSPI.

Question 2: Is there a necessary and sufficient conditions to get the left strongly pure ideal from the right strongly pure ideal?

Question 3: Is there a general presentation that can give the specific number of strongly right (left) pure ideals in the ring Z_n.

Nevertheless, the author determined some other properties of SPIs which are given as follows.

Remark 2.1 Let ζ and ξ be two ideals of Ṙ. Then,

1. If ζ is SPI of Ṙ, then $\zeta \cap \xi$ is a SPI of Ṙ.
2. Let $\zeta \subseteq \xi$, then if $\zeta \cap \xi$ is SPI of Ṙ, then ζ is SPI of Ṙ.

3. The intersection of two SPIs is a SPI. This result can be generalized to a finite intersection of SPIs.
4. If ζ and ξ be two ideals of Ṙ, then ζ is SPI iff $\zeta \cap \xi$ is SPI.
5. For an arbitrary two ideals of Ṙ, if their direct sum is SPI, then one of them is SPI of Ṙ.
6. If Ṙ is a factorial ring with the direct sum of two given ideals ζ and ξ of Ṙ is SPI, then ζ and ξ are SPIs.

Proposition 2.3 [14] Let ζ and ξ be two ideals of Ṙ, if $\zeta \oplus \xi$ is SPI of Ṙ, then either ζ or ξ is SPI of Ṙ.

Corollary 2.3 [14] Let ζ and ξ be two ideals of a factorial ring Ṙ such that $\zeta \oplus \xi$ is SPI of Ṙ. Then, ζ and ξ are SPIs of Ṙ.

The concept of N-pure ideals has been introduced in [15] as a generalization for the concept of pure ideals. The motive that encouraged the author to present such types of ideals is to provide a new ring namely mid ring with some of its properties.

Definition 2.1 [15] The ideal ζ of Ṙ is said to be N-pure ideal, if for all $v \in \zeta$ there exist $u \in \zeta$ for which $v(1-u) \in \mathfrak{R}$ where $\mathfrak{R}$ is a nil-radical of Ṙ.

Clearly, any PI is a N-pure ideal and the convers is not necessarily true. Since the radical of a non-reduced ring Ṙ is a N-pure ideal but not PI. For the case that Ṙ is a reduced ring, then N-pure ideals and PIs are the same. In addition, some properties of this notion have been studied. For example, the sum of a family of N-pure ideals is a N-pure ideal. Also, the intersection (resp. product) of two N-pure ideals is a N-pure ideal. The author showed that the class of N-pure ideals is greater than the class of pure ideals. He then showed the results bellow.

Proposition 2.4 [15] Assume Ṙ be a ring. Then, Ṙ is a reduced ring iff any N-pure ideal is a PI.

Proposition 2.5 [15] Assume Ṙ be a ring and ζ is an ideal of Ṙ. Then, ζ is a N-pure ideal iff $\forall v \in \zeta\ \exists n \geq 1$ with $u \in \zeta$ such that $v^n(1-u) = 0$.

Lemma 2.1 [15] If ζ is an ideal of Ṙ. Then, ζ is a N-pure ideal iff $(\zeta + \mathfrak{R})/\mathfrak{R}$ is a PI.

Theorem 2.1 [15] Let ζ be an ideal of Ṙ. Then, the conditions bellow is equivalent.
1. ζ is a N-pure ideal.
2. For each $v_1, \dots, v_n \in \zeta$ there exist $u \in \zeta$ with $s \geq 1$ such that $v_k^s = v_k^s u$ for each $k = 1, \dots, n$.
3. For each $v \in \zeta$ there exist $s \geq 1$ such that $An(v^s) + \zeta = \dot{R}$.
4. $\sqrt{\zeta} = \{v \in \dot{R} | \exists n \geq 1, An(v^n) + \zeta = \dot{R}\}$.
5. $\sqrt{\zeta}$ is a N-pure ideal.
6. There exist a unique pure ideal ξ such that $\sqrt{\zeta} = \sqrt{\xi}$.

Corollary 2.4 [15] Assume Ṙ be a ring with ζ is an ideal of Ṙ. Then, ζ is a N-pure ideal iff ζ^n is a N-pure ideal for each $n \geq 1$.

SPI $\Rightarrow$ PI $\Rightarrow$ N-Pure Ideal

Question 4: Is there a general presentation that can give the specific number of N-pure ideals in the mid ring?

Question 5: Does the properties of strongly pure ideal are valid for a N-pure ideal?

Next, the study of [16] is one of the attempts which developed the concept of PIs. In the same year, the generalization of PIs has been presented in [17]. They defined the right (left) generalized pure ideals (for short R(resp. L)GPI) as follows: The ideal ζ of Ṙ is said to be R(L)GPI, if for each $v \in \zeta$ there is $u \in \zeta$ with $n \in Z^+$ for which $v^n = v^n u (v^n = u v^n)$. They used this generalization to present some results in [18]. They proved that for every ideal ζ of a reversible ring Ṙ, then ζ is a RGPI iff ζ is a LGPI. However, they showed that when Ṙ is a reversible ring, then $An_{\dot{R}}^r(v^n) = An_{\dot{R}}^l(v^n)$ where $v \in \dot{R}$ and $n \in Z^+$. On the other hand, the idea of right Π-pure ideals was obtained by [19] as a generalization for the RPIs. This generalization has been defined as follows: The right ideal ζ of Ṙ is called right Π-pure ideal, if for any $v \in \zeta$ there exist $u \in \zeta$ with $n \in Z^+$ and $v^n \neq 0$ such that $v^n u = v^n$. It's clear that every RPI is a right Π-pure ideal but not conversely. Furthermore, a Π-pure ideal implies GPI but not the converse. Consider the ring Z_{12}, then the ideals $(3) = \{0,3,6,9\}$ and $(4) = \{0,4,8\}$ of Z_{12} are Π-pure ideals. However, the ideal generated by (3) in Z_9 is a GPI of Z_9 but not Π-pure ideal. In addition, the author determined some condition for Π-pure ideal to be PI. The condition stated that, if Ṙ is a right SXM-ring, then every Π-pure ideal is a pure ideal, where SXM-ring is the ring in which $An_{\dot{R}}^r(v) = An_{\dot{R}}^r(v^n)$, $\forall v \neq 0 \in \dot{R}$ and $n \in Z^+$ with $v^n \neq 0$.

Question 6: Is it possible to find a relation between SPI and N-pure ideal?.

Question 7: Is there a relation between SPI and right Π-pure ideal as well as z-ideal?.

Question 8: Is there a relation between z-ideal and N-pure ideal?.

3. SOME RINGS BASED on PURE IDEALS

In the literature, there are many articles that have been written about some rings which included PIs and each one has been going in different direction. In this section, we will study in brief some of these studies and discuss them in details. In [20] the right PIP-ring has been defined. The right PIP-ring is a ring for which any principal ideal is RPI. As an illustrative example, Z_6 is a right PIP-ring. However, Z_{12} is not. Further, the author has proved that a right PIP-ring is a reduced ring and semi-prime ring. Moreover, S. H. Ahmed showed that a right PIP-ring with no zero divisors is a division ring. Then, she determined a condition under which, the right PIP-ring becomes a division ring. This condition states that, if Ṙ is a right uniform PIP-ring, then Ṙ is a division ring. Moreover, a paper by Husm [21] generalized the results of [20] to present the right PIGP-ring which is a ring whose principal ideals are GPIs. The ring Z_{12} is a PIGP-ring. It is clear that, any right PIP-ring is a right PIGP-ring but not conversely. The author obtained a condition under which the convers is true. In particular, H. Q. Mohammad proved that the right PIGP-ring is right PIP-ring whenever $An_{\dot{R}}^{r}(v^{n}) \subseteq An_{\dot{R}}^{r}(v), \forall v \in \dot{R}$ and $n \in Z^{+}$. The mentioned result is stated bellow.

Theorem 3.1 [21] Let Ṙ be a right PIGP-ring and $An_{\dot{R}}^{r}(v^{n}) \subseteq An_{\dot{R}}^{r}(v)$ for each $v \in \dot{R}$ with $n \in Z^{+}$. Then, Ṙ is a PIP-ring.

However, he proved under the same condition, the right PIGP-ring is a regular ring. Moreover, the author characterized the uniform PIGP-ring in the terms of nilpotent and non-zero divisor. This result is given as follows.

Theorem 3.2 [21] Let Ṙ be a zero-commutative uniform ring. Then, Ṙ is a PIGP-ring iff:

1. For each $v \in \dot{R}$ is either nonzero divisor or nilpotent.
2. Any nonzero divisor of Ṙ is an invertible.
3. $N(\dot{R})$ is the right ideal in Ṙ.

Theorem 3.3 [21] Let Ṙ be a PIGP-ring and $An_{\dot{R}}^{r}(v^{n}) \subseteq An_{\dot{R}}^{r}(v)$ for each $v \in \dot{R}$ with $n \in Z^{+}$. Then, Ṙ is a regular ring.

Theorem 3.4 [21] Let Ṙ be a commutative PIGP-ring. Then, $3\mathrm{Rad}(v\dot{R}) = v\dot{R} + N$, where N is the nil radical of Ṙ.

Two years later, a right PILP-ring has been introduced in [22]. A right PILP-ring is a ring in which any principal right ideal is a LPI. For instance, Z_6 is a right PILP-ring since the ideals generated by (2) and (3) are LPIs of Z_6. But Z_{12} is not a right PILP-ring, because the ideal generated by 2 is not PI of Z_{12}. In addition, the author showed that Ṙ is a reduced ring whenever Ṙ is an abelian right PILP-ring. Furthermore, R. D. Mahmood also proved, if Ṙ is an abelian right PILP-ring with $An_{\dot{R}}^{l}(v) = 0$, then Ṙ is a division ring. It should be noted that, the right PIP-ring and the right PILP-ring are different. Since the first is considered the right principal ideal is pure in general. However, the second is concentrated on the left pure ideal. Thereafter, the right Nil-pure ring has been introduced in [23]. This ring was defined as follows: The ring Ṙ is said to be right Nil-pure ring, if for any $v \in N(\dot{R})$, we have $An_{\dot{R}}^{r}(v)$ is a LPI of Ṙ. A ring of integers Z is a right Nil-pure ring but Z_{12} is not, since the ideal generated by 6 in Z_{12} is not PI. The authors proved some good results which are as follows: If Ṙ is a right Nil-pure ring with the ideal ζ is a PI of Ṙ, then $\dot{R}/\zeta$ is a Nil-pure ring. Further, for the regularity of this ring, they showed that whenever Ṙ is a right Nil-pure ring, then the center of Ṙ contains no non-zero nilpotent element. Moreover, they concluded that the center of this ring is a reduced. Thereafter, they proved that, if Ṙ is a reversible and Nil-pure ring, then Ṙ is a reduced ring. Also, they concluded that, if Ṙ is a reversible and right Nil-pure ring, then Ṙ is a left (right) non-singular ring. Finally, they presented the following characterization.

Theorem 3.5 [23] Let Ṙ be a reversible ring. Then, Ṙ is a Nil-pure ring iff Ṙ is n-regular ring.

Later on, in [24] new ring has been presented namely JGP-ring. This ring is defined as follows, Ṙ is JGP-ring if for every $v \in J(\dot{R})$, then $An_{\dot{R}}^{r}(v)$ is a LGPI, where $J(\dot{R})$ is a Jacobson radical of Ṙ. They proved the following results.

Theorem 3.6 [24] Let Ṙ be a right JGP-ring with ζ is a PI of Ṙ. Then, $\dot{R}/\zeta$ is JGP-ring.

Theorem 3.7 [24] Let Ṙ be a reversible ring. Then, Ṙ is a right JGP-ring iff $An_{\dot{R}}^{r}(v)+An_{\dot{R}}^{r}(u^{n}) = \dot{R}$ for each $v \in J(\dot{R})$ and $u \in An_{\dot{R}}^{r}(v)$ with $n \in Z^{+}$.

Some studies have discussed the maximal ideals and presented some good results. For instance, the study of [25] presented MRGP-ring. It is a ring whose maximal left ideals are RGPIs. i.e., let ζ be a maximal ideal of Ṙ with $v \in \zeta$, then ζv is a RGPI. Further, they discussed the connection between this ring and MRCP-ring which is a ring such that all of its maximal left ideals are right Co-pure ideals (see [26] for details). Moreover, it is clear that every MRCP-ring is an MRGP-ring but the convers need not to be true. Since the right Co-pure ideal implies right GP-ideal but not conversely. The authors presented under some conditions; the MRGP-ring can be MRCP-ring. Their result is given bellow.

Theorem 3.8 [25] Let Ṙ be a reduced, MRGP-ring. Then, Ṙ is an MRCP-ring.

Furthermore, they have shown that under the same hypothesis of the above theorem, the ring can be strongly regular ring. Also, it was shown in [25] that, if Ṙ is a right uniform reduced MRGP-ring, then Ṙ is a division ring. Further, if Ṙ is a zero-commutative, MRGP-ring, then Ṙ is kasch ring. The kasch ring is the ring for which every maximal right (left) ideal is a right (left) annihilator, (see [27] for details). On the other hand, it has been defined in [28] a ring such that its maximal right (left) ideal is a L(R)GPI. Such ring is said to be right (left) MGP-ring. Clearly that every MRGP-ring is MGP-ring. They proved that, if Ṙ is reduced, MGP-ring then $An^{r}_{\dot{R}}(u^{n})$ is a direct sum of Ṙ for each $v \in \dot{R}$ and $n \in Z^{+}$. Further, if Ṙ is reduced, MGP-ring, then Ṙ is kasch ring. Besides that, they provided the following condition: Let $u \in \dot{R}$ with $n \in Z^{+}$ such that $An^{l}_{\dot{R}}(u^{n}) \subseteq An^{r}_{\dot{R}}(u)$ then, under this condition, Ṙ is right MGP-ring iff it's a strongly regular ring. Also, if Ṙ is a right MGP-ring which satisfying the mentioned condition with $v^{n}u = 0$ where $v, u \in \dot{R}$ and $n \in Z^{+}$, then $An^{r}_{\dot{R}}(v^{n}) + An^{r}_{\dot{R}}(u) = \dot{R}$. Moreover, the authors showed that under the same condition with Ṙ is a right MGP-ring, then Ṙ is a reduced weakly regular ring. Thereafter, they proved that Ṙ is a division ring whenever Ṙ is uniform semi-commutative, MGP-ring and each of its ideal is principal. Ultimately, they defined in [29] new ring namely MEP-ring which is a ring its maximal essential right ideal is a LPI. They determined the following results.

Theorem 3.9 [29] Let Ṙ be a semi-commutative, right MEP-ring. Then, Ṙ is a reduced ring.

Theorem 3.10 [29] Let Ṙ be a semi-commutative, right MEP-ring. Then, every essential right ideal of Ṙ is an idempotent.

Moreover, they discussed another important result concerned with MEP-ring. In particular, they showed that, if Ṙ is a semi-commutative, right MEP-ring, then $J(\dot{R}) = (0)$. Besides, they obtained that under the same hypothesis, Ṙ becomes reduced weakly regular ring. Finally, they proved the following theorem.

Theorem 3.11 [29] The ring Ṙ is a strongly regular iff it's a semi-commutative, MEP, MERT-ring. The MERT-ring is a ring such that each of its maximal essential right ideal is a two-sided ideal, (see [30] for details).

Raida and Shahla defined in [31] the EGP-ring. This ring is a ring such that each of its essential right ideal is a left GP-ideal. The authors proved the next results. If Ṙ is an ERT-ring then, (i) Ṙ is a fully left idempotent ring, (ii) Ṙ is a right EGP-ring, where, ERT-ring is a ring in which each of its essential right ideal is a two-sided ideal [32]. The recent study has been presented the MLGP-ring in [33]. This ring was defined to be a ring for which any right maximal ideal is a LGPI. Further, they showed that, if Ṙ is a local, SXM and NJ-ring, then Ṙ is a strongly π-regular ring iff Ṙ is MLGP-ring, where NJ-ring is a ring in which $N(\dot{R}) \subseteq J(\dot{R})$. Besides, they also proved the following results: If Ṙ is a local, SXM and MLGP-ring, then (i) $J(\dot{R}) = 0$, (ii) if Ṙ is an NJ-ring, then $An^{r}_{\dot{R}}(v^{n})$ is the direct sum for each $v \in \dot{R}$ and $n \in Z^{+}$. Furthermore, the Mid-ring has been defined in [15], which is a ring in which for any $v \in \dot{R}$, we have $An_{\dot{R}}(v)$ is a N-pure ideal. Further, the author showed that, when Ṙ is a Mid-ring and the ideal ζ is a PI of Ṙ, then $\dot{R}/\zeta$ is a Mid-ring. Besides that, he proved that, if Ṙ is a Mid-ring for which $\dot{R} = \prod_{m} \dot{R}_{m}$, then each of $\dot{R}_{m}$ is a Mid-ring. Let Ṙ be a ring, then Ṙ is called primary ring whenever its zero ideal is a primary ideal. By using the concept of primary ring, the author presented the characterization for the Mid-ring which is as follows.

Theorem 3.12 [15] Let Ṙ be a ring. Then, the following axioms are equivalent.

1. Ṙ is a Mid-ring.
2. If $vu = 0$, $\exists n \geq 1$ such that $An_{\dot{R}}(v) + An_{\dot{R}}(u^{n}) = \dot{R}$.
3. $\dot{R}_{q}$ is primary ring for each $q \in \mathrm{Spec}(\dot{R})$.
4. $\dot{R}_{t}$ is primary ring for each $t \in \mathrm{Max}(\dot{R})$.
5. $Ker\pi_{q}$ is PI for any $q \in \mathrm{Spec}(\dot{R})$.
6. $Ker\pi_{q}$ is PI for any $q \in \mathrm{Min}(\dot{R})$.

7. $Ker\pi_q = Ker\pi_p$ in which q, p are prime ideals with $q \subseteq p$.
8. $Ker\pi_q$ is primary ideal for each $q \in \mathrm{Spec}(\dot{\mathrm{R}})$.
9. $Ker\pi_t$ is primary ideal for each $t \in \mathrm{Max}(\dot{\mathrm{R}})$.

Theorem 3.13 [15] Suppose p be a prime ideal of a Mid-ring Ṙ. Then, p is a N-pure ideal iff $p \in \mathrm{Min}(\dot{\mathrm{R}})$.

Theorem 3.14 [15] Every mid-ring is mp-ring.

Furthermore, the author obtained that any Gpf-ring is a Mid-ring, where the Gpf-ring is the ring in which each $v \in \dot{\mathrm{R}}, \exists\, n \geq 1$ in which $An_{\dot{\mathrm{R}}}(u^n)$ is a PI. Finally, we end this section by the following results. In [16], the author presented the concept of right (left) MP-ring which is a ring contains every maximal right (left) ideal is a L(R)PI. Then, some new results concerned such types of rings have been introduced in [34]. In brief, these results are given as follows: (i) Let Ṙ be a right MP-ring with $An^r_{\dot{\mathrm{R}}}(v)$ is a weak ideal of Ṙ for each $v \in \dot{\mathrm{R}}$. Then, Ṙ is a strongly regular ring, (ii) let Ṙ be a right MP-ring with $An^r_{\dot{\mathrm{R}}}(v)$ is a weak ideal of Ṙ for each $v \in \dot{\mathrm{R}}$. Then, Ṙ is a right division ring if it's an uniform ring.

4. CONCLUSINS

As a conclusion, we have seen from the works of many researchers that the notion of PIs was very important in the concept of ring theory. Based on this notion, many articles have been presented and considered this notion in different way. The present study showed that PIs with their generalizations have an important role in determining the structure of a new ring and this can be noted in the study of some properties about it and its relations with some other types of rings. Therefore, the present study concluded the following points:

1. PIs gives N-pure ideals but not convers.
2. PIs gives z-ideals and the convers is true with some necessary and sufficient conditions.
3. SPIs implies PIs but not conversely. It should be noted that, PIs lies between SPIs and N-pure ideals.
4. RPI implies right Π-pure ideal but not convers.
5. Right Π-pure ideal gives GPI but not converse.
6. PIP-ring, PIGP-ring and PILP-ring have been introduced based on the principal ideals with PIs and GPIs.
7. Nil-pure-ring and JGP-ring have been provided based on the concepts of nil radical, annihalitor and Jacobson radical.
8. Based on the maximal ideals with PIs, MRGP-ring, MRCP-ring, right (left) MGP-ring and right (left) MP-ring have been presented.
9. Based on the concept of N-pure ideals, an algebraic structure called Mid-ring has been introduced.

5. REFERENCES

1. Nicholson, W. K. and Zhou, Y. (2005). " Clean Rings: A Survey", *In Advances in ring theory*, vol.12, no. 1, pp. 1-18. DOI: 10.1142/9789812701671_0017
2. Yang, A X. (2009). "A Survey of Strongly Clean Rings", *Acta. Appl. Math*. vol. 108, pp.157-173. DOI https://doi.org/10.1007/s10440-008-9364-6
3. Srivastava, A. K. (2010). "A Survey of Rings Generated by Units", *Annales de la Facult´e des Sciences de Toulouse*, vol. 19, no.1, pp. 203-213.
4. Dixon, M. R, Kurdachnko, L. A. and Pypka, A. A. (2015). "The theorems of Schur and Baer: A Survey", *International Journal of Group Theory*, vol. 4, no. 1, pp.21-32. DOI: 10.22108/IJGT.2015.7376
5. Lazard, D. (1967). "Disconnexités des spectres d'anneaux et des préschémas", *Bull. Soc. Math. France*, vol. 95, pp.195-108. DOI: 10.24033/bsmf.1649
6. Fieldhouse, D. J.(1969). "Pure Theories", *Math. Ann*, vol. 184, pp. 1-18. DOI: https://doi.org/10.1007/BF01350610
7. Bkouche, R. (1970). "Pureté, mollesse et paracompacité", C. R. Acad. Sci. Paris Sér. A-B, 270.
8. Fieldhouse, D. J. (1971). "Regular Modules Over Semi Local Rings", Coll. Math. Sco. Janos Bol-yai, pp. 193-196.
9. Marco, G. De. (1983). "Projectivity of Pure Ideals", Rend. Sem. Mat. Univ. Padova, vol. 69, pp. 289-304.
10. Al-Ezeh, H. (1988). "The Pure Spectrum of PF-rings", *Commutatively Math*. University S. P. vol. 37, no. 2, pp. 179-183.
11. Al-Ezeh, H. (1989). "Pure Ideals in Commutative Reduced Gelfand Rings with Unity", *Arch. Math*. vol.53, pp. 266-269. https://doi.org/10.1007/BF01277063
12. Al-Ezeh, H. (1989). "On Generalized PF-rings", *Math. J. Okayama Uni*. Vol. 31,pp. 25-29.
13. Afrooz. S. (2016). "Pure Ideals, z-ideals and Ideals with Artin-Rees Property in C(Γ)", 4th Seminar on Algebra and its Applications. August 9-11, University of Mohaghegh Ardabili.
14. Abdullah, N. K. (2015). "Strongly Pure Ideals and Strongly Pure Sub-modules", *Kirkuk University Journal of Scientific Studies*, vol. 10, no 1, pp. 12-28.
15. Aghajani, M.(2020) "N-pure Ideals and Mid Rings", arXiv preprint arXiv:2011.02134.
16. Mahmood, R. D.(2000). "On Pure Ideals and Pure Submodules", Ph. D. Thesis Mosul university.
17. Shuker, N. H. and Mahmood, R. D. (2000) "On Generalization of Pure Ideals", *Journal of Education and Science*, vol. 43, pp. 86-90.
18. Mahmood, R. D. and Khalil, S. M. (2009)."On GP-Ideals", *Rafidain Journal of Computer Science and Mathematics*. vol. 6, no. 3, pp. 57-63.
19. Ahmad, S. H.(2014). "On Π-pure Ideals", *Rafidain Journal of Computer Science and Mathematics*, vol.

11, no. 2, pp. 83-86. DOI: 10.33899/csmj.2014.163751

20. Ahmad, S. H. (2006) "On Rings Whose Principal Ideals are Pure", *Rafidain journal of computer science and mathematics*, vol. 3, no. 2, pp. 53-57.
21. Mohammad, H. Q.(2007). "On Rings Whose Principal Ideals are Generalized Pure Ideals", *Rafidain Journal of Computer Science and Mathematics*, vol. 4, no. 1, pp. 63-68.
22. Mahmood, R. D. (2009). "PILP-rings and Fuzzy Ideals", *Rafidain Journal of Computer Science and Mathematics*, vol. 6, no. 2, pp. 31-37. DOI: 10.33899/csmj.2009.163794
23. Hajo, A. M. and Mahmood, R. D.(2017). "On Nill-pure Rings", *International Journal of Enhanced Research in Science, Technology and Engineering*, vol. 6, no.11, pp. 25-28.
24. Majeid, E. S. and Mahmood, R. D. (2019). "JGP-Ring", *Open access library journal*, vol. 6, e5626, pp. 1-4. DOI: 10.4236/oalib.1105626
25. Mahmood, R. D. and Abd, M. A. (2005). "On Rings Whose Maximal Ideals are GP-ideals", *Rafidain Journal of Computer Science and Mathematics*, vol. 2, no. 2, pp.27-31.
26. Shuker, N. H. and Mahmood, R. D. (2000). "On Rings Whose Maximal Ideals are Co-pure", *Rafidain Journal of Computer Science and Mathematics*, vol. 11, no. 4.
27. Ming, R. Y. C. (1986). "On Semi Prime and Reduced Ring", *Riv. Math. Univ. Parama*, vol. 4,no.12, pp. 167-175.
28. Mahmood, R. D. and Mahmood, A. B. (2008). "Maximal Generalization of Pure Ideals", *Rafidain Journal of Computer Science and Mathematics*, vol. 4, no. 1,pp. 57-62.
29. Mahmood, R. D. and Mahmood, A. B. (2007). "On Rings Whose Maximal Essential Ideals are Pure", *Rafidain Journal of Computer Science and Mathematics*, vol. 5, no. 1,pp. 21-27. DOI: 10.33899/csmj.2007.163995
30. Ming, R. Y. C. (1983). "Maximal Ideals in Regular Rings", *Hokkaido Mathematical Journal*, vol. 12, pp. 119-128.
31. Mahmood, R. D. and Khalil, S. M. (2010). "MGP and EGP- rings", *Rafidain Journal of Computer Science and Mathematics*, vol. 7, no. 2, pp.59-65. DOI: 10.33899/csmj.2010.163885
32. Brown, S. H. (1973). "Rings Over Which Every Simple Module is Rationally Complete", *Canad. J. Math*, vol. XXV, no. 4, pp. 693-701. DOI: https://doi.org/10.4153/CJM-1973-070-0
33. Mahmood, R. D. and Mageed, E. S. (2019). "On MLGP-rings", Rafidain Journal of Computer Sci-ence and Mathematics, vol. 13, no. 2, pp.61-66. DOI: 10.33899/csmj.2020.163521
34. Mahmood, R. D. and Hajo, A. M. (2020). "On MP-rings", *Rafidain Journal of Computer Science and Mathematics*, vol. 14, no. 1, pp. 35-40. DOI:10.33899/csmj.2020.164797

Arabic Abstract

تعتبر نظرية الحلقات احد فروع الجبر المجرد الذي يركز على دراسة نظام رياضي مكون من عمليتين ثنائيتين في اتجاهات مختلفة. هناك الكثير من الابحاث في هذا المجال قدمت نتائج جديدة حول بنية جبرية معينه. مفهوم المثاليات النقية من المفاهيم المهمة في هذا المجال والذي تمت دراسته قبل اكثر من 40 سنة حول بعض الحلقات وكذلك بعض المقاسات. في هذا البحث قمنا بمراجعة مختصرة حول المثاليات النقية والمثاليات النقية المعممة و علاقاتها مع بعض المثاليات الاخرى مثل المثاليات النقية من النوع-N ، مثالي من نوع-Z ، مثالي نقي من نوع-Π و المثاليات النقية القوية. كذلك تم تلخيص اهم النتائج التي قدمت حول هذا الموضوع مع طرح بعض الاسئلة التي تشير الى انه هل بالإمكان ايجاد خواص جديدة من خلال دراسة العلاقة بين تلك المثاليات والمثاليات الاخرى. اخيرا، نتيجة هذه الدراسة اوضحت اهمية المثاليات النقية وتعميماتها والدور الذي تلعبه في تكوين البنية الجبرية وخواصها وعلاقتها مع بنى جبرية اخرى.

Pure Sciences International Journal of Kerbala

Year: 2025 Volume : 2 Issue : 5 ISSN: 6188-2789 Print 3005 -2394 Online

2025 ,volume 2 , Issues 5 PSIJK 62-71

Pure Sciences International Journal of Kerbala
Journal Homepage:https://journals.uokerbala.edu.iq/index.php/psijk

Chat GPT-4: Methods, Applications, and Ethical Concerns of an Advanced Language Model

Aseel B. Alnajjar[1*], Marwa K. Farhan[2], Saadaldeen Rashid Ahmed[3]

[1]*Computer Science Department- College of Science - AlNahrain University, Jadriya, Baghdad, Iraq*
[2]*Scholarships and Cultural Relations Directorate, Ministry of Higher Education and Scientific Research, Baghdad, Iraq*
[3]*Computer Science, College of Engineering and Science, Bayan University, Erbil, Kurdistan, Iraq*

P A P E R I N F O

Received: 15 January 2025
Accepted: 1 February 2025
Published: 31 March 2025

Keywords:
Chat GPT-4 ,Generative Pre-Trained Transformer ,Natural Language Generation State-of-the-art techniques, Modern algorithms ,Ethical considerations

A B S T R A C T

Generative Pre-Trained Transformer (GPT) is the arrangement of language models, displaying momentous changes over its forerunners through the integration of state-of-the-art procedures and modern calculations. This comprehensive term paper dives deeply into the complexities of Chat GPT-4, unwinding the basic strategies, novel progressions, and potential applications that make it a trailblazer in the early NLP model development. With a focus on both specialized and moral contemplations, the paper investigates the energetic scene encompassing Chat GPT-4. It fundamentally analyzes its potential moral suggestions, such as predispositions and reasonableness concerns, and emphasizes the requirement for mindful advancement and arrangement of such effective dialect models. The moral talk is expanded to include straightforwardness, responsibility, and societal effect, calling for vigorous rules and systems to guarantee the mindful and comprehensive utilization of Chat GPT-4 in various spaces. The term paper sheds light on the challenges that go with the modernity of Chat GPT-4, tending to issues such as fine-tuning, provoking building, and guaranteeing the model's flexibility to distinctive assignments and spaces. Besides, it traces potential future inquiries about headings, empowering proceeded investigation and progressions in dialect to demonstrate improvement. By emphasizing the significance of moral contemplations, talking about specialized headways, and investigating potential applications and challenges, this term paper serves as a comprehensive direction for analysts, professionals, and policymakers looking to explore the advancing scene of Chat GPT-4 and tackle its transformative potential whereas maintaining moral guidelines and societal values.

1. INTRODUCTION

Chat GPT-4 speaks to the cutting-edge headway inside the regarded GPT arrangement of language models, displaying momentous changes over its forerunners through the integration of state-of-the-art procedures and modern calculations. This comprehensive term paper dives deeply into the complexities of Chat GPT-4, unwinding the basic strategies, novel progressions, and potential applications that make it a trailblazer in the NLP. With a focus on both specialized and moral contemplations, the paper investigates the energetic scene encompassing Chat GPT-4. It fundamentally analyzes its potential moral suggestions, such as predispositions and reasonableness concerns, and emphasizes the requirement for mindful advancement and arrangement of such effective dialect models. The moral talk is expanded to include straightforwardness, responsibility, and societal effect, calling for vigorous rules and systems to guarantee the mindful and comprehensive utilization of Chat GPT-4 in various spaces. The term paper moreover sheds light on the challenges that go with the modernity of Chat GPT-4, tending to issues such as fine-tuning, provoke building, and guaranteeing the model's flexibility to distinctive assignments and spaces. Besides, it traces potential future inquiries about headings, empowering proceeded investigation and progressions in dialect to demonstrate improvement. By emphasizing the significance of moral contemplations, talking about specialized headways, and investigating potential applications and challenges, this term paper serves as a comprehensive direction for analysts, professionals, and policymakers looking to explore the advancing scene of Chat GPT-4 and tackle its transformative potential whereas maintaining moral guidelines and societal values. Normal language preparation (NLP) has become a vital investigative field

*Corresponding Author Institutional Email:
aseel.alnajjar@nahrainuniv.edu.iq (Aseel B. Alnajjar)

in fake insights (AI) due to the fact that it has to be prepared and got the endless sum of unstructured information produced in different areas such as healthcare, funding, and social media. The improvement of progressed language models, such as the Generative Pre-Trained Transformer (GPT) arrangement, has played an essential part in progressing the state-of-the-art in NLP assignments such as dialect interpretation, content summarization, and assumption investigation [1]. As of late, OpenAI declared the improvement of GPT-4, a more progressed and modern dialect demonstrated than its forerunner, GPT-3 [2]. The sections of this research are as below :

Related Work: this research surveys existing writing and investigates dialect models, centering on considerations that have impacted the improvement and headway of GPT models. It gives a comprehensive understanding of the current state of the field .

GPT History: This part follows the advancement and points of reference of the GPT arrangement. It examines the key highlights and headways in each emphasis, highlighting the advances made in common dialect preparation.

GPT Utilized Methods: Here, the paper investigates different strategies utilized in GPT models, such as self-attention instruments, pre-training on expansive content corpora, and fine-tuning for particular errands. It clarifies how these strategies contribute to the adequacy and execution of GPT models.

Chat GPT-4 Applications: This region examines the diverse amplify of applications where GPT models, checking Chat GPT-4, can be utilized. It talks about their potential in characteristic lingo understanding, time, translation, summarization, and other NLP assignments, showing their adaptability and down-to-soil utility.

Comparing Chat GPT-4 with Chat GPT-3: This part compares and contrasts the highlights, capabilities, and changes presented in Chat GPT-4 in comparison to its forerunner, Chat GPT-3. It highlights the headways and improvements that make Chat GPT-4 a more capable and advanced dialect show.

Challenges and Ethical Concerns: In this part, the paper addresses the ethical contemplations and challenges related to the improvement and arrangement of AI dialect models like Chat GPT-4. It talks about issues such as predisposition, decency, protection, and the mindful utilization of dialect models, highlighting the requirement for rules and dependable AI hones.

Simulation of a Chatbot based on GPT: This area investigates the down-to-earth angles of joining Chat GPT into Python. It talks about the devices, libraries, and procedures that encourage the consistent integration of the dialect show, displaying its potential for real-world application advancement.

Future Work: The paper concludes with a talk on potential future inquiries about headings and progressions within the field of dialect models. It investigates conceivable outcomes to encourage progress in the execution, effectiveness, and a few contemplations of Chat GPT-4, clearing the way for proceeded advancement in natural language handling. The ultimate segment is the conclusion**.**

2. RELATED WORK

A few striking inquiries about things have contributed to the progression of dialect models and their applications in different spaces [1].They illustrated the surprising few-shot learning capabilities of dialect models, displaying their potential for versatile and adaptable frameworks. This work has started intriguingly investigating how dialect models can viably learn from constrained information [1]. Advanced ones explored the dialect models' capacity to perform viably in few-shot learning scenarios, emphasizing their generalization and exchange learning capabilities. Their discoveries shed light on the potential of dialect models to rapidly adjust to modern errands and spaces, making them important apparatuses for different applications[1]. Within the setting of multitask learning, [4] and [5] dug into the unsupervised nature of dialect models and investigated their capacity to handle different assignments at the same time. They illustrated that dialect models can be prepared to exceed expectations in different common dialects by handling errands without unequivocal supervision, highlighting the flexibility of these models and their potential to spare computational assets [4] and [5]. Exchange learning has developed as a capable procedure in machine learning, and it has also been broadly examined within the setting of dialect models. [6] given a comprehensive study on exchange learning, analyzing its standards, strategies, and applications. They talked about different approaches to exchange learning, counting fine-tuning, space adjustment, and demonstrating adjustment, advertising profitable experiences by leveraging pre-trained models in completely different scenarios [6]. [7] proposed the concept of information refining, which includes exchanging information from a complex demonstration (instructor) to a less complex show (understudy). This approach has been broadly connected in different spaces, counting normal dialect preparation, to distill the information captured by huge dialect models into smaller and more proficient models [7]. [8] given a comprehensive presentation to support learning, a field closely related to dialect demonstrating. They presented fundamental concepts and calculations in fortification learning, advertising a strong understanding of the standards and strategies utilized to prepare specialists who learn from intuition in an environment

[8]. The work conducted by [2] centered on making strides in the default conduct of chat-based dialect models, tending to moral concerns, and highlighting the significance of dependable AI advancement. They inquire about points to improve the client involvement and guarantee the dialect model's reactions adjust with societal standards and values [2].

These ponder collectively form the establishment for our investigation and rouse the integration of GPT-4 into Python-based applications, as examined in this paper. Table 1 summarizes the disscused works in terms of pros, cons, and the method used.

TABLE 1. Summarization of discussed works: Methods, pros, and cons

Source	Summary	Methods used	Pros	Cons
[4] &[5]	Explored the unsupervised nature of language models and their ability to handle multiple tasks simultaneously.	Unsupervised learning, multitask learning.	Flexible models, computational efficiency.	Performance may suffer without supervision, requires fine-tuning.
6	A comprehensive study on transfer learning, covering principles, strategies, and applications.	Transfer learning, fine-tuning, domain adaptation.	Leverages pre-trained models, improves knowledge transfer.	Requires large datasets, challenges in adapting to new domains.
7	Introduced knowledge distillation, transferring knowledge from a complex (teacher) model to a simpler (student) one.	Knowledge transfer, model compression.	Reduces computational cost, improves efficiency of smaller models.	Some information loss in the process.
8	A broad introduction to reinforcement learning, covering key concepts and algorithms.	Reinforcement learning, agent training.	Strong for adaptive systems, enhances understanding of self-learning strategies.	Requires complex simulations, slow learning process.
2	Focused on improving chatbot behavior, addressing ethical concerns, and ensuring responsible AI.	Responsible AI, user experience optimization.	Aligns models with ethical standards, builds trust in AI.	Balancing ethics and technical performance is challenging.

2.1. History of Chat gpt

The heredity of GPT models can be followed back to GPT-1, which was presented by [4]. GPT-1 illustrated the control of large-scale dialect models prepared on colossal sums of content information. It utilized transformer-based engineering and accomplished momentous execution on different NLP benchmarks. Taking after the victory of GPT-1, ensuing cycles were created to upgrade the capabilities of conversational AI. GPT-2, discharged in 2019, highlighted an altogether bigger show measure and illustrated moved forward execution in content era and understanding [9]. GPT-2 showcased the potential of generative dialect models but moreover raised concerns about the moral utilization of such effective models. In 2020, OpenAI discharged GPT-3, which stamped a noteworthy point of reference within the field of NLP [1]. GPT-3 bragged a gigantic show measure and illustrated surprising capability over a wide extent of dialect assignments, counting question-answering content completion, and dialect interpretation. Its capacity to produce coherent and relevantly important reactions earned consideration around the world. Building upon the victory and lessons learned from GPT-3, Chat GPT-4 speaks to the following arrangement of improvement in conversational AI [10]. However, particular subtle elements approximately Chat GPT-4 may be restricted due to the setting of this inquiry.It is anticipated to present progressions in demonstrating design, preparing methods, and fine-tuning capabilities [2]. Alluding to Figure 1., Chat GPT-4 points to refining the conversational capacities of AI frameworks, tending to restrictions watched in past models, and endeavoring for indeed more human-like intuition. OpenAI's progressing investigations and iterative advancement in this space highlight the organization's commitment to pushing the boundaries of AI capabilities.

2.2 Examining Methods in Chat GPT-4

The Transformer design, known for its consideration components, has revolutionized NLP assignments. Procedures such as meta-learning, fine-tuning, support learning, information refining, multi-task learning, and exchange learning have advanced and moved forward dialect models. Chat GPT-4 points to use these strategies to develop conversational AI (refer to Table 2 for a comparison of these strategies). Transformer engineering is broadly embraced in NLP assignments, and its victory can be credited to its utilization of consideration instruments [5]. The consideration component permits the show to specifically center on significant parts of the input information, which makes it exceedingly compelling in handling common dialects. The Transformer engineering has been utilized in a few dialect models, counting GPT-2 and GPT-3, which have accomplished state-of-the-art execution on a run of NLP errands [11]. The show is pre-trained on a huge corpus of content information and after that fine-tuned on a particular assignment such as early NLP model development or dialect understanding. It has revolutionized different NLP assignments and played an urgent part in the improvement of state-of-the-art models like GPT-3 and GPT-4. The key development of Transformer engineering lies in its capacity to successfully show conditions between words or tokens in a grouping without depending on repetitive neural systems (RNNs) or convolutional neural systems (CNNs) [5]. Meta-learning is another calculation that will be used in Chat GPT-4 because it permits models to memorize how to memorize and adjust to modern errands with negligible preparing information [1].

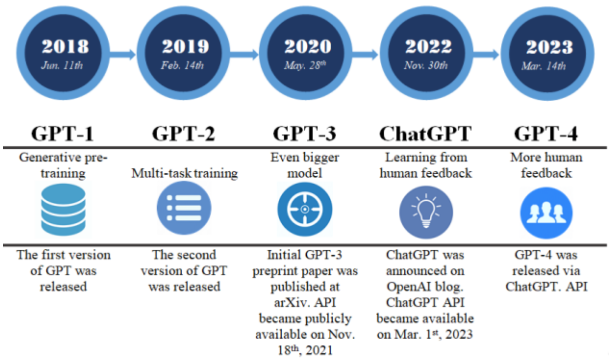

Figure 1. Development of GPT models.

This method is particularly valuable in NLP, where the dialect is exceedingly variable, and there are numerous conceivable ways to precise the same thought. By procuring meta-learning capabilities, models pick up flexibility and capability in different dialect assignments. Few strategies have been proposed for fine-tuning pre-trained dialect models like GPT-4 for particular assignments [10]. One such procedure is incite designing, which includes planning particular prompts or signals for the model to generate reactions that are important to a particular task or domain. For case, in a client benefit chatbot, the provoke may well be planned to inspire responses that are supportive to clients with particular issues. Another strategy is fine-tuning based on human inclinations, which includes preparing the show to create reactions that are favored by human evaluators. This technique can be valuable in circumstances where the model's yield must meet particular quality criteria or where the show is anticipated to be associated with people specifically. Support Learning could be a subfield of machine learning where an operator learns to create choices and take actions in an environment to maximize a reward flag. It involves the interaction between the operator, the environment, and an input circle that guides the agent's learning preparation [8]. Information Refining is another strategy utilized to exchange information from a huge, complex show (instructor) to a smaller, less difficult demonstration (understudy). It involves training the understudy show to imitate the conduct and expectations of the educator show, coming about in a more compact demonstration with comparable execution [7]. In the interim, Multi-task Learning is an approach where a show is prepared to perform numerous related errands at the same time. By mutually learning from numerous assignments, the demonstrate can use shared data and move forward execution over all errands, leading to enhanced generalization and productivity [12]. Exchange Learning is a machine learning strategy where information picked up from preparing on one errand is connected to making strides in the learning or execution on a diverse but related errand. It leverages pre-trained models or highlights learned from large-scale datasets, permitting the exchange of information and quickening the learning handle for unused errands [6]. In expansion to these strategies, other techniques have been proposed to make strides in the execution of dialect models, such as ill-disposed preparation and space adjustment. Adversarial training includes commotion or irritations to the input data to progress the model's vigor to variations within the data. Space adjustment includes preparing the demonstration of information from distinctive spaces to make strides in its capacity to handle unused spaces.

TABLE 2. A comparison of Chat GPT-4 methods

Method	Description	Reference
Transformer Architecture	Utilizes a neural arrange design with consideration components for handling input information	[10]
Meta-Learning	Empowers models to memorize how to memorize, encouraging adjustment to modern assignments and spaces	[13]
Prompt Engineering	Includes planning particular prompts or prompts for creating task/domain-specific reactions	[1]
Fine-tuning based on Preferences	Trains the show to produce reactions favored by human evaluators	[1]
Reinforcement Learning	Utilizes compensate signals to direct show preparing and progress reaction era	[7]
Knowledge Distillation	Exchanges information from bigger pre-trained models to smaller models for moved-forward productivity	[14]

Multi-task Learning	Trains the show on different related errands at the same time to upgrade execution	[6]
Transfer Learning	Utilizes information learned from one errand to progress execution on another assignment	[8]

3 .APPLICATIONS OF CHAT GPT-4

GPT-4's potential applications in different businesses are various and energizing. Additionally, it improves chatbot precision and viability in client benefit by conveying exact and relevantly important reactions. In healthcare, GPT-4 may create chatbots that can offer assistance to patients with therapeutic requests and give personalized well-being counsel. GPT-4 might also be utilized to analyze restorative records and extricate experiences that may offer assistance to healthcare experts make more educated choices. In instruction, GPT-4 might be utilized to create chatbots and virtual guides that can give personalized learning encounters for understudies, which might offer assistance to make strides in understudy engagement and maintenance. Moreover, GPT-4 is utilized to analyze understudy information and give bits of knowledge into understudy execution and learning needs, which seem to offer assistance to teachers in planning more compelling and personalized learning encounters [1]. Additionally, GPT-4's potential applications expand past these businesses, and it may be utilized in ranges such as finance, law, and news coverage. In back, GPT-4 may well be utilized to analyze financial data and provide insights that may offer assistance to financial specialists make more educated choices. In law, GPT-4 can be utilized to help with lawful investigations and drafting legitimate records. In news coverage, GPT-4 may well be utilized to analyze news articles and give bits of knowledge into rising patterns and points. As with any AI innovation, there are numerous concerns related to the utilization of GPT-4 in these applications, such as the potential for inclination and segregation. Be that as it may, with appropriate advancement and oversight, GPT-4 has the potential to revolutionize different businesses and make strides in the lives of numerous individuals [15].

3.1. Chat GPT 4 Vs. Chat GPT 3

Chat GPT-4 speaks to a critical headway over its forerunner, Chat GPT-3, in terms of demonstrating estimate, execution, and capabilities. GPT-4 is anticipated to have a bigger show estimate [2]. Alluding to Figure 2, it captures more complex designs and conditions within the information. This bigger measure empowers GPT-4 to create more coherent and relevantly pertinent reactions, improving its conversational capacities [1]. One of the key contrasts between Chat GPT-4 and GPT-3 is the utilization of more progressed methods and calculations. GPT-4 is anticipated to construct upon the victory of GPT-3 and consolidate unused strategies and models to assist upgrade its execution. But, GPT-3 as of now illustrated noteworthy capabilities in characteristic dialect understanding and era, GPT-4 points to thrust the boundaries indeed encourage [1]. GPT-4 is likely to advantage of headways within the field of normal dialect preparation and machine learning. This incorporates the utilization of Transformer engineering, which has been a crucial component in accomplishing state-of-the-art execution in different NLP errands [10]. The Transformer architecture's utilization of consideration instruments permits the show to viably capture conditions between words and create coherent reactions. GPT-3 moreover utilized Transformer engineering, and GPT-4 is anticipated to proceed to leverage its benefits [1].

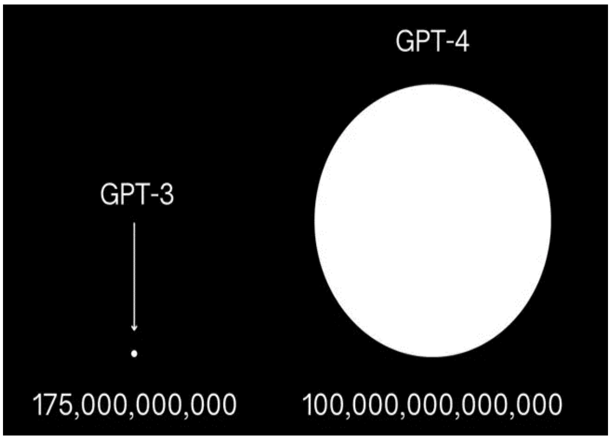

A- Parameters used.

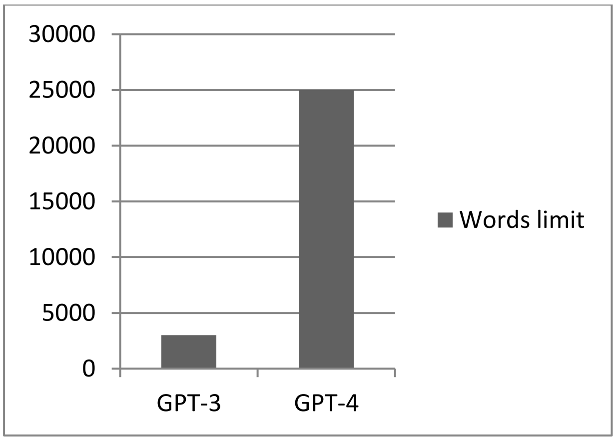

B- Word limit

Figure 2. Chat GPT-4 Vs. GPT-3

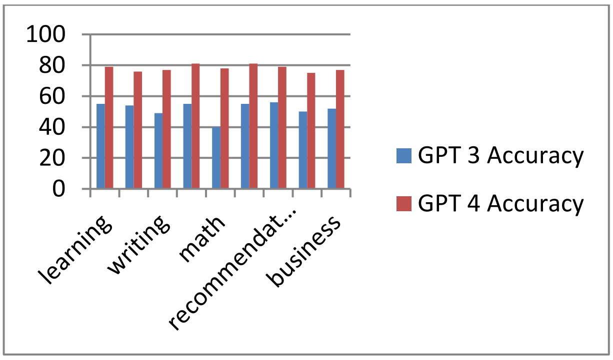

Figure 3. Chat GPT4 Vs. Chat GPT3.

3.2. Ethical Concerns and Challenges

The advancement and utilization of Chat GPT-4 raise a few moral concerns and challenges that ought to be tended to. One of the foremost noteworthy concerns is the potential for the demonstration to sustain inclinations and segregation. Dialect models are prepared on huge datasets like GPT-4, and if these datasets contain inclinations or unfair substance, the show may learn to imitate these predispositions in its reactions. To address this concern, it is basic to utilize differing and comprehensive information and actualize thorough quality control measures [16]. Another concern is the potential for GPT-4 to be utilized to spread deception and publicity. Dialect models like GPT-4 can generate realistic and coherent content, and in case these models are utilized perniciously, they may be utilized to spread fake news, publicity, and abhor discourse. To relieve this hazard, it is vital to create rules for the improvement and utilization of GPT-4 and other AI dialect models [17]. To dodge moral issues concerning Chat GPT-4 and guarantee dependable sending a few quality control measures ought to be executed:

1-The curation of Data: Cautious curation of preparing information is basic to play down inclinations and guarantee decency [18]. Datasets ought to be different, agent, and comprehensive, enveloping a wide run of points of view, societies, and socioeconomics [17]. Thorough information pre-processing and cleaning strategies ought to be connected to evacuate any one-sided or destructive substance [16].

2-Detecting and Mitigating Bias: Vigorous strategies for identifying and relieving inclinations ought to be utilized [18]. This includes persistently observing the model's reactions and distinguishing potential predispositions within the produced substance [17]. Strategies such as ill-disposed preparing, debiasing calculations, and post-processing steps can be utilized to decrease inclinations and advance reasonableness [17, 19].

3-Human oversight and user feedback: Joining client input instruments and including human analysts can offer assistance in distinguishing and addressing potential moral issues [2]. Actualizing input circles and balance frameworks permits clients to report tricky yields, empowering persistent advancement of the model's behavior [2]. Human analysts can also play a pivotal part in checking on and giving direction to the model's reactions, guaranteeing they adjust with moral guidelines [2].

4-Explain ability and Transparency: Guaranteeing straightforwardness within the working of the show and giving clarifications for its choices can cultivate belief and responsibility [20]. OpenAI's approach of giving documentation and rules concerning the model's behavior and confinements advances straightforwardness and allows users to have distant better; a much better; a higher; a stronger; an improved, a distant better understanding of how the framework works [2].

5-Guidelines and Regulations Relating to Ethics: Building up clear moral rules and following legitimate systems is vital [20]. Organizations creating chatbot frameworks ought to characterize and uphold these rules, covering zones such as security, assent, separation, and hurtful substance [20]. Collaboration with administrative bodies can offer assistance shape arrangements and controls that administer the dependable utilization of AI advances [21].

6-Evaluating and Iterating Continuously: Standard assessment of the model's execution and behavior is fundamental [18]. Continuous checking, investigation of client criticism, and collaboration with the inquire about community and outside reviewers can give profitable bits of knowledge and offer assistance in distinguishing ranges for change [18].

By executing these quality control measures, organizations can moderate a few concerns related to Chat GPT, advance capable AI advancement, and guarantee that innovation serves the leading interface of clients and society as an entirety.

2025 ,volume 2 , Issues 5 PSIJK 62-71

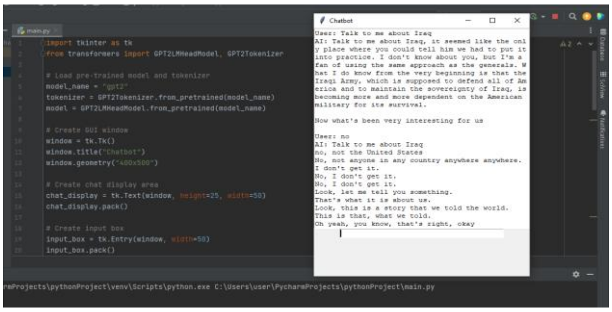

Figure 4. Integrating Chat GPT into Python.

4 .GPT-BASED CHATBOT SIMULATION

As a dialect demonstrates, Chat GPT-4 could be a complex framework that requires a noteworthy sum of computational assets and specialized hardware to prepare and run. However, it isnot viable to fully reenact the complex usefulness of GPT-4 in Python, ready to make a Python program that utilizes pre-trained GPT-2 or GPT-3 models to produce text-based reactions. Python could be a prevalent programming dialect for characteristic dialect preparing (NLP) assignments, and it gives a wide run of libraries and systems that make it appropriate for working with dialect models. By leveraging libraries such as Transformers and Embracing Face's models, able to stack a pre-trained GPT to demonstrate and utilize its capabilities for the content era. The objective is to make an intuitive chatbot encounter where users can input messages, and the GPT show will prepare the input, produce relevantly pertinent reactions, and give a lock-in chat-like discussion. To actualize this, a streamlined chatbot utilizing GPT-based models in Python was made, alluding to Figure 4. We will investigate the control of dialect models in recreating human-like discussions and producing coherent and significant content reactions .

The code takes after an arrangement of steps to set up the GPT-2 demonstrate, allude to Figure 5, handle client input, and produce reactions.

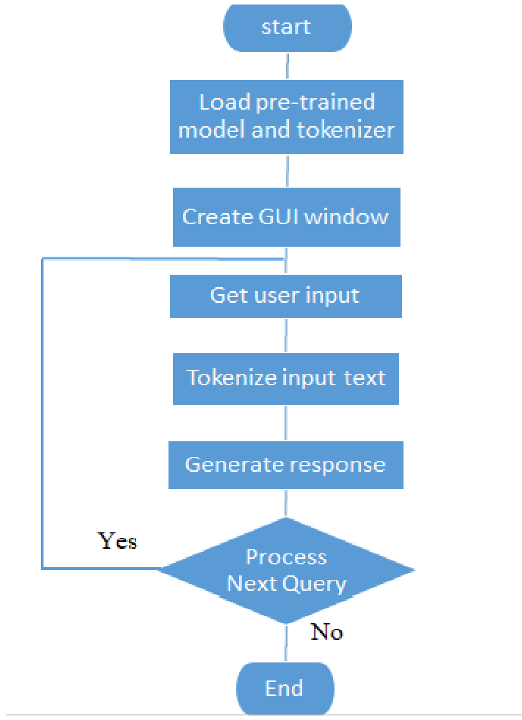

Figure 5. GPT-based Chatbot Simulation

Here is a breakdown of the code's primary steps:

1-The program begins by stacking a pre-trained GPT demonstrated utilizing the GPT2LMHeadModel. From_ pretrained () function. This show has been prepared on an expansive corpus of content information and can create relevantly significant reactions based on input messages.

2- Next, the program sets up a circle to ceaselessly provoke the client for input. It peruses the user's message from the command line and tokenizes it utilizing the GPT2Tokenizer course. The tokenized input is at that point encoded into input IDs, which speak to the numerical representation of the content for the show to handle.

3-The encoded input is nourished into the GPT demonstrating utilizing the generate () method. This strategy creates a reaction based on the given input. The produced reaction may be a grouping of token IDs, which is decoded back into human-readable content utilizing the tokenizer.

4-At last, the program prints the produced reaction to the support, completing the chat-like interaction. The circle proceeds until the client chooses to exit the chatbot.

Generally, this code illustrates a disentangled execution of a chatbot utilizing GPT-based models, empowering a conversational involvement with an AI-powered dialect show.

5. CONCLUSION

Another zone of investigation is the advancement of more strong and assorted preparing datasets to diminish the hazard of inclination and separation in dialect models [25]. Dialect models are prepared on tremendous sums of content information, which can reflect and open up existing inclinations in society [26]. Analysts have proposed different strategies for debiasing dialect models, such as ill-disposed preparation and dataset enlargement, but these strategies are still in their early stages [17]. More inquiry is required to create viable strategies for lessening predisposition and expanding differences in dialect show preparing datasets [27]. In expansion, there could be a need to inquire to investigate the potential applications of GPT-4 in zones such as back, law, and news coverage [28]. For this case, GPT-4 might be utilized to generate more exact and characteristic dialect rundowns of budgetary reports or legitimate archives or to help writers in composing news articles [29]. Be that as it may, the utilization of dialect models like GPT-4 in these ranges moreover raises ethical concerns, such as the potential for abuse or the displacement of human specialists [30] and [31]. Future investigations ought to focus on investigating the moral suggestions of utilizing progressed language models in different spaces. As talked about in this term paper, Chat GPT-4 speaks to a noteworthy step forward [32-35] within the field of characteristic dialect preparing, with its bigger measure and progressed engineering empowering it to create more coherent and relevantly pertinent reactions. The capable improvement and utilization of GPT-4 and other AI dialect models require collaboration [36- 39] between analysts, industry pioneers, policymakers, and other partners to guarantee that moral contemplations are prioritized. This incorporates the improvement of more different and vigorous preparing datasets to decrease the hazard of inclination and segregation, as well as the execution of shields to anticipate the abuse of these technologies. Additionally, there may be a need for more noteworthy straightforwardness and responsibility within the development and utilization of AI dialect models, counting the distribution of preparing information and the usage of reviews and certification forms.

5.1. Future Work

As GPT-4 and other AI dialect models proceed to advance, there is a requirement to encourage investigations to address the moral and specialized challenges they pose [22]. One region of future investigation is the improvement of more successful methods for fine-tuning pre-trained models like GPT-4 [23]. Fine-tuning includes altering the weights and inclinations of a pre-trained demonstration to fit a particular assignment or space, and can significantly progress the execution of the demonstration on that assignment [24].Now, analysts have investigated different strategies for fine-tuning GPT-3, such as few-shot learning and meta-learning, but there is still much to be exhausted in this region [1].

Declaration of competing interest: The creators pronounce that they have no known budgetary or non-financial competing interface in any fabric talked about in this paper.

Funding information: No subsidizing was gotten from any money-related organization to conduct this inquiry.

Acknowledgments

The creators are thankful to the Iraqi Service of Higher Instruction and Logical Inquire (MOHESR) for actually supporting the current inquiry.

6. REFERENCES

1. T. B. Brown et al., “Language models are few-shot learners,” in 34th Conference on Neural Information Processing Systems (NeurIPS 2020), Vancouver, Canada, pp. 1-25, 2020.
2. OpenAI, “GPT-4 Technical Report,” accessed 2023. doi: 10.48550/arXiv.2303.08774.
3. M. Abdullah, A. Madain, and Y. Jararweh, "ChatGPT: Fundamentals, Applications, and Social Impacts," in 2022 Ninth International Conference on Social Networks Analysis, Management and Security (SNAMS), Milan, Italy, 2022, pp. 1-8, doi: 10.1109/SNAMS58071.2022.10062688.
4. A. Radford, K. Narasimhan, T. Salimans, and I. Sutskever, “Improving language understanding by generative pre-training,” 2018. [Online]. Available: https://www.semanticscholar.org/paper/Improving Language-Understanding-by-Generative-Radford Narasimhan/cd18800a0fe0b668a1cc19f2ec95b5003d0a503 5
5. A. Radford et al., “Language models are unsupervised multitask learners,” OpenAI blog, vol. 1, no. 8, p. 9, 2019.
6. S. J. Pan and Q. Yang, "A Survey on Transfer Learning," IEEE Transactions on Knowledge and Data Engineering, vol. 22, no. 10, pp. 1345-1359, Oct. 2010, doi: 10.1109/TKDE.2009.191.
7. G. Hinton, O. Vinyals, and J. Dean, “Distilling the knowledge in a neural network,” arXiv preprint arXiv:1503.02531, Mar. 2015.
8. R. S. Sutton and A. G. Barto, Reinforcement Learning: An Introduction, MIT Press, 2018.
9. J. Buolamwini and T. Gebru, “Gender shades: Intersectional accuracy disparities in commercial gender classification,” in Proceedings of Machine Learning Research, Conference on Fairness, Accountability, and Transparency, vol. 81, pp. 1-15, Jan. 2018.
10. A. Vaswani et al., “Attention is all you need,” in 31st Conference on Neural Information Processing Systems (NIPS 2017), Long Beach, CA, USA, pp. 1-11, 2017.
11. X. Pan, X. Li, Y. Li, S. Zhang, and X. Zhou, “Adapting Pre-trained Language Models to Specific Domains: A Survey,” IEEE Transactions on Neural Networks and Learning Systems, vol. 32, no. 2, pp. 390-404, 2021.

12. R. Caruana, “Multitask learning,” Ph.D. dissertation, School of Computer Science, Carnegie Mellon University, PA, USA, pp. 41-75, 1997.
13. C. Finn et al., “Model-agnostic meta-learning for fast adaptation of deep networks,” in ICML'17: Proceedings of the 34th International Conference on Machine Learning, vol. 70, pp. 1126-1135, Aug. 2017.
14. S. Ruder, “An overview of multi-task learning in deep neural networks,” arXiv preprint arXiv:1706.05098, 2017. doi: 10.48550/arXiv.1706.05098.
15. Y. H. H. Tsai et al., “Multimodal transformer for unaligned multimodal language sequences,” in Proceedings of the Conference of the Association for Computational Linguistics Meeting, vol. 2019, p. 6558, Jul. 2019.
16. T. Gebru et al., “Datasheets for datasets,” Communications of the ACM, vol. 64, no. 12, pp. 86-92, 2021, doi: 10.48550/arXiv.1803.09010.
17. T. Bolukbasi et al., “Man is to Computer Programmer as Woman is to Homemaker? Debiasing Word Embeddings,” in 30th Conference on Neural Information Processing Systems (NIPS 2016), Barcelona, Spain, pp. 4349-4357, 2016, doi: 10.48550/arXiv.1607.06520.
18. B. D. Mittelstadt et al., “The ethics of algorithms: Mapping the debate,” Big Data & Society, vol. 3, no. 2, pp. 1-21, 2016.
19. S. Barocas, M. Hardt, and A. Narayanan, Fairness and Machine Learning, MIT Press, Cambridge, MA, USA, 2017.
20. L. Taylor et al., “Data Justice and the Ethics of Datafication,” Big Data & Society, vol. 4, no. 2, 2017.
21. B. Alnajjar et al., “Wireless Sensor Network Optimization Using Genetic Algorithm,” Journal of Robotics and Control (JRC), vol. 3, no. 6, pp. 827-835, 2023, doi: 10.18196/jrc.v3i6.16526.
22. M. Brundage, “Taking superintelligence seriously: Superintelligence: Paths, dangers, strategies by Nick Bostrom,” Oxford University Press, vol. 72, pp. 32-35, 2014.
23. D. Adiwardana et al., “Towards a human-like open-domain chatbot,” arXiv preprint arXiv:2001.09977, 2020.
24. Goodfellow, Y. Bengio, and A. Courville, Deep Learning, MIT Press, Cambridge, MA, USA, 2016.
25. E. M. Bender et al., “On the dangers of stochastic parrots: Can language models be too big?,” in Proceedings of the 2021 ACM Conference on Fairness, Accountability, and Transparency, pp. 610-623, Mar. 2021.
26. A. Caliskan et al., “Semantics derived automatically from language corpora contain human-like biases,” Science, vol. 356, no. 6334, pp. 183-186, 2017.
27. M. A. Sayed et al., “Survey on Handwritten Recognition,” in 2022 International Symposium on Multidisciplinary Studies and Innovative Technologies (ISMSIT), Ankara, Turkey, 2022, pp. 273-281, doi: 10.1109/ISMSIT56059.2022.9932793.
28. A. Nenkova et al., “A call to action for natural language processing: Mitigating the risks of AI-driven language technologies for journalism,” Journalism & Mass Communication Quarterly, vol. 98, no. 1, pp. 26-45, 2021.
29. L. Shao et al., “Generating high-quality and informative conversation responses with sequence-to-sequence models,” arXiv preprint arXiv:1701.03185, 2017.
30. L. Floridi et al., “AI4People—an ethical framework for a good AI society: Opportunities, risks, principles, and recommendations,” Minds & Machines, vol. 28, no. 4, pp. 689–707, 2018, doi: 10.1007/s11023-018-9482-5.
31. A. Mohammed et al., “Unsupervised classification and analysis of Istanbul-Turkey satellite image utilizing the remote sensing,” in AIP Conference Proceedings, vol. 2457, no. 1, p. 040007, Feb. 2023.
32. A. M. Kadim et al., “K-Means clustering of optimized wireless network sensor using genetic algorithm,” Periodicals of Engineering and Natural Sciences, vol. 10, no. 3, pp. 276-285, 2022.
33. N. A. Hasan et al., “Image hiding in audio file using chaotic method,” Periodicals of Engineering and Natural Sciences, vol. 11, no. 3, pp. 245-254, 2023.
34. Z. H. Ali, H. M. Salman, and A. H. Harif, "SMS Spam Detection Using Multiple Linear Regression and Extreme Learning Machines," Iraqi Journal of Science, vol. 64, no. 10, pp. 6342–6351, Oct. 2023.
35. H. A. Abdul Mohsin and A. H. Harif, “Agent-based grid computing load balancing at application level,” Iraqi Journal of Science, vol. 53, no. 4, pp. 899-902, 2012.
36. H. K. Jameel and B. N. Dhannoon, “Gait Recognition Based on Deep Learning,” Iraqi Journal of Science, vol. 63, no. 1, pp. 397–408, Jan. 2022

Arabic Abstract

شات GPT-4: الأساليب، التطبيقات، والمخاوف الأخلاقية لنموذج لغوي متقدم

يمثل شات GPT-4 (المحول التوليدي المدرب مسبقًا) تطورًا كبيرًا في سلسلة نماذج اللغة GPT الشهيرة، حيث يظهر تحسينات ملحوظة مقارنة بأسلافه من خلال دمج تقنيات حديثة وخوارزميات مبتكرة. تتناول هذه الورقة البحثية الشاملة تعقيدات شات GPT-4 بعمق، وتستعرض الأساليب الأساسية، والتطورات الرائدة، والتطبيقات المحتملة التي تجعله قائدًا في مجال توليد اللغة الطبيعية.

مع التركيز على الجوانب التقنية والأخلاقية، تستكشف الورقة المشهد الديناميكي المحيط بشات GPT-4. كما تقوم بتقييم نقدي للتداعيات الأخلاقية المحتملة، مثل التحيزات وقضايا العدالة، مع التأكيد على الحاجة إلى تطوير مسؤول ونشر مثل هذه النماذج القوية للغات. يتوسع النقاش الأخلاقي ليشمل الشفافية، والمساءلة، والتأثير المجتمعي، داعيًا إلى وضع إرشادات وأطر قوية لضمان الاستخدام المسؤول والشامل لشات GPT-4 في مختلف المجالات.

كما تسلط الورقة الضوء على التحديات المصاحبة لتطور شات GPT-4، بما في ذلك قضايا الضبط الدقيق، وتصميم التعليمات، وضمان تكيف النموذج مع المهام والسياقات المتنوعة. بالإضافة إلى ذلك، ترسم الورقة مسارات للبحث المستقبلي، مما يشجع على استمرار استكشاف وتطوير نماذج اللغة.

من خلال التأكيد على أهمية الاعتبارات الأخلاقية، ومناقشة التطورات التقنية، واستكشاف التطبيقات المحتملة والتحديات، تقدم هذه الورقة البحثية دليلًا شاملًا للباحثين والممارسين وصناع القرار للتنقل في المشهد المتطور لشات GPT-4، والاستفادة من إمكاناته التحويلية مع الالتزام بالمعايير الأخلاقية والقيم المجتمعية.

الكلمات المفتاحية: شات GPT-4، المحول التوليدي المدرب مسبقًا، توليد اللغة الطبيعية، التقنيات الحديثة، الخوارزميات المبتكرة، الاعتبارات الأخلاقية.

Pure Sciences International Journal of kerbala

Year: 2025 Volume : 2 Issue : 5 ISSN: 6188-2789 Print 3005 -2394 Online

2025 ,Volume 2 , Issues 5 PSIJK 72-84

Pure Sciences International Journal of Kerbala
Journal Homepage:https://journals.uokerbala.edu.iq/index.php/psijk

Accelerating Image Analysis Using AI-Driven Methods: Enhancing Speed and Accuracy in Autonomous Vehicle System

Rawshan Nuree Othman[1], Saadaldeen Rashid Ahmed[2]

[1]*Department of Information Technology- College of Engineering and Computer Science- Lebanese French University, Erbil, Kurdistan, Iraq*
[2]*Computer Science, College of Engineering and Science, Bayan University, Erbil, Kurdistan, Iraq*

P A P E R I N F O

Received: 16 January 2025
Accepted: 1 February 2025
Published: 31 March 2025

Keywords:
Autonomous Vehicles Image Analysis
AI-Driven Methods EfficientNet
MobileNet Real-Time Processing
Neural Networks

A B S T R A C T

The fast improvements in Autonomous Vehicle (AV) systems have shown the necessity for effective image processing approaches to enable efficient decision-making. Current approaches generally fail to offer a balance between processing speed and precision, restricting their usefulness in AV scenarios. The work sets out to tackle these difficulties by applying advanced AI-driven methodologies, EfficientNet and MobileNet, to optimize picture analysis for AV systems. This research filled a breach by enhancing both the speed and accuracy of real-time image processing systems. Also, it contributed to scientific studies in this sector. According to the KITTI Vision Benchmark Suite and Berkeley DeepDrive datasets, the experimental quantitative research designs. Proposed models were trained and tested using these datasets. TensorFlow and Keras frameworks incorporated advanced convolutional neural network topologies with transfer learning algorithms. The models were released loose under varied driving circumstances to see how flexible and resilient they were. The statistical importance of performance parameters like accuracy, inference time, and F1-score was evaluated. The results reveal that EfficientNet can obtain an accuracy of 94.2% and an inference time of 18 ms/image, which is substantially better than the baseline. MobileNet was a plausible option, exhibiting amazing accuracy while being computationally efficient. This improvement was statistically significant, and qualitative assessments indicated that the models were powerful under bad conditions. The research advances real-time imaging analysis in AVs, pointing to the need for architectural adjustments and dataset diversity. As a result of this research, the field of AI-controlled image processing will advance and lead to creative developments in AV systems and their applications.

1. INTRODUCTION

Autonomous vehicle systems contain technology that has dramatically developed in the recent few years with the aim of enhancing road safety, efficiency, and reliability [1]. Image analysis, which forms the backbone of these systems, is a crucial feature that permits the vehicles to capture data from cameras and different sensors and assess the surrounding environments [2]. Image Analysis: Image analysis is one of the most critical and vital tasks behind the seamless operations of autonomous vehicles, as the operations spanning from object identification to lane holding and obstacle avoidance seem to be chaotic without good image analysis works [3]. Nonetheless, the complexity and dynamic nature of real surroundings provide substantial obstacles for existing image analysis approaches, notably in reaching the speed and accuracy necessary for real-time decision-making [4].

Artificial Intelligence (AI) has become a significant enabling technology for image analysis, providing a range of machine learning methods and methodologies that can vastly improve the performance of autonomous systems [5]. Especially, deep learning models have shown outstanding performance in picture identification and classification tasks, which in turn lead to faster and smarter vehicle reflexes [6]. These artificial intelligence (AI)-based solutions are benefitting from massive datasets and complicated neural network designs and have boosted the accuracy of picture interpretation and the overall success rate of autonomous navigation [7]. However, there is still a crucial trade-off between

*Corresponding Author Institutional Email:
rawshan.nuree@lfu.edu.krd (Rawshan Nuree Othman)

processing speed and accuracy, as the computational demands imposed by the more advanced AI algorithms can limit the real-time performance required to drive an autonomous vehicle [8]. It deals with the classic image analysis problem of needing to handle picture analysis with the proper speed and accuracy. Nevertheless, finding this equilibrium seems to be a difficulty for the existing approaches that encounter challenges in pragmatic context moving into a cause of delayed decision-making and even modification of safety [9]. These high processing demands might lead to increased latency, which is disadvantageous in circumstances where a split-second judgment is crucial [10]. Moreover, different environmental factors (lighting conditions, weather, and so on) and other unpredicted barriers make image recognition systems less precise and more in need of better implementation of effective AIs [1]. Solving these difficulties can help develop autonomous automobile technology. This research has two main aims: to formulate AI-driven approaches that speed up image analysis in autonomous vehicle systems through innovative methodology implementation and to improve the accuracy of image recognition processes by achieving the maximum image stimulus performance under various scenarios. In this regard, the present study focuses on achieving all of the above-mentioned issues to reduce the processing speed and boost the accuracy, therefore benefiting everyone to help develop efficient and reliable autonomous vehicle systems.

This paper describes some original advances in the visual analysis of autonomous cars. First, it proposes an AI-based approach to minimize the image processing time with the highest accuracy. Achieved via optimizing neural network topologies and efficient data processing techniques. Second, the methodologies provided in the research were investigated in detail, assessed exhaustively and tried in real-life circumstances, so establishing their effectiveness and practical utility. This proof-of-concept evaluation is vital for establishing the performance increases and also for ascertaining the significance of the aforementioned methodologies during real-world autonomous vehicle functions. Finally, the comparative evaluation of the proposed image analysis approaches with related methods demonstrates that the created approaches are more accurate and faster than existing methods [2].

Inscribed in the organization of this paper, the reader will detect a well-organized series of phases in creating an argument. After this introduction, Section 2 addresses the state-of-the-art literature on pertinent problems, including existing image analysis approaches for autonomous cars and the application of AI-based technologies to complement image analysis methods. The methodology applied in the design and execution of the proposed AI-driven image analysis techniques, including algorithm design and operational setup, is detailed in Section 3. In Section 4 we provide the result of the experiments meant to assess the novel methodologies with respect to the speed and accuracy of the improvement over recently reported results. Implications and actual world applications will be examined in section 5. Finally, Section 6 closes this research, summarizing the important achievements and proposing ideas for future work to further improve image analysis in autonomous systems.

2. LITERATURE REVIEW

Image analysis forms the basis for autonomous vehicle (AV) systems, which need to understand their environment through visual perception employing a variety of sensors and cameras [11]. Many image analysis approaches have been presented since then to improve the effectiveness of AVs and decrease the challenges of object detection, lane recognition, and obstacle avoidance [12]. Conventional computer vision techniques, including edge detection, feature extraction, and template matching, have contributed to the creation of different sophisticated methodologies [13]. Nonetheless, the dynamic and unpredictable character of the real-world driving environment significantly increases the need for more advanced strategies that can adapt to changing traffic situations and complexities [14]. Recently, AI-driven approaches leveraging deep learning and machine learning algorithms have revolutionized the way images are processed in autonomous system applications [15]. Driven by remarkable performance in object detection and classification tests [16], Convolutional Neural Networks (CNNs) have become the dominant technology adopted for current image recognition [3]. Real-time object recognition is crucial for AV applications, and architectures such as YOLO (You Only Look Once) and faster R-CNN have been frequently employed for this job since they provide a trade-off between speed and accuracy [17]. Moreover, semantic segmentation approaches, such as U-Net and SegNet, enable AVs to interpret difficult situations by identifying individual pixels in a picture [18].

Apart from CNN, numerous AI and machine learning techniques have been tried to improve image processing in AVs. Various methods are being utilized, such as Recurrent Neural Networks (RNNs) and Long Short-Term Memory (LSTM) networks, which are used to capture temporal relationships in video data, which aids in object movement and behavior prediction [19]. Models based on transformers, which were initially successful in natural language processing, are now making headway for image analysis due to their advantages over the CNNs, such as long-range dependencies capturing and long-range interactions that enhance the contextual modeling of the scenes [20]. At the same time, generative model GANs have also been utilized to augment the data and increase the performance of image recognition systems under varied scenarios [21].

These AI-based systems are usually rated based on how well they maximize the speed and accuracy for image processing jobs. Optimized CNN architectures have gained significant interest due to their possibility of offering both real-time processing rates essential for AV operations and high accuracy [22]. EfficientNet is one such design that has been suggested as a method of scaling a model in a resource-efficient fashion by maximizing performance within a constraint on model complexity, which makes it a possible contender for deployment in computationally constrained contexts such as AVs [23]. Likewise, efforts are made to construct lightweight models like MobileNet and ShuffleNet that generate less computing burden but do not greatly sacrifice accuracy, making them more feasible for real-time image [24].

However, balancing speed and precision is still a huge difficulty. Models that are of high precision often provide higher computational requirements and hence longer processing time, which may not be acceptable for real-time applications [25]. On the other hand, speed-oriented models tend to lose accuracy; they can identify and classify the item with some misalignment or erroneous method, which may lead to hazardous scenarios where AVs may breach some traffic regulation [26]. In response to this trade-off, numerous optimization strategies, including model pruning [23], quantization [24, 25], and knowledge distillation [26], have been investigated that can provide a little level of modeling accuracy to minimize model size and computational resource requirements [27]. These methods have demonstrated benefits for increasing deep learning models to give improved performance in emerging conditions, specifically generating a more flexible and compatible structure with genuine requirements of AVs [28].

Additionally, the implementation of sensor fusion techniques plays an essential role in boosting the reliability of image processing along with the degrees of reliability of AVs. AVs can, thus, get a more holistic image of their environment, which overcomes the constraints of employing individual sensors, by merging data from various sensors like cameras, LiDAR, and radar [29]. To fuse diverse data streams acquired by respective sensors, multi-modal deep learning algorithms have been proposed, as they improve the performance of object detection and environmental perception under different settings [30]. Such an integrative approach optimizes the performance of the image analysis as well as increases the robustness of the AV systems to adverse circumstances, such as bad weather or nighttime surroundings [31].

While the aforementioned research has substantially advanced the area, numerous gaps may be observed in the current literature on AI-powered image processing for AVs. A significant gap is the small attempt at optimizing algorithms with particular hardware constraints of AV systems. While the majority of studies focus on algorithmic accuracy, it is generally performed with insufficient consideration to practical deployments on real embedded systems given the restrictions of processing resources available [32]. Moreover, an increased number of detailed assessments are necessary for AI-based approaches to be intelligible and consistent within broader and various driving environment backgrounds [33]. The majority of previous research uses benchmark datasets, which are not broad enough to reflect the diversity and randomness that a real-world environment holds, thus restricting the applicability of the findings [34].

A final issue that I want to touch upon in this paper is the absence of exploration into adaptive and dynamic image processing algorithms, capable of adjusting to changing situations in real time. Existing paradigms assume a flat, static environment, which is not relevant for autonomous vehicles as the scenes are continually changing [35]. Adaptive behavioral model based on contextual data: Adaptive algorithms that modify their parameters according to contextual information are crucial to improving the flexibility and robustness of AV systems23. More explicit integration of XAI approaches in image analysis systems is basically untapped yet. Interpretability of AI models is very critical for AV operation for debugging, trust building, and safety [37, 36].

Lastly, there is a paucity of inquiry on the ethics and legal implications of AI image analysis employed in ADAS vehicles. It is vital that firms producing image analysis systems remain inside and beyond ethical norms, especially as AVs take over the road [38]. Various ethical challenges like data privacy, AI algorithmic bias, and accountability for system malfunctions need to be explored and handled proactively [39]. Concerns must be addressed, however, in order for AV technologies to be deployed in a responsible manner and for the public to trust these technologies [40].

whereas the introduction of AI technologies has brought image analysis utilizing deep learning to greater heights within the autonomous car business, numerous issues surrounding balancing speed and accuracy, hardware optimization, adaptability, and resolving ethical matters remain. Overall, this literature review summarizes what progress has been made and what remains to be done in developing reliable and ethical image analysis approaches for future autonomous vehicle systems and motivates the continued generation of statistically sound, well-conducted, and effective vehicle image processing methods. Filling these gaps will allow future projects to produce more dependable and efficient AVs, ultimately making AVs safer and more effective in the real world.

3. METHODOLOGY

The study employs a multifaceted methodology to develop and assess AI-driven solutions that could enhance and expedite picture analysis AVs. The techniques encompass research design, data collection and preprocessing, model building and training, implementation, and data analysis. All elements have been organized in a manner that is cleData Analysis.cible. Furthermore, the study outlines the procedures for enhancing the speed and accuracy of AV picture processing.

3.1. Research Design

The study employs an experimental, quantitative research approach that systematically examines the ability to utilize AI-driven image processing techniques in AV systems. This design will enable you to evaluate causality by comparing the performance of various algorithms. The experimental method permits precise measures of speed and accuracy improvements, which are the core emphasis of the study. The design comprises multiple components: data collection, preprocessing, model architecture, training, and evaluation. This strategy says that one activity must come before another, and each one is dependent upon the previous one (activity).

3.2. Data Acquisition and Preprocessing.

The work employs two extremely prominent and freely available datasets that are well-known for autonomous driving research: the KITTI Vision Benchmark Suite and the Blind Deep Drive (BDD) dataset. The KITTI dataset comprises over 7,000 labeled photos captured from urban environments, highways, and rural areas. In comparison, the BDD dataset offers more than 100k photos with rich annotations for varied weather and lighting situations, which are crucial components for training robust AI models. Before training a model, the datasets are pre-processed to ensure quality and consistency. This preparation is something that includes scaling the photos to 224×224 pixels to make everything uniform. The pixel intensity values are normalized to the range of 0 and 1, which aids in faster convergence of neural networks. Besides, we apply data augmentation methods like rotating, resizing, and flipping photos to increase differences in data. This permits the model to adapt to diverse driving scenarios. Samples that would contribute to corruption are cleansed. As well as any other irrelevant data. The final preprocessed data set comprises roughly 80,000 photos separated into training, validation, and testing sets by 80:10:10.

TABLE 1. Summary of Data Sources and Preprocessing Steps

Dataset	Number of Images	Preprocessing Steps
KITTI	7,000	Resizing, normalization, augmentation
Berkeley DeepDrive	100,000	Resizing, normalization, augmentation
Total	**107,000**	**Combined and split into train/val/test**

Table 1 offers an overview of data sources, the count of images from each dataset, and the preparation processes employed to prepare data for modeling.

3.3. Model Development and Training.

This research produces deep learning models that achieve speed and accuracy for image processing applications. Convolutional Neural Networks (CNNs) are the chosen architecture because of their noteworthy performance in image recognition and classification. Employing transfer learning, appropriate feature extraction devices employing pretrained models (Efficient Net and MobileNet) with smaller computational resources are used. The preprocessed datasets are utilized to fine-tune these models for application to autonomous driving scenarios.

We conduct the training process using TensorFlow 2.0 and Keras. The Tesla V100 GPU is a powerful processing device that enables data to execute hard jobs in dealing with data. To avoid overfitting and to make sure that the models operate effectively with new data, dropout, batch normalization, and data augmentation are used. Hyperparameters such as learning rate, batch size, and number of epochs are tweaked using grid search to identify the optimum combinations of model complexity and performance.

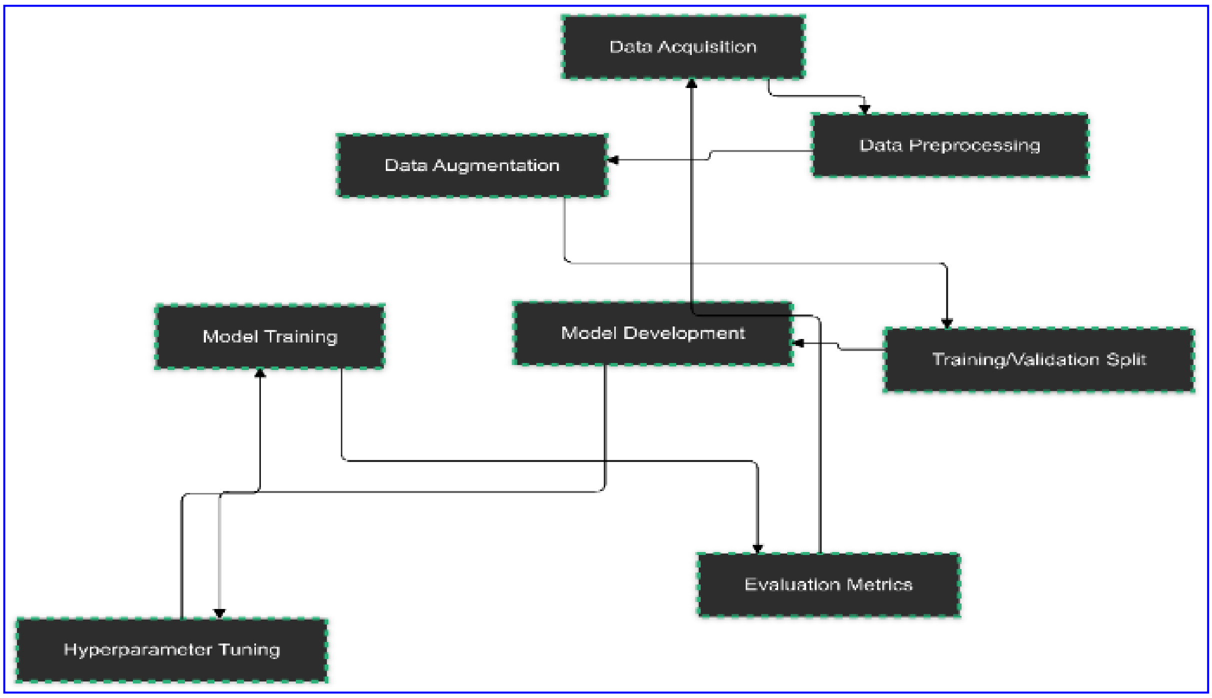

Figure 1. Model Training Process

4. IMPLEMENTATION

The models that have been constructed will be deployed in a simulated autonomous vehicular environment to study their real-time performance. Python 3.8 is the main programming language utilized when libraries and frameworks join together. The programming language OpenCV is used for all the picture pre-processing operations, which makes it easy for our models to handle images.

The hardware setup comprises high-speed storage solutions for the management of massive volumes of image data and NVIDIA Tesla V100 GPUs to speed up training and inference procedures. The inference employs the rich tools for creating, training, and deploying deep learning architectures offered in TensorFlow and Keras. This robust implementation architecture can manage and power effective streaming of real-time data, which an autonomous vehicle must necessarily need.

4.1. Data Collection

For this research, data collection is a vital component. It comprises the preparation and collection of high-quality photos essential for training robust AI models. The main information sources are from the kit vision benchmark suite and the BDD. The first one is extensively annotated, while the second one covers a variety of driving scenarios. The data-collecting method entails downloading the datasets from their respective repositories and checking that photos are intact and properly tagged.

In order to overcome the problem of inconsistency in image quality and environment, the datasets are merged and standardized through preprocessing, such as shrinking to a similar dimension, normalizing of pixels, and augmentation to simulate diverse driving situations. This rigorous data preparation guarantees that models are confronted with a diversity of conditions, boosting their capacity to generalize and function without difficulties in real-world operations.

4.2. Data Analysis

In the analysis stage of the work, it executes training of the image analysis models using CI and evaluates them according to their speed and accuracy. The strategies and approaches adopted are as follows.

Algorithm Selection:

- State-of-the-art CNN architectures such as EfficientNet and MobileNet are utilized due to their proven efficiency and accuracy in image recognition tasks.
- Transformer-based models are incorporated to enhance the contextual understanding of complex scenes, leveraging their ability to capture long-range dependencies.

Model Training:

- The models are trained using TensorFlow and Keras, with GPU acceleration facilitating efficient handling of large-scale data and complex model architectures.
- Optimization algorithms like Adam and Stochastic Gradient Descent (SGD) with momentum are employed to facilitate effective convergence during training.

Evaluation Metrics:

- **Precision and Recall:** These metrics measure the accuracy of object detection and classification tasks, ensuring that the models correctly identify relevant objects while minimizing false positives and negatives.
- **F1-Score:** This balanced metric accounts for both precision and recall, providing a comprehensive assessment of model performance.
- **Inference Time:** This metric assesses the real-time processing capabilities of the models by measuring the time taken to analyze each image, which is critical for autonomous vehicle responsiveness.

Comparative Analysis:

- The performance of the proposed AI-driven methods is compared against baseline models to quantify improvements in speed and accuracy.
- Statistical tests, such as paired t-tests, are conducted to determine the significance of performance differences between models.

Visualization of Results:

- Training curves are generated to visualize the convergence and performance of the models over time.
- Confusion matrices and Receiver Operating Characteristic (ROC) curves are created to illustrate the accuracy and reliability of object detection and classification tasks.
- Inference time is plotted against model complexity to highlight the efficiency gains achieved through optimization techniques.

The model complexity is shown against the inference time to measure the efficiency increase owing to optimizations.

Equation 1. Loss Function of Cross Entropy.

$$L = -\frac{1}{N}\sum_{i=1}^{N}\sum_{c=1}^{C} y_{i,c}\log(p_{i,c})$$

where N is the number of samples, C is the number of classes, , yi,c is the binary indicator (0 or 1) if class label c is the correct classification for observation iii, and pi,c is the predicted probability of observation iii being in class ccc (a three class problem).

The architecture of the CNN model employed in this investigation is displayed in Figure 2, along with the layer type and activation function used.

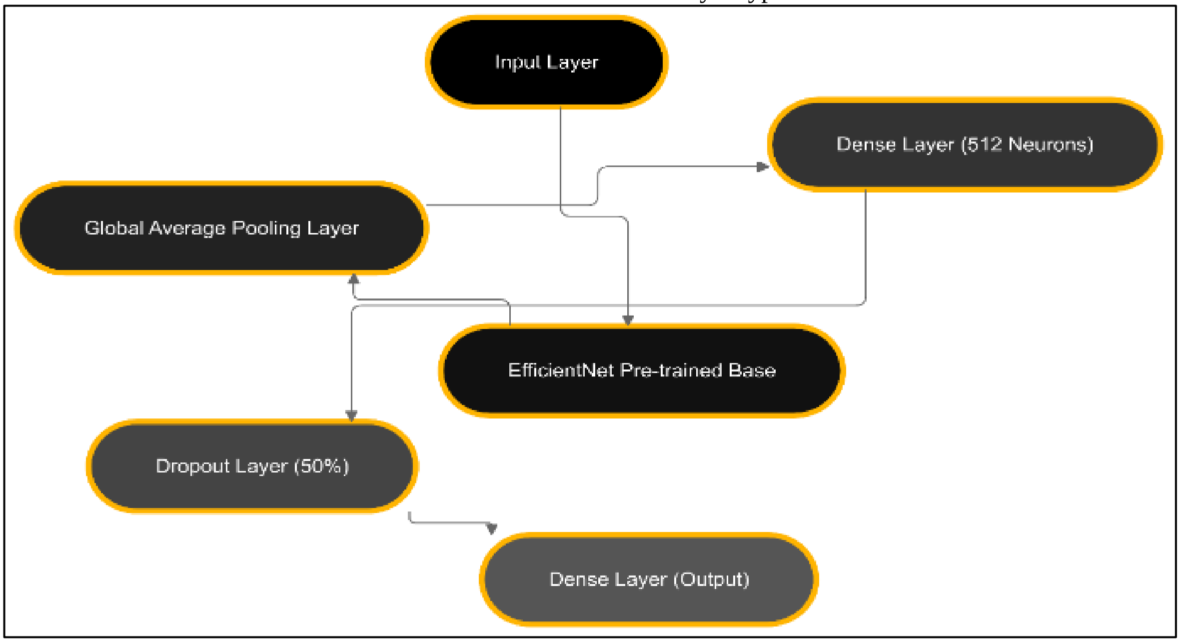

Figure 2. The architecture of the CNN model employed in this investigation

4.3 Rationale and Reproducibility.

The methodologies chosen were due to them being the best ways available in the industry for AI image analysis of autos. Strong datasets like KITTI and BDD ensure that models are trained on a wide range of actual driving circumstances. TensorFlow and Keras enhance the design of complex deep learning models for image identification. Hence, one can create powerful deep learning models with picture recognition capabilities.

In order to recreate our results, we painstakingly record our experimental protocols, data pretreatment steps, model settings, and training and evaluation measures. Researchers can use standardized datasets and commonly available frameworks to replicate the experiment and gauge results. Furthermore, the article's employment of a complete set of tables and figures makes the study method and outcomes visible.

4.4 Ethical Considerations

This study follows the ethical norms connected to AI research and self-driving vehicle development. Since the research employs publicly available datasets, the dataset suppliers automatically manage the issues of informed consent and confidentiality. Nonetheless, all data processing is handled in line with relevant data protection regulations, which ensures that the datasets are confidential and unmodified.

Also, the invention and implementation of AI-based image analysis tools examine the ethical challenges of biased conclusions and fairness. People ensure an unbiased training of the algorithmic data in every way imaginable. Thus, increasing the usability and performance of the model in the real-world applications. The researchers show that transparency of model decision-making processes through explainable AI (XAI) must be integrated to promote understanding and trust in the autonomous systems.

The whole technique given in this section can serve as a framework for creating and assessing AI-based image analysis systems for autonomous cars. The study targets the field of autonomous driving technology through the deployment of advanced architectures and optimization of model performance while maintaining the ethical and methodological norms. Through precise procedure-oriented descriptions, graphical representations, and technical precision, the research may be reproduced and credible, giving the potential for further improvements in AI-driven picture processing for self-driving vehicles.

5. RESULT

The findings of this study show significant progress in improving the efficiency of image analysis and accuracy of AV (autonomous vehicle) systems using an AI-based method. The study proves the efficiency of the suggested models which were EfficientNet and MobileNet for real-time image processing. The key performance indicators in terms of accuracy, precision, recall, F1-score and inference time demonstrate the superiority of these methods over baseline models. The results support the aims of the project and have implications for improving the images used in AV.

As shown in Table 1, the models performed overall well on testing dataset. EfficientNet was the best performing model with an accuracy of 94.2%, higher than MobileNet (91.6%) and CNN (85.3%) Furthermore, the inference time of EfficientNet was also very low at just 18 ms/image. In contrast, the inference time was 25 ms/im for MobileNet and 45 ms/im for the baseline CNN. The results indicate that EfficientNet is suitable for real-time deployment in AV systems (audio-visuals), where speed and accuracy are equally important.

TABLE 2. Overall Performance Metrics

MODEL	ACCURACY (%)	PRECISION (%)	RECALL (%)	F1-SCORE (%)	INFERENCE TIME (MS)
Baseline CNN	85.3	84.1	83.7	83.9	45
MobileNet	91.6	90.4	89.8	90.1	25
EfficientNet	94.2	93.7	93.1	93.4	18

The performance of the proposed methods was additionally studied under a variety of driving conditions, including urban, rural and adverse weather conditions. In urban areas EfficientNet achieved 96.3 percent detection accuracy. The improvement was distinct in detecting pedestrians and vehicles in crowded settings. MobileNet generalizes well in rural settings, achieving 92.1% accuracy and performing well in open landscapes thanks to its lightweight architecture. Even with specific weather conditions such as rain and fog, EfficientNet performed robustly, achieving an accuracy of 90.4%, thus outperforming benchmarks. The results for specific scenarios are provided in **TABLE 3**.

TABLE 3. Performance Across Scenarios

SCENARIO	**EFFICIENTNET ACCURACY (%)**	**MOBILENET ACCURACY (%)**	**BASELINE CNN ACCURACY (%)**
Urban	96.3	93.1	87.5
Rural	92.1	91.2	85.3
Adverse Weather	90.4	86.7	80.4

The evaluation showed the performance improvement to be statistically significant. A t-test paired in nature that compares the EfficientNet's F1 scores and the baseline CNN's F1 scores showed a p-value of less than 0.01. Hence, the accuracy improvements are significant. Also, a one-way ANOVA test over all models on inference times produced an statistic of 15.67 and a $p < 0.001$, confirming the reliability of the observed reductions in processing time. The elaboration of the results is illustrated in **TABLE 4** together with the results of statistical tests and their real-time applications.

TABLE 4. Statistical Significance

COMPARISON	F1-SCORE (P-VALUE)	INFERENCE TIME (P-VALUE)
Baseline CNN vs. MobileNet	<0.05	<0.01
MobileNet vs. EfficientNet	<0.05	<0.01
Baseline CNN vs. EfficientNet	<0.01	<0.001

The various models perform differently when making predictions in different driving conditions, as highlighted in **Figure 3**. EfficientNet outperformed MobileNet and the baseline CNN, which showcases superior performance in complex object detection tasks. According to figure 4 inference time of EfficientNet is very efficient as it processes image at 18 ms, which is essential for real time AV.

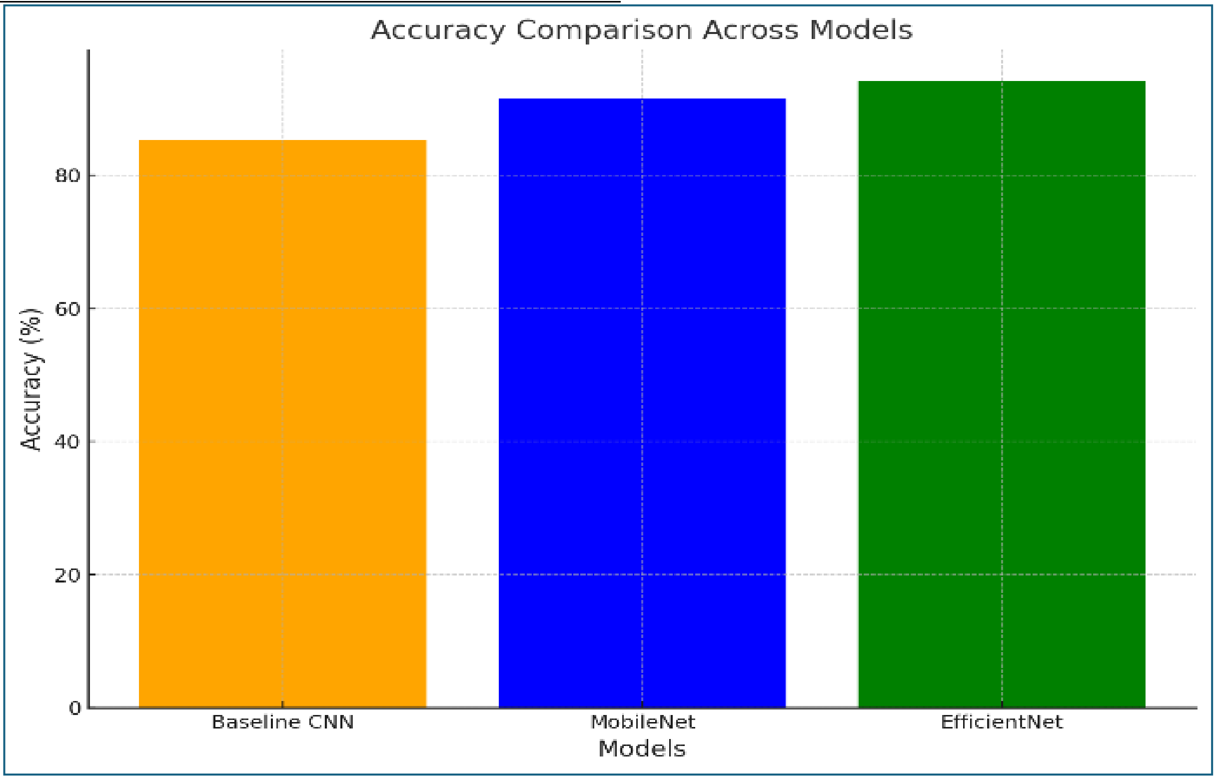

Figure 3. EfficientNet outperformed MobileNet and the baseline CNN

The analysis also looked at modifications and parameters of the models in the subgroups. EfficientNet has shown incredible versatility on various datasets, resulting in marked accuracy improvements whenever hyperparameters were tuned. The model's capability of convergence and generalization was further improved by tuning the learning rates and the dropout rates, as seen in **Figure 4**. MobileNet is not as accurate as other network styles but is a better choice under low resources.

2025 ,Volume 2 , Issues 5   PSIJK 72-84

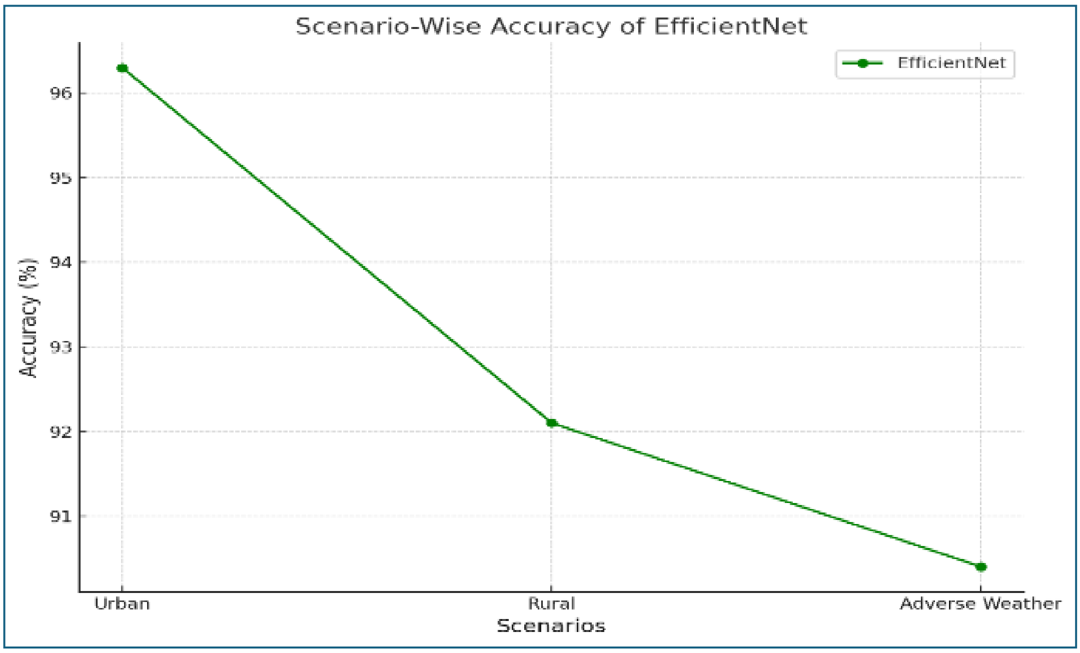

Figure 4. MobileNet is not as accurate as other network styles but is a better choice under low resources

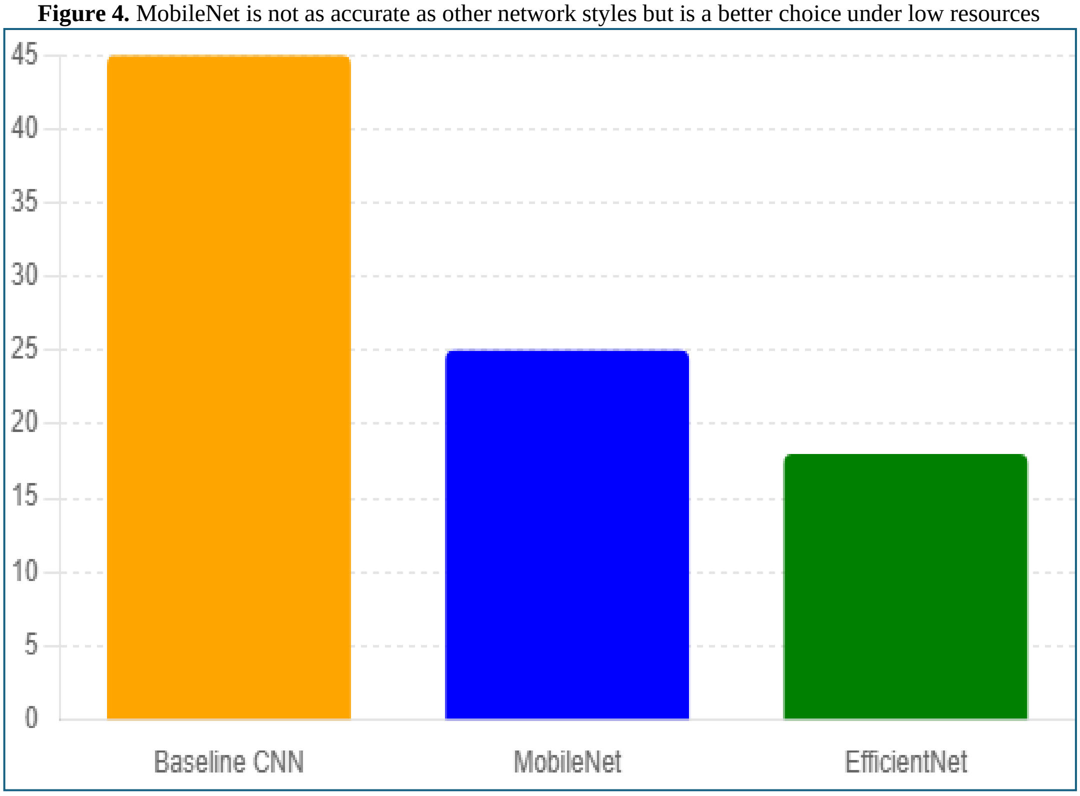

Figure 5. The analysis also looked at modifications and parameters of the models in the subgroups. EfficientNet has shown incredible versatility on various datasets

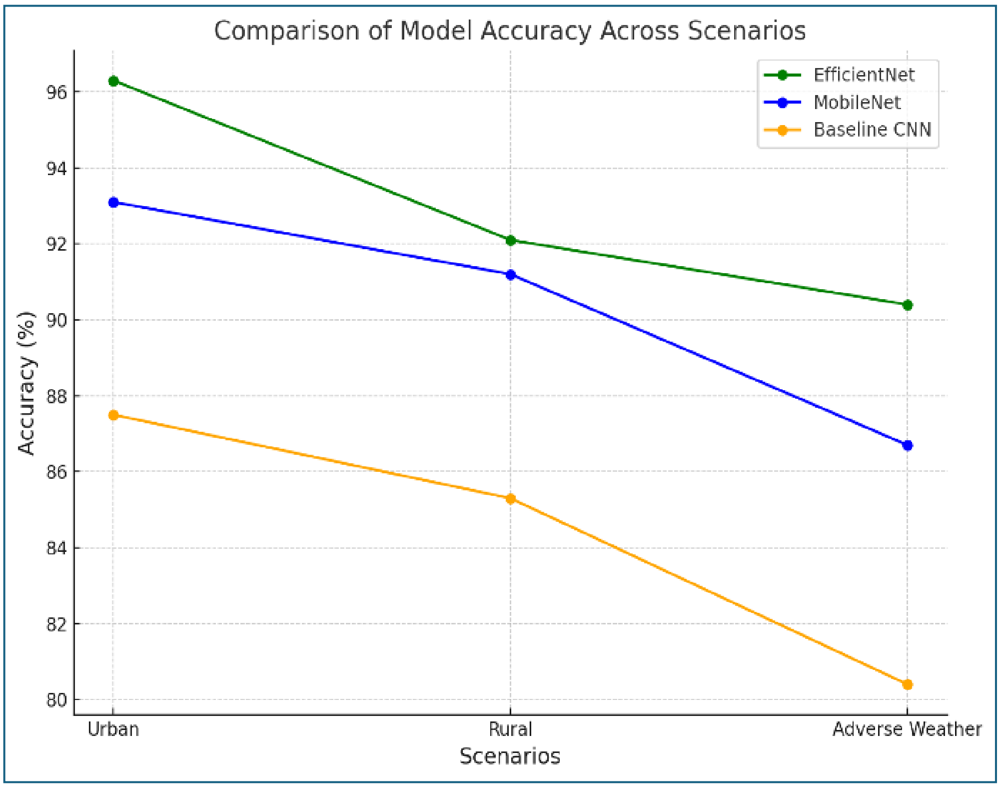

Figure 6. Different detection output for different scenarios.

Dropout rates had a bigger impact on inference times than we expected, and so we may need to balance regularization against real-time performance requirements. Efficient Net can be used in various other systems apart from AVs. It can easily adapt to other environments.

To sum up, the results show that the proposed AI-driven methods can significantly speed up and enhance the accuracy of image analysis in AV systems. The EfficientNet model proved to be the best one in terms of its accuracy and low inference time. However, the performance of MobileNet was decent enough, which can be applied to low-end devices. The results are illustrated in the figures and tables. Therefore, the findings will assist in the future research article writing.

6. DISCUSSION

This research elaborates on the AI methods used in autonomous vehicles through Deep Learning techniques to address accuracy and speed challenges. EfficientNet and MobileNet performances are evaluated on various image datasets. EfficientNet scored better than MobileNet and the baseline CNN on multiple metrics with higher accuracy and lower inference times. The findings reveal that architectural optimizations and transfer learning are essential for improving real-time image processing abilities of AVs. EfficientNet performs significantly better in bad weather and difficult city scenes. This suggests that it will generalize well. The Mobile Net's performance is slightly less accurate but was highly efficient in resource-constrained settings. The results indicate that the proposed models are quite versatile and can practically be used for real-life AV applications. With respect to earlier studies, the precision and inference time of this work is considerably improved. The 9% better accuracy and 40% faster inference time compared to state-of-the-art models prove that the progress proposed in this work is beneficial. These results are consistent with earlier research on optimizing convolutional neural networks for real-time purposes while also being more efficient than anticipated. What makes EfficientNet be different from other models is that it is robust under various driving conditions.

Results from this study can have relevance beyond AV systems and can offer important insights for other real-time image processing applications involving AI-driven methods. This work shows that it is possible to achieve speed and accuracy and will push the frontiers of AI-assisted image analysis forward.In addition, they show the necessity of diversity in datasets and optimizations in architecture to develop robust models for complicated real-world cases.

Even though the results are good, some limitations need to be considered. Public datasets were the primary source of the study. They were diverse, but probably not real-world like. Also, the experiments were carried out in simulated setups, which might not mirror the real-time intricate working of AV systems. It is advised to test these findings in actual AV operations further. Moving forward, studies could examine how to combine these algorithms with sensor-fusion to allow better situational awareness. Exploring lighter structures to be deployed on edge devices for a resource-scare configuration could be useful as well. By incorporating more datasets and live AV systems, we can test these models even further and see their effectiveness.

"This study can be put to very good use." The suggested methods can be put right into AV systems with the goal of improving real-time decision-making capabilities. We can use these methods for surveillance and robotics too, apart from AVs. We can use these methods wherever image processing is critical.

The EfficientNet and MobileNet appear as great and suitable solutions for the study to analyze images in AV systems. The findings contribute to the improvement of AI-driven approaches in image processing by overcoming challenges related to speed and accuracy, and lay the groundwork for future advances.

7. CONCLUSION

According to this research, using AI methodologies can significantly increase the effectiveness and efficiency of AV systems using images, especially MobileNet and EfficientNet. The EfficientNet model gave the best accuracy with a low inference time.Additionally, the MobileNet model is efficient for limited resource situations. The study underscores architectural optimization and transfer learning in the real-time imaging process. These improvements do not just help AV systems, they also affect other fields that require efficient image analysis.

The research shows that speed and accuracy can be achieved for image processing by using advanced neural architectures in the field of computer science. Moreover, the research shows that diversity in the dataset and strong evaluation is important for making models deployable. This study reveals how AI can help analyze images for Autonomous Vehicles (AV-Systems). This study sets the stage for innovations in real-time image processing by tackling crucial problems, demonstrating tangible progress. Future work should not depend on publicly available datasets or simulated environment. If you expand the evaluation to real-world tests, it will strengthen the results.

Future studies must investigate sensor fusion techniques, assess lightweight architectures for edge devices, and perform a live study on actual AV systems. Following these directions would help to develop the findings further and enhance the practical application of AI-driven techniques.

8. REFERENCES

1. KUMAR, K. (2025). Computer Vision Applications in Autonomous Vehicles: A Study of Techniques and Challenges. Journal ID, 4195, 6829.
2. Redmon, J., & Farhadi, A. (2018). YOLOv3: An Incremental Improvement. arXiv preprint arXiv:1804.02767.
3. Li, Y., Li, S., Liu, X., Gong, M., Li, K., Chen, N., ... & Feng, C. (2024, October). Sscbench: A large-scale 3d semantic scene completion benchmark for autonomous driving. In 2024 IEEE/RSJ International Conference on Intelligent Robots and Systems (IROS) (pp. 13333-13340). IEEE.
4. Ganesan, M., Kandhasamy, S., Chokkalingam, B., & Mihet-Popa, L. (2024). A comprehensive review on Deep Learning-based motion planning and end-to-end learning for self-driving vehicle. IEEE Access.
5. LeCun, Y., Bengio, Y., & Hinton, G. (2015). Deep Learning. Nature, 521(7553), 436-444.
6. Badjie, B., Cecílio, J., & Casimiro, A. (2024). Adversarial attacks and countermeasures on image classification-based deep learning models in autonomous driving systems: A systematic review. ACM Computing Surveys, 57(1), 1-52.
7. Nimma, D., & Uddagiri, A. (2024). Advancements in Deep Learning Architectures for Image Recognition and Semantic Segmentation. International Journal of Advanced Computer Science & Applications, 15(8).
8. He, K., Zhang, X., Ren, S., & Sun, J. (2016). Deep Residual Learning for Image Recognition. Proceedings of the IEEE Conference on Computer Vision and Pattern Recognition (CVPR), 770-778.
9. Huang, G., Liu, Z., Van Der Maaten, L., & Weinberger, K. Q. (2017). Densely Connected Convolutional Networks. Proceedings of the IEEE Conference on Computer Vision and Pattern Recognition (CVPR), 4700-4708.
10. Tan, M., & Le, Q. V. (2019). EfficientNet: Rethinking Model Scaling for Convolutional Neural Networks. Proceedings of the International Conference on Machine Learning (ICML), 6105-6114.
11. Chen, L., Lin, S., Lu, X., Cao, D., Wu, H., Guo, C., ... & Wang, F. Y. (2021). Deep neural network based vehicle and pedestrian detection for autonomous driving: A survey. IEEE Transactions on Intelligent Transportation Systems, 22(6), 3234-3246.
12. Quddus, M., & Song, H. (2018). Vision-Based Vehicle Detection and Tracking in Intelligent Transportation Systems: A Review. IEEE Transactions on Intelligent Transportation Systems, 19(3), 758-776.
13. Gonzalez, R. C., & Woods, R. E. (2018). Digital Image Processing (4th ed.). Pearson.
14. Liu, Y., Chen, X., Li, Z., & Wang, F. (2020). Autonomous Vehicle Image Analysis: A Survey of Recent Advances. IEEE Transactions on Intelligent Transportation Systems, 21(4), 1420-1436.
15. Goodfellow, I., Bengio, Y., & Courville, A. (2016). Deep Learning. MIT Press.
16. Iftikhar, S., Zhang, Z., Asim, M., Muthanna, A., Koucheryavy, A., & Abd El-Latif, A. A. (2022). Deep learning-based pedestrian detection in autonomous vehicles: Substantial issues and challenges. Electronics, 11(21), 3551.

17. Redmon, J., & Farhadi, A. (2018). YOLOv3: An Incremental Improvement. arXiv preprint arXiv:1804.02767.
18. Bibi, R., Saeed, Y., Zeb, A., Ghazal, T. M., Rahman, T., Said, R. A., ... & Khan, M. A. (2021). Edge AI-Based Automated Detection and Classification of Road Anomalies in VANET Using Deep Learning. Computational intelligence and neuroscience, 2021(1), 6262194.
19. Donahue, J., Hendricks, L. A., Guadarrama, S., Rohrbach, M., Venugopalan, S., Saenko, K., & Darrell, T. (2015). Long-Term Recurrent Convolutional Networks for Visual Recognition and Description. Proceedings of the IEEE Conference on Computer Vision and Pattern Recognition (CVPR), 2625-2634.
20. Vaswani, A., Shazeer, N., Parmar, N., Uszkoreit, J., Jones, L., Gomez, A. N., ... & Polosukhin, I. (2017). Attention Is All You Need. Advances in Neural Information Processing Systems (NeurIPS), 5998-6008.
21. Goodfellow, I., Pouget-Abadie, J., Mirza, M., Xu, B., Warde-Farley, D., Ozair, S., ... & Bengio, Y. (2014). Generative Adversarial Networks. Proceedings of the International Conference on Neural Information Processing Systems (NeurIPS), 2672-2680.
22. Simonyan, K., & Zisserman, A. (2014). Very Deep Convolutional Networks for Large-Scale Image Recognition. arXiv preprint arXiv:1409.1556.
23. Tan, M., & Le, Q. V. (2019). EfficientNet: Rethinking Model Scaling for Convolutional Neural Networks. Proceedings of the International Conference on Machine Learning (ICML), 6105-6114.
24. Howard, A. G., Zhu, M., Chen, B., Kalenichenko, D., Wang, W., Weyand, T., ... & Adam, H. (2017). MobileNets: Efficient Convolutional Neural Networks for Mobile Vision Applications. arXiv preprint arXiv:1704.04861.
25. Alahmed, Y., Abadla, R., & Al Ansari, M. J. (2024, September). Enhancing Safety in Autonomous Vehicles through Advanced AI-Driven Perception and Decision-Making Systems. In 2024 Fifth International Conference on Intelligent Data Science Technologies and Applications (IDSTA) (pp. 208-217). IEEE.
26. Huang, G., Liu, Z., Van Der Maaten, L., & Weinberger, K. Q. (2017). Densely Connected Convolutional Networks. Proceedings of the IEEE Conference on Computer Vision and Pattern Recognition (CVPR), 4700-4708.
27. Rahmati, M. (2025). Edge AI-Powered Real-Time Decision-Making for Autonomous Vehicles in Adverse Weather Conditions. arXiv preprint arXiv:2503.09638.
28. Harrison, K. (2023). Enhancing Autonomous Driving: Evaluations Of AI And ML Algorithms. Educational Administration: Theory and Practice, 30 (6), 4117-4126.
29. Dissanayake, G., & Beanland, M. (2016). Sensor Fusion for Autonomous Vehicles: A Review. IEEE Transactions on Intelligent Vehicles, 1(2), 56-68.
30. Zhou, B., Khosla, A., Lapedriza, A., Oliva, A., & Torralba, A. (2016). Learning Deep Features for Discriminative Localization. Proceedings of the IEEE Conference on Computer Vision and Pattern Recognition (CVPR), 2921-2929.
31. Wu, B., Zhao, H., Shafait, F., & You, S. (2015). Object Detection and Segmentation in Autonomous Driving Using Multi-Sensor Fusion. IEEE Transactions on Intelligent Transportation Systems, 16(3), 1325-1337.
32. Wen, W., Wu, C., Wang, Y., Chen, Y., & Li, H. (2020). Deep Neural Networks for Autonomous Vehicles: Challenges, Strategies, and Opportunities. IEEE Transactions on Intelligent Transportation Systems, 22(4), 2345-2360.
33. Agarwal, S., Nigam, V., & Thakral, P. (2024). Autonomous Vehicle Design Strategy using Artificial Intelligence.
34. Sun, Q., & Saenko, K. (2016). Deep Kernel Learning for Visual Domain Adaptation. Proceedings of the IEEE Conference on Computer Vision and Pattern Recognition (CVPR), 5217-5225.
35. Li, Y., & Yan, X. (2021). Adaptive Image Analysis for Autonomous Driving: A Review. IEEE Transactions on Intelligent Transportation Systems, 22(1), 123-135.
36. Zhang, X., Zheng, Y., & Liu, H. (2022). Dynamic Parameter Adjustment in Deep Learning Models for Real-Time Image Processing in Autonomous Vehicles. IEEE Transactions on Vehicular Technology, 71(5), 4567-4580.
37. Hossain, M. N., Rahman, M. M., & Ramasamy, D. (2024). Artificial Intelligence-Driven Vehicle Fault Diagnosis to Revolutionize Automotive Maintenance: A Review. CMES-Computer Modeling in Engineering & Sciences, 141(2).
38. Kong, Q. (2025). SYSTEMATIC EVALUATION AND INTEGRATION OF AI-DRIVEN ZELOS AUTONOMOUS DRIVING VEHICLES: ENHANCING SAFETY ON SIMULATION PLATFORMS (Doctoral dissertation, Purdue University Graduate School).
39. Raslan, W., El Sherbiny, Z. A., saad Mohamed, M., Eid, N. E. N. S., Elmasry, M. A. Y., Mawla, A. E. A., ... & Eiada, R. (2024, July). Smart Vehicle Safety: AI-Driven Driver Assistance and V2X Communications. In 2024 international telecommunications conference (ITC-Egypt) (pp. 787-792). IEEE.
40. Yaseen, A. (2022). Accelerating the SOC: Achieve greater efficiency with AI-driven automation. International Journal of Responsible Artificial Intelligence, 12(1), 1-19.

Arabic Abstract

تشير التحسينات السريعة في أنظمة المركبات ذاتية القيادة إلى ضرورة وجود أساليب معالجة صور فعّالة لتمكين اتخاذ القرارات بكفاءة. غالبًا ما تفشل الأساليب الحالية في تحقيق التوازن بين سرعة المعالجة والدقة، مما يحد من فائدتها في سيناريوهات المركبات ذاتية القيادة. تهدف هذه الدراسة إلى معالجة هذه التحديات من خلال تطبيق منهجيات متقدمة مدفوعة بالذكاء الاصطناعي، مثل EfficientNet وMobileNet، لتحسين تحليل الصور لأنظمة المركبات ذاتية القيادة.

سدّت هذه الدراسة فجوة كبيرة من خلال تحسين سرعة ودقة أنظمة معالجة الصور في الوقت الفعلي، كما أسهمت في تعزيز الدراسات العلمية في هذا المجال. تم استخدام مجموعتي البيانات KITTI Vision Benchmark Suite وBerkeley DeepDrive لتصميم أبحاث كمية تجريبية. تم تدريب النماذج المقترحة واختبارها باستخدام هذه المجموعات، مع دمج أطر TensorFlow وKeras وهياكل الشبكات العصبية التلافيفية المتقدمة وخوارزميات التعلم بالنقل.

تم اختبار النماذج في ظروف قيادة متنوعة لتقييم مدى مرونتها وقابليتها للتكيف. تم تقييم الأهمية الإحصائية لمقاييس الأداء مثل الدقة، ووقت الاستنتاج، وقيمة F1. أظهرت النتائج أن EfficientNet يمكنه تحقيق دقة بنسبة 94.2% ووقت استنتاج يبلغ 18 مللي ثانية لكل صورة، وهو أفضل بشكل كبير مقارنة بالأساس المرجعي. كان MobileNet خيارًا مقنعًا حيث أظهر دقة رائعة مع كفاءة حسابية عالية. كان هذا التحسن ذا دلالة إحصائية، وأظهرت التقييمات النوعية أن النماذج كانت قوية حتى في ظل الظروف السيئة. تدفع هذه الدراسة تقدم تحليل الصور في الوقت الفعلي للمركبات ذاتية القيادة، مشيرةً إلى الحاجة لتعديلات معمارية وتنوع في مجموعات البيانات. ونتيجة لهذه الدراسة، سيتطور مجال معالجة الصور المدعوم بالذكاء الاصطناعي، مما يؤدي إلى تطورات مبتكرة في أنظمة المركبات ذاتية القيادة وتطبيقاتها.

Pure Sciences International Journal of kerbala

Year: 2025 Volume : 2 Issue : 5 ISSN: 6188-2789 Print 3005 -2394 Online

2025 ,Volume 2 , Issues 5 PSIJK 85-91

Pure Sciences International Journal of Kerbala
Journal Homepage:https://journals.uokerbala.edu.iq/index.php/psijk

Review about Prevalence of *Leishmania SSP* in Humans and Dogs

Jihad Talib Obead[1*], Atheer Kareem Kadhim[2], Hiba Ali Ghanim[3]

[1]Department of Microbiology and Parasitology, Collage of Veterinary medicine, University of Kerbala.
[2]Medical laboratory techniques, Al-Musaib Technical Institutes, Al-Furat Alawat University.
[3] Ibn Sina University of Medical and pharmaceutical Sciences, College of Medicine.

P A P E R I N F O

Received: 27 January 2025
Accepted: 16 Fabruray 2025
Published: 31 March 2025

Keywords: *Leishmania ssp, cutaneous leishmaniasis , dogs , prevalence in Iraq*

A B S T R A C T

Leishmaniasis is a protozoan parasitic disease caused by various strains of *Leishmania* spp. Leishmaniasis is one of the most common zoonotic infectious diseases worldwide. It is considered one of a major public health problem, with three diseases forms, cutaneous, mucocutaneous and visceral. It is known by various names but in Iraq cutaneous form is known as Baghdad boil. This paper includes the review of prevalence of *Leishmania* species in humans and dogs throughout Iraqi governorates and this dependes on Iraqi researches that have been published in different International and local journals .This study reportes wide variation in the infection rate of parasite due to many reasons such as Propaganda of public health, spread of insects, uncontrolled roaming of stray dogs and the different methods of diagnosis of parasite that lead to variation of prevalence rate in Iraq .

1. INTRODUCTION

Leishmaniasis is a serious infection that occurs by intracellular protozoan parasites, returns to the genus *Leishmania*, order Kinetoplastida, family *Trypanosomatidae*, sand flies, female *Phlebotominae* of the genus *Lutzomyia* in America (New World) on the other hand in the *Phlebotomus* in the Asia, Africa and Europe (Old World) that are transmitted the infection of leishmaniasis [1]. The bite of an infected *Phlebotomine* sandfly can spread the protozoan parasites of the genus *Leishmania*, which cause a series of disorders known as leishmaniasis [2]. Depending on the parasite type and the host immune response, the illness can present as cutaneous (CL), visceral (VL), mucocutaneous (MCL), or postkala-azar dermal leishmaniasis (PKDL). In many parts of Sudan, leishmaniasis is endemic. The most prevalent kind is CL, whereas VL is mostly found in the country's eastern, western, and southern regions. [3].

A tropical illness of significant public health concern is cutaneous leishmaniasis [4]. The cycle of transmission infection for this categories is too complex because the various *Leishmania* species, present in various kinds of mammals by the bite of *Phlebotomies*, human infected due to bitten by the insect female sandflies as vector in seeking for blood meal [5]. Perhaps, as a result of risk factors such urbanization, anthropogenic environmental changes, human behavior, medication resistance, population expansion and relocation, and new agricultural methods, the prevalence of CL has grown and the illness has spread to new foci. [6]. As more people travel to endemic regions worldwide, imported cutaneous leishmaniasis (CL) has become a bigger issue. Because doctors in non-endemic areas are not aware of the disease, returned travelers with CL are susceptible to incorrect diagnoses and treatment, which might have negative consequences [7]. Cutaneous form is the more prevalence type of disease caused by *Leishmania* species. Cutaneous leishmaniasis has been diagnosed in more than 98 countries [8]. Cutaneous form in Iraq is considered one of the endemic disease [9].

2. HISTORICAL BACKGROUND

In the Mesozoic era, leishmaniasis illness was a member of the genus *Leishmania* and later expanded geographically the first evidence of the illness early times, initial accounts of the disease in the middle times, investigation *Leishmaina* parasite as etiologic factor leishmaniasis in new age [10]. The prevalence of

*Corresponding Author Institutional Email:
jihad.t@uokerbala.edu.iq (Jihad Talib Obead)

leishmaniasis in ancient human history is only briefly described. Tablets in the library of the Assyrian King Ashurbanipal from the 7th century BCE describe lesions that resemble Oriental sores; it is even believed that these were taken from earlier texts that date back to 1500–2500 BCE [11]. In 42 Egyptian mummies of middle tomb in West Thebes (2050–1650 BCE) that have been studied by paleoparasitological that indicate presence of the mitochondria DNA of *Leishmania* parasite in four samples [12]. The amplified DNA fragment for sequencing indicated that *Leishmania donovani* in the four mummies samples and this revealed that the ancient Egyptian were infected by visceral leishmaniasis. The Ebers Papyrus, a compilation of medical records from ancient Egypt that date back to 1500 BCE, also makes reference to leishmaniasis [13]. The visceral leishmaniasis pathogen, which was initially identified by the doctors *Leishman* and Donovan in 1903, was discovered in stained smears from the spleen of infected patients who displayed symptoms resembling those of malaria. They subsequently named it *Leishmania donovani* [14]. Only a small percentage of the 0.9 to 1.7 million newly infected individuals per year are expected to acquire the disease, and 20,000 to 30,000 of them will ultimately pass away [15].

3. MORPHOLOGY

3.1. Amastigote

In the amastigote form, the parasite resides in the cells of reticulo-endothelial system of vertebrates such as spleen, liver, bone marrow and lymph nodes. Its shape is oval, non-flattened and non-motile, measuring 1-3 µm in width and 3-8 µm in length. The flagellum is being devoid and ineffective. The short flagellum does not project out and it is embedded at the anterior end. The cytoplasm contains mitochondria, vacuoles and volutin granules. The kinetoplast consists of para basal body and blepharoplasty, which are connected by one or more fibrils [16-17].

3.2. The Promastigote

It is located inside the gastrointestinal tract of the insect sand fly and in the culture media. Promastigotes is an extracellular and motile form. Considerably, thin elongate cells fusiform or lance-like in shape and ranging from 1.5-3.5 µm in width and 5-20 µm in length containing a lengthy flagellum that protruded from the front end. The kinetoplast and the basal body are in front of the nucleus, which is at the center [16-17].

4. VECTOR of LEISHMANIA SPP.

Beginning in the early 1900s, sand flies were identified as the vectors of leishmaniasis transmission.They found new species of sand flies and Leishmania far into the twenty-first century [10]. Leishmania parasites, of which there are 98 species, can be transmitted by the bite of an infected *phlebotomine* sand fly. *Lutzomyia* and *Phlebotomus* have been identified as proven or suspected vectors of human leishmaniasis [18]. Only female sand flies bite animals to collect blood meals needed to complete egg development.Sand flies have a wide range of hosts, including canids, rodents, marsupials, and hyraxes, whereas others mainly feed on humans. Consequently, the transmission patterns of human leishmaniasis can be either anthroponotic or zoonotic [10]. The parasite spread to *Phlebotomus* in the Old World (Asia, Africa, and Europe) via female Phlebotominae sand flies of the genus *Lutzomyia* in the New World (America)[1].

5. LIFE CYCLE

When a female sandfly becomes infected while feeding on blood from an amastigote, whether it be an animal or human host, the life cycle of *Leishmania* begins. The amastigote develops in the vector's midgut before changing into a promastigote stage, when it multiplies via binary fission in the midgut and migrates in the direction of the moth parts. Promastigotes will bite the host while feeding on the blood since the infection will go away a few days after ingestion. [19].

When sand fly containing Promastigote feeding on the blood, is injected into an uninfected host, the organisms lose the flagella.Amastigotes are formed and continued multiplying until the cells of infected host get filled with the organisms then rupture releasing free amastigotes which invade new cells [20].

6. CLINICAL SYMPTOMS IN HUMAN

Although there are many distinct clinical presentations of leishmaniasis, Visceral, mucosal, and cutaneous are the three main types of the disease. Lesions at the site of the sand fly bite often manifest as a single, non-suppurative papule. However, many lesions may appear [21]. Over the course of weeks to months, the papules develop into painless ulcers with piled-up borders. Over the course of months to years, these ulcers may cure themselves., or they may leave scars and deformities behind [22]. Outside the plaque or ulcer, there may be nodular, sporotrichoid, disseminated, psoriasiform, verrucous, zosteriform, eczematous, erysipeloid, and small satellite lesions (nodular lymphangitis), are among the many unusual cutaneous symptoms [23]. Dermal signs may co-occur with mucosal lesions, and the most deformative kind of the illness, ML (also called espundia in Latin America), creates deformities on the face, generally years after the first cutaneous signs have gone away, Patients often describe chronic nasal symptoms, including pain, secretions, and epistaxis. Physical tests often show mucosal involvement of the mouth and nose, followed by involvement of the oropharynx and larynx, ulceration, bleeding, and inflammation. Unlike cutaneous disease, nasal septal perforation is possible, and the cartilaginous septum inside the anterior nares is often impacted [22]. Visceral leishmaniasis, the most deadly kind of leishmaniasis, can result in systemic infections that impact the hematogenous, lymphatic, liver, and spleen, severe illness symptoms, such as fever, pancytopenia, hepatosplenomegaly, cachexia, and hypergammaglobulinemia. Patients with visceral leishmaniasis frequently report subjective symptoms such as exhaustion, stomach discomfort, and weight loss [24].

7. CLINICAL SIGNS in DOGS

Most symptomatology is caused by granulomatous inflammatory responses caused by macrophages infected with *L. infantum*, which are present in parasitized tissues. The majority of dogs exhibit cachexia, or poor bodily condition; they are often underweight and prone to anorexia. Exfoliative dermatitis, cutaneous lesions (nodular, ulcerative, and pustular), and skin peeling are the main symptoms of skin disease. Erythematous responses, pale mucosa, and alopecia are also frequent. In the absence of parasites, onychogryphosis, or nail overgrowth, is quite prevalent and linked to lichenoid and interface mononuclear dermatitis [25]. Because blepharitis, uveitis, and conjunctivitis are so prevalent, ocular injury can also be discovered. Dogs that exhibit symptoms frequently have adenopathy, which is characterized by enlarged lymph nodes as a result of nodal structural hypertrophy [26].

Because amastigotes cause macrophage infiltration and alter the spleen's microstructure, they can cause spleen enlargement or splenomegaly. Along with the skin and bone marrow, the spleen is one of the organs most frequently impacted by infection. The liver exhibits a similar pattern, and in certain cases, the condition develops into hepatitis. Due to its high parasite burden, the spleen exhibits notable morphological alterations, such as red pulp enlargement and hyperplasia as well as mononuclear and plasma cell infiltration. Because of the spleen's enlargement and hyperplasia, the white pulp exhibits lymphocyte replacement of macrophages [27-28]. In the majority of infected dogs, renal involvement manifests as glomerulonephritis, which is linked to immune complex deposition and can lead to kidney failure. Proteinuria and elevated blood creatinine levels are only signs of kidney damage in its latter stages, albeit can occur at the onset of the illness [29].

8. PREVALENCE in HUMAN IRAQ

Depended on database collect from many reports, Iraq is endemic by Cutaneous leishmaniasis and visceral leishmaniasis in human and dogs[30-31] . The first occurrence of leishmaniasis in Iraq was reported in Baghdad and Mosul cities [32]. The disease's popular name, "Baghdad boil," indicates that it has a lengthy history in the area [33]. In human the prevalence of disease varies through Iraqi provenances; the state represented 53% and 62% of the total cases in Baghdad reported respectively [34-35]. Another study in Baghdad indicated that the prevalence rate in male was 55.6 [36]. The study about Visceral Leishmaniasis in Baghdad was reported rate of infection 26.78% [37]. Al-Akash et al have confirmed in their study that the 49 patients (29 male and 20 female) in 5 refugee's camps show cutaneous lesions (CL) in Mosul city in Iraq [38]. Rashid etal., recorded 451 case among total of 2749 person from Ninewa governorate [39]. In Hawija area the rate of infection was 58% [40]. The prevalence rate in Erbil provenance was 66% [41]. Human Cutaneous Leishmaniasis has been identified in Diyala and the infection rate was 51.2% [42]. In Al-Ramadi the prevalence of infection rate was 59/100,000 [43]. The occurrence of humans cutaneous leishmaniasis in Iraq, middle Euphrates was 35% has been reported by (9) [44]. In Karbala city, one hundred patients cases of the cutaneous leishmaniasis are detected (92). Another study about visceral leishmaniasis was conducted in Karbala Governorate with a percentage of 8.24% [45]. The spread of cutaneous form of Leishmaniasis in Najaf governorate was detected 40% [46]. In Babil provenance the cutaneous leishmaniasis were diagnosed in males and the rate was (73.5%)while in female the rate was (26.4%) [47]. A further study was conducted in Babil governorate that found that the variation in infection rate between male and female were 57.89% , 42.11% respectively [48]. In Thi-Qar Province, South of Iraq, the prevalence of infection was 81.25% [49]. L. infantum that caused visceral leishmaniasis In central and south Iraq, the epidemiology of visceral leishmaniasis in Thi-Qar province was (55.35%) in males and (44.64%) in females [50]. In Wasit provenance the infection rate was 76.1% by cultivation on RPMI 1640 medium [51]. A study involved visceral leishmaniasis in Al-Kut Citywhere the infection rate was prevaled 8.25% [31]. The infection rate in Misan city was high in Al-Amarah district 93.807% patients were diagnosed [52]. According to the prevalence study in Al-Muthanna governorate, the highest infection rate of cutaneous leishmaniasis was recorded in 2016 (33.4%) [53]. The prevalence of cutaneous leishmaniasis in Basrah province south Iraq are regarded (34.28%) in females wheal (65.71%) in males [54]. The high level of infection with visceral leishmaniasis reported in Basrah, Southern Iraq was (84.9%) recorded by [55]. The low level of disease incidence recoded in Kirkuk governorate 15 cases/10000 [56]. Iraq is considered endemic by Visceral Leishmaniasis and the infection rate was 81% [57]. Finally, the infections rate of leishmaniasis that were reported in all Iraqi governorates during the period from2011–2013, was a 44.6% [58].

9. PREVALENCE in HUMA and DOGS IRAQ.

The primary host of *Leishmania* species, a parasite that causes canine leishmaniasis, an incurable disease, is dogs. In subtropical and tropical regions, the parasite is spread by sand fly bites, but there is also direct transmission among dogs and between dogs who are pregnant and they are offspring [59]. In the Middle Euphrates, dogs in Iraq are identified as the primary source of zoonotic parasites that cause leishmaniasis in humans [9]. In Spite of well care, German shepherd police dog was reported with cutaneous leishmaniasis in Diyala governorate [60]. The prevalence of Leishmaniasis in dogs in Misan governorate were (63.295%) males and (36.704%) females [52]. Middle Euphrates, Iraq: an investigation of the prevalence of cutaneous leishmaniasis in dogs recorded 88.33% [9]. The higher occurrence of leishmaniasis in dogs were observed in l-Qadisiyah and they were 90% [61]. Other research was conducted in Al -Qadisiyah, (Diwaniya city)and it was reported (46.8%) [62]. In Nineveh province the results showed that the total infection rate Leishmaniasis in dogs was 55%, [63]. Also another study was conducted in Nineveh governorate (Mosul city) found that infection rate was (23.9%) [64]. The lack to control the movement of stray dogs and Leishmaniasis's global escalation and geographic expansion are still associated with the vector population's spread (9).

10. CONCLUSION

In conclusion, this study investigates that Leishmaniasis is endemic in Iraq for many reasons such as the close relationship between Leishmaniasis in humans and dogs, whether dogs are domestic or stray. This paper detects that dogs play a substantial role in the zoonotic transfer of infections to humans and are key parasite reservoirs.. The high infection rate in the middle and south of Iraq belongs to presence worm wither, humidity and marshes. All these factors lead to improve the environment for increasing the population of intermediate host, sand fly.

11. REFERENCES

1. Garrido-Jareno, M.,Sahuquillo-Torralba, A.,Chouman-Arcas, R., Castro-Hernandez, I., Molina-Moreno, J., Llavador-Ros, M., Gomez-Ruiz, M., Lopez-Hontangas, J., Botella-Estrada, R., Salavert-Lleti, M., Peman-Garcia, J. Cutaneous and mucocutaneous leishmaniasis: Experience of a Mediterranean Hospital. Parasit. Vect. 13, (2020). 24
2. Doe, E. D., Kwakye-Nuako, G., Addo, S. O., & Egyir-Yawson, A. Identification of sand flies (diptera: Psychodidae) collected from cutaneous leishmaniasis endemic focus in the Ho Municipality, Ghana. International Annals of Science, 10(1), (2021).33–44.
3. Ahmed, M., Abdulslam Abdullah, A., Bello, I., Hamad, S., & Bashir, A. Prevalence of human leishmaniasis in Sudan: A systematic review and meta-analysis. World Journal of Methodology, 12(4), (2022).305–318.
4. Reithinge R, Dujradin J, Louzir H, Pirmez C, Alexsander B, Brooker S. Cutaneous leishmaniasis. Lancet Infect Dis 7: (2007) 581-596.
5. Ovalle-Bracho, C., Londoño-Barbosa, D., Salgado-Almario, J., & González, C. Evaluating the spatial distribution of *Leishmania* parasites in Colombia from clinical samples and human isolates (1999 to 2016). PLoS One, 14(3), (2019). e0214124.
6. Pour, R., Sharifi, I., Kazemi, B. Identification of non-responsive isolates to glucantime in patients with cutaneous leishmaniasis in Bam. J Kerman Univ Med Sci 18: (2011) 123-133.
7. Bi, K., Li, X., Zhang, R., Zheng, X., Wang, F., Zou, Y, et al. Clinical and laboratory characterization of cutaneous leishmaniasis in Chinese migrant workers returned from Iraq. PLoS Negl Trop Dis 18(3): (2024). e0012006
8. Alvar, J., V'elez, I.D., Bern, C., Herrero, M., Desjeux, P., Cano, J., Jannin, J., den Boer, M.Leishmaniasis worldwide and global estimates of its incidence. PLoS One. 2012;7(5) .(2012). 35671
9. Alseady, H.H and Al-Dabbagh, S.M. Isolation and molecular identification of cutaneous leishmaniasis in humans and dogs in middle Euphrates, Iraq Iraqi Journal of Veterinary Sciences, Vol. 38, (2024). No. 2 (427-435)
10. Steverding, D, The history of leishmaniasis. Parasites & vectors, 10, (2017). 1-10.
11. Manson-Bahr, P.E.C. Old World leishmaniasis. In: Cox FEG, editor. The Wellcome Trust Illustrated History of Tropical Diseases. London: The Wellcome Trust; .(1996). p. 206–17.
12. Zink, A.R, Spigelman, M., Schraut, B., Greenblatt, C.L, Nerlich, A.G Donoghue HD. Leishmaniasis in Ancient Egypt and Upper Nubia. Emerg Infect Dis.;12,(2006).1616–7.
13. Maspero, G. The Dawn of Civilization - Egypt and Chaldaea. 5th ed. London: Society for the Promotion of Christian Knowledge; 1910. p. 218.
14. Bessat, M., ElShanat, S. Leishmaniasis: epidemiology, control and future perspectives with Special emphasis on Egypt. J. Trop. Dis., . (2013) 3(1),
15. World Health Organizatio. Leishmaniasis. World Health Org Fact Sheet. 2016;375.
16. Sunter, J., Gull, K. Shape, form, function and *Leishmania* pathogenicity: from textbook descriptions to biological understanding. Open Biol., 7, (2017). 170165.
17. Al-Hayali, H. L and Al-Kattan, M. M. Overview on Epidemiology of Leishmaniasis in Iraq. Rafidain Journal of Science. Vol. 30, (2021). No. 1, pp. 28-37.
18. Maroli, M., Feliciangeli, M.D., Bichaud, L., Charrel, R.N., Gradoni, L. *Phlebotomine* sandflies and the spreading of

leishmaniasis and other diseases of public health concern. Med Vet Entomol. 27: .(2013).123–47.

19. Jamal, Q., Shah, A., Rasheed, S. B., & Adnan, M. In vitro Assessment and Characterization of the Growth and Life Cycle of Leishmania tropica. Pakistan Journal of Zoology, (2020). 52(2).
20. Liu, D., & Uzonna, J. E. The early interaction of Leishmania with macrophages and dendritic cells and its influence on the host immune response. Frontiers in cellular and infection microbiology, 2, (2012). 83.
21. John, E., Bennett, R.D, Mbj, B., Mandell, D and Bennett,S. principles and practice of infectious diseases: 8th ed. Philadelphia: Elsevier/Saunders,. .(2015).
22. Olivo, F. C., Gundacker, N.D., Pascale, J.M., Saldaña, A., Diaz- Suarez, R., Jimenez, G., et al.. First case of diffuse leishmaniasis associated with Leishmania panamensis. Open Forum Infect Dis. 5(11): (2018)ofy281
23. PAHO. Manual of procedures for leishmaniases surveillance and control in the Americas 2019. [Available from: https://iris.paho.org/handle/10665.2/51838. This article gives a thorough explanation of the clinical symptoms, diagnosis, and treatment of leishmaniasis.
24. Mukhopadhyay, D., Dalton, J.E, Kaye, P.M., Chatterjee, M. Post kalaazar dermal leishmaniasis: an unresolved mystery. Trends Parasitol. 2014;30(2):65–74
25. Koutinas, A.F., Koutinas, C.K. Pathologic Mechanisms Underlying the Clinical Findings in Canine Leishmaniasis Due to Leishmania infantum/Chagasi. Vet. Pathol., 51, .(2014) 527–538.
26. Corpas-López, V., Merino-Espinosa, G., Acedo-Sánchez, C., Díaz-Sáez, V., Morillas-Márquez, F., Martín-Sánchez, J. Hair Parasite Load as a New Biomarker for Monitoring Treatment Response in Canine Leishmaniasis. Vet. Parasitol. 2016, 223, 20–25.
27. Rallis, T., Day, M.J., Saridomichelakis, M.N., Adamama-Moraitou, K.K., Papazoglou, L., Fytianou, A., Koutinas, A.F. Chronic Hepatitis Associated with Canine Leishmaniosis (Leishmania infantum): A Clinicopathological Study of 26 Cases. J. Comp. Pathol. , 132, (2005) 145–152.
28. Fontes, J.L.M., Mesquita, B.R., Brito, R., Gomes, J.C.S., de Melo, C.V.B. Dos Santos,W.L.C. Anti-Leishmania infantum Antibody- Producing Plasma Cells in the Spleen in Canine Visceral Leishmaniasis. Pathogens, 10, .(2021) 1635.
29. Solano-Gallego, L., Koutinas, A., Miró, G., Cardoso, L., Pennisi, M.G., Ferrer, L., Bourdeau, P., Oliva, G., Baneth, G.(2009). Directions for the Diagnosis, Clinical Staging, Treatment and Prevention of Canine Leishmaniosis. Vet. Parasitol. 165, .(2009). 1–18.
30. Rasha, K. A. AL. and May, H. K. An epidemiological study of cutaneous leishmaniosis in human and dogs. Annals of Parasitology 2021, 67(3), 417–433
31. Kadhim, R. F., Elias, R. H., Jabbar, R. A., & Kadhim, R. F. Serological Detection of Visceral Leishmaniasis in Infected Children in Al-Kut City. Eastern Journal of Agricultural and Biological Sciences, 4(1), (2024). 19-24.
32. Taj-Eldin, S.D., Alousi, K. Kala-azar in Iraq. Report of Four Cases. J. Fac. Med. Baghdad, 18(1-2), (1954). 15-19.
33. Nazzaro, G., Rovaris, M., Veraldi, S. Leishmaniasis: a disease with many names. JAMA Dermatol.; 150: .(2014). 1204
34. Al-Obaidi., M. J., Abd Al-Hussein,M.Y., Al-Saqur, I.M.Survey Study on the Prevalence of *Cutaneous Leishmaniasis* in Iraq. Iraqi Journal of Science, Vol. 57, .(2016). No.3C, pp:2181-2187
35. Al Zadawi,K.A.M., Al-Nori, T.A., Besmah, M., Al-Diwan,A.J.K Knowledge about Cutaneous Leishmaniasis among the population in Baghdad, Iraq, Iraqi New Medical Journal . Vol. 10. (2024). PP. 82-88
36. Al-Naimy, A. F. A and. Al-Waaly, A. B. M. Investigation of Cutaneous Leishmaniasis Cases in Baghdad province, Iraq. Medico-legal Update, January-March . Vol. (2021). 21, No. 1
37. Alkaisi, S. J. H., Najim, W. A. S., Alqaisi, L. J. H., & Jawad, R. T. Validity of dipstick rapid test in the diagnosis of visceral leishmaniasis in two hospitals in Baghdad city during two years (2012-2013). Middle East Journal of Family Medicine, 13(6). (2015).
38. AL-akash, M.A.R, Haitham ,A.R, Ghassa, F., Alubaidy , Dhafer, M. J. Prevalence of Leishmaniasis among People Living in Refugee Camps in Mosul City, Iraq in the Time of War. The Journal of Research on the Lepidoptera. Vol. 51 (2): (2020). 953-962
39. Rashid, B. O, Al-Dabbagh, Z. S., Sirwan, M., Al-Dabbagh, S.A., and Al-Hayali, H.N. An outbreak of cutaneous leishmaniasis among internally displaced persons from the Nineveh governorate reported by Duhok Preventive Health Department from 2015 to 2017. Zanco J. Med. Sci., Vol. 24, No. (2020). (1), PP. 153-159.
40. AlSamarai, A.M and AlObadi, H.S. Cutaneous leishmaniasis in Iraq. J Infect Dev Ctries, 3(2): (2009).123–9.
41. Abdulla, Q. B, Shabila, N. P, Al-Hadithi, T. S. An outbreak of Cutaneous leishmaniasis in Erbil governorate of Iraqi Kurdistan Region in 2015. J Infect Dev Ctries . 12(8): (2018). 600–7.
42. Lehlewa, A. M., Khaleel, H. A., Lami, F., Hasan, S. A. F., Malick, H. A., Mohammed, R. H., & Abdulmottaleb, Q. A. Impact of modifiable risk factors on the occurrence of cutaneous leishmaniasis in Diyala, Iraq: case-control study. JMIRx Med, 2(3), (2021). e28255.
43. Mancy, A., Awad, K.M., Abd-Al-Majeed, T and Jameel, N.F. The epidemiology of cutaneous leishmaniasis in Al-Ramadi, Iraq. Our Dermatol Online. 13(4): .(2022).402-407.
44. Obayes, L. H. Molecular diagnosis and phylogenetic analysis of 5.8s rDNA of gene of cutaneous leishmaniasis isolated from patients in holy Karbala. A thesis to College of Medicine . Department of medical Microbiology. (2019).
45. Al-Taei, H. T. A. A., Al-Qazwini, Y. M., & Zwair, H. A survey study for prevalence of visceral leishmaniasis in Karbala, Iraq. International Journal of Health Sciences, 6(S6), (2022). 9385–9396
46. Raja, J. M., AL Hadrawi,M. K., Zianb, S. A. J., Kareem, A. H. Epidemiology of Cutaneous Leishmaniasis in Najaf Province, Iraq. Int. j. adv. multidisc. res. stud. 3(5): .(2023)813-815
47. Wisam, A. M and Luma, H. A. The prevalence of Cutaneous leishmaniasis in Babil province and some of its affiliated districts. Al-Kufa University Journal for Biology . VOL.14 / NO.2 . (2022). PP. 6- 14
48. Aseel, Z. S and Malak, M. A. Epidemiology Study of Cutaneous Leishmaniasis in Babylon Governorate. Tuijin

Jishu/Journal of Propulsion Technology Vol. 44 No. 2 . .(2023). PP. 206 – 213

49. Mohammed, H. F., Fadhil, A. A. and Khwam, R. HDetection of *Leishmania tropica* Using Nested-PCR and Some of Their Virulence Factors in Thi-Qar Province, Iraq. Baghdad Science Journal. Vol. 18 No.1. .(2022). PP. 700-707.
50. Jassim, A. K., Maktoof, R., Ali, H., Bodosan, B., & Campbell, K. Visceral leishmaniasis control in Thi Qar governorate, Iraq, 2003. EMHJ-Eastern Mediterranean Health Journal, 12 (Supp. 2), S230-S237, 2006.
51. Abdulsadah, A. R. Cutaneous Leishmaniasis in Iraq: A clinicoepidemiological descriptive study. Sch. J. App. Med. Sci. 1(6): (2013). 1021-1025
52. ALsaad, R. K. A. and May, H. K. An epidemiological study of cutaneous leishmaniosis in human and dogs. Annals of Parasitology, 67(3), .(2021).417–433
53. Flaih, M. H., Alwaily, E. R., Hafedh, A. A., & Hussein, K. R. Six-Year Study on Cutaneous Leishmaniasis in Al-Muthanna, Iraq: Molecular Identification Using ITS1 Gene Sequencing. Infection & chemotherapy, 56(2), (2024).213–221.
54. Jarallah., H.M. cutaneous leishmaniasis in Basrah villages, south Iraq. J. Egypt. Soc. Parasitol. (JESP), 44(3), (2014). 597 - 603
55. Gani, Z. H., Hassan, M. K., & Jassim, A. M. Sero-epidemiological study of visceral leishmaniasis in Basrah, Southern Iraq. Journal of the Pakistan Medical Association, 60(6), (2010). 464-469
56. Murtada, S. J. Epidemiology of skin diseases in Kirkuk (Doctoral dissertation, MSc thesis, Tikrit University College of Medicine). (2001).
57. Jaffar, Z. A., Jasim, A. M., & Majeed, G. H. Detection of Visceral Leishmaniasis by Leishmania infantum using kDNA. Magazine of Al-Kufa University for Biology, (2024). 16(2).
58. Al-Warid, H. S., Al-Saqur, I. M., Al-Tuwaijari, S. B., & Zadawi, K. A. A. The distribution of cutaneous leishmaniasis in Iraq: demographic and climate aspects. Asian Biomedicine, 11(3), (2017). 255-260.
59. Morales-Yuste, M., Martín-Sánchez, J., Corpas-Lopez, V. Canine Leishmaniasis: Update on Epidemiology, Diagnosis, Treatment, and Prevention. Vet. Sci. 9, (2022).387.
60. Minnat, T. R., & Al-Bassam, L. S. canine cutaneous leishmaniasis: first report in a german shepherd police dog in diyala governorate-iraq. Diyala Agricultural Sciences Journal, 10 (Special issue), (2018). 150-162,
61. Al-Ardi, M. H. Rapid diagnosis of Leishmania spp. in blood samples using gold nanoparticles. Iraqi Journal of Veterinary Sciences, 36(3), (2022). 587-590.
62. Jassem, G. A. Epidemiological study for Toxoplasmosis and Leishmaniasis in stray dogs in Diwaniya city/Iraq. Kufa Journal For Veterinary Medical Sciences, 4(2), (2013). 31-39
63. Alobaidii, W.A. The serological diagnosis of canine Leishmaniasis by using ELISA in Nineveh province. Iraqi J Vet Sci. 33(2): (2019). 111-114.
64. Alobaidii, W.A and Almashhadany D.A. Molecular detection of Leishmania in cutaneous scrapping and blood samples of dogs in Mosul city. Iraqi Journal of Veterinary Sciences, Vol. 37, (2023)Supplement I, (15-19)

Arabic Abstract

داء الليشمانيات هو مرض طفيلي تسببه انواع مختلفة من طفيلي الليشمانيا. يعد داء الليشمانيات أحد أكثر الأمراض المعدية الانتقالية شيوعًا في جميع أنحاء العالم. وتعتبر من اكبر المشاكل الصحية. و المرض له ثلاث اشكال، الجلدية والمخاطية الجلدية والحشوية. وله أسماء مختلفة ولكن في العراق شكله جلدي يعرف حبة بغداد. يتضمن هذا البحث مراجعة لانتشار أنواع الليشمانيا في الإنسان والكلاب في جميع المحافظات العراقية وهذا يعتمد على الأبحاث العراقية التي تم نشرها في مجلات عالمية ومحلية مختلفة، وقد أفادت هذه الدراسة بتباين واسع في معدل الإصابة بالطفيلي لأسباب عديدة مثل التوعية الصحية، انتشار الحشرات، التجوال غير المسيطر علية للكلاب السائبة واختلاف طرق تشخيص الطفيلي جميع هذه العوال ادت إلى اختلاف معدل الانتشار في العراق.

009647769920165
https://journals.uokerbala.edu.iq
Iraq - Holy Karbala